THE ROLE OF GROWTH HORMONE AND ITS MEDIATOR INSULIN-LIKE GROWTH FACTOR-I IN GROWTH, METABOLISM, AND MAMMARY DEVELOPMENT

A Dissertation

Presented to the Faculty of the Graduate School

of Cornell University

In Partial Fulfillment of the Requirements for the Degree of

Doctor of Philosophy

by

Sarah Louise Giesy

January 2009

THE ROLE OF GROWTH HORMONE AND ITS MEDIATOR INSULIN-LIKE GROWTH FACTOR-I IN GROWTH, METABOLISM, AND MAMMARY DEVELOPMENT

Sarah Louise Giesy, Ph. D.

Cornell University 2009

The somatotropic axis is one of the major hormonal systems regulating growth, development, and metabolism. Growth hormone (GH) can act directly on target tissues or indirectly by stimulating insulin-like growth factor (IGF-I) through the JAK2-Stat5 pathway. The first objective of this dissertation was to test whether exogenous GH could stimulate growth, development, and insulin resistance in the absence of functional Stat5 proteins. Wild type (WT) and Stat5 mutant ($Stat5^{\Delta N}$) mice were treated with exogenous GH for 4 weeks. $Stat5^{\Delta N}$ mice grew at a slower rate and had lower hepatic IGF-I expression and plasma IGF-I than WT animals. GH stimulated growth in WT animals but had absolutely no effect in $Stat5^{\Delta N}$ mice. GH increased hepatic IGF-I expression and plasma IGF-I in WT mice but failed to do so in $Stat5^{\Delta N}$ mice. GH-stimulated IGF-I expression also occurred in the muscle and adipose of WT mice only. GH-treated $Stat5^{\Delta N}$ mice were protected from GH-induced insulin resistance. This protection was associated with lack of GH-stimulated expression of p85α mRNA in insulin sensitive tissues.

GH plays a critical role in mammary development through its modulation of mammary production of IGF-I and IGF binding proteins (IGFBPs). One component of the IGF system that has not been studied in mammary development is the acid labile subunit (ALS). ALS is thought to function exclusively by forming ternary

complexes with IGF-I and IGFBP-3 or -5 to build a reservoir of circulating IGF-I. The second objective was to evaluate the role of ALS in mammary gland development using null ALS mice. Null ALS mice had three specific mammary defects, namely delayed ductal elongation, impaired ductal branching in early pregnancy, and delayed involution following lactation. In contrast, mammary development during late pregnancy and lactation appeared normal in null ALS mice. ALS mRNA was detected in the mouse mammary gland, and levels of expression were comparable to liver during pregnancy, lactation, and involution. Therefore, mammary defects seen in null ALS mice cannot be attributed solely to disruption of the circulating IGF system and could relate partly to local ALS expression.

BIOGRAPHICAL SKETCH

Sarah Louise Giesy was born in St. Maries, Idaho on January 4th, 1978 to Steven and Peggy Cuvala. Sarah has a younger brother, Nathan, and a younger sister, Lauren with whom she has shared numerous adventures. The Cuvala family made their home in the Benewah Valley on just over 200 acres of land. Sarah was an active participant in 4-H and showed market hogs, sheep, and horses at the county fair. Sarah attended school in St. Maries and graduated salutatorian from St. Maries High School in 1996. After graduation she moved to Moscow, Idaho to attend the University of Idaho and pursue a degree in Animal Science. Sarah quickly became interested in scientific research while working in the laboratory of Dr. Susan Duckett. While at the University of Idaho, she met Jay Giesy. The summer of 2000 was a whirlwind for Sarah. She graduated summa cum laude in May, married Jay in July, and moved across the country to Ithaca, NY in August to begin her graduate career at Cornell University. Sarah completed her Master's degree in Animal Science under the direction of Dr. Yves Boisclair in February 2004 and continued on to pursue a Ph.D. She and her husband welcomed their daughter, Dillan Louise, into their family in October 2004. Six days after passing her B exam, Sarah gave birth to their second daughter, Ashton Jae. Upon completion of the requirements for her Ph.D., Sarah plans to spend time with her family.

To my family: Jay, Dillan, and Ashton Giesy

ACKNOWLEDGMENTS

I have many people to thank for their help and support throughout my graduate program. First, I must thank my husband, Jay. Without his love and support, I would not be where I am today. I appreciate all his patience and the sacrifices he has made through the years. My daughter, Dillan, has allowed me to experience the joys of motherhood, and she has kept me on my toes throughout my Ph.D. program. I also must thank my daughter Ashton for sticking to 'the plan:' defense, Christmas, then baby. Next, I would like to thank my family. Their love and guidance have helped to shape me into the person I am today. They have always encouraged me throughout all my endeavors. Though we have been separated by several thousands of miles, their support has remained as ever strong. I also must thank the Giesy family as they have provided many words of praise and encouragement throughout my graduate career.

I would like to thank my advisor, Yves Boisclair, for all his guidance and support throughout my program. Thank you to Drs. Alan Bell, Susan Quirk, and Mark Roberson for taking the time to participate on my committee and advise me throughout my Ph.D. program. Numerous people have helped me throughout my graduate career. I thank Richard Ehrhardt for his technical advice and Ramona Ehrhardt for performing RIAs. I also thank Bob Cowan for providing technical advice. Thank you to Dr. Long for allowing me to photograph slides using his microscope. I also thank Shuai Li for instructing me on use of the microscope and immunohistochemistry procedures. I value the friendships I have made with many of the graduate students in the department. They help me to remember to relax some and enjoy life. And finally, I must thank the Department of Animal Science for the financial support provided to me throughout my program.

TABLE OF CONTENTS

LIST OF FIGURES

LIST OF TABLES

LIST OF ABBREVIATIONS

aa	amino acid
Alb	albumin promoter
Alfp	alpha fetoprotein enhancer
ALS	acid labile subunit
AUC	area under the curve
BCA	bicinchoninic acid
Bcl	B-cell lymphoma protein
bGH-TG	bovine growth hormone transgenic
bp	base pair
BSA	bovine serum albumin
BW	body weight
cDNA	complementary deoxyribonucleic acid
ChIP	chromatin precipitation
Ci	curie (= 3.7×10^{10} disintegrations/second)
CIS	cytokine inducible SH2 domain containing protein
Cre	Cre recombinase
d	day
DAPI	4´,6-diamidino-2-phenylindole
DNA	deoxyribonucleic acid
DNase	deoxyribonuclease
dNTPs	deoxynucleotide triphosphates
dpm	disintegrations per minute
E	embryonic day
EMSAs	electrophoretic mobility shift assays

ER	estrogen receptor
ERK	extracellular signal-regulated kinase
FFA	free fatty acids
GAS	γ-interferon activated sequence
GH	growth hormone
GHa	growth hormone antagonist
GHR	growth hormone receptor
GHRE	growth hormone response element
GR	glucocorticoid receptor
Grb2	growth factor receptor binding protein-2
h	hour
HRP	horseradish peroxidase
H&E	hematoxylin and eosin
IGF	insulin-like growth factor
IGF-IR	insulin-like growth factor receptor
IGFBP	insulin-like growth factor binding protein
IGFs	insulin-like growth factor-I and –II
IR	insulin receptor
IRS	insulin receptor substrate
ITT	insulin tolerance test
JAK	Janus kinase
kb	kilobase
kDa	kilodalton
LID	liver IGF-I deficient
MAPK	mitogen-activated protein kinase
MEK	MAP ERK kinase

min	minute
MMTV	mouse mammary tumor virus
mRNA	messenger ribonucleic acid
Myf5	myogenic factor 5 promoter
nt	nucleotide
P	postnatal day
PBS	phosphate buffered saline
PCR	polymerase chain reaction
PDK-1	3-phosphoinositide-dependent kinase-1
Pdx1	pancreatic and duodenal homeobox 1 promoter
PH	pleckstrin homology
PIAS	protein inhibitors of activated Stats
PIP2	phosphatidylinositol-3,4-bisphosphate
PIP3	phosphatidylinositol-3,4,5-triphosphate
PI3K	phosphatidylinositol 3-kinase
PRLR	prolactin receptor
PTP	phosphotyrosine phosphatase
PVP	polyvinylpyrrolidone
RIA	radioimmunoassay
RNA	ribonucleic acid
RNase	ribonuclease
RPA	ribonuclease protection assay
SDS	sodium dodecyl sulphate
SDS-PAGE	SDS-polyacrylamide gel electrophoresis
SHP	SH2-containing phosphatases
SH2	Src homology domain

SOCS	suppressors of cytokine signaling
SOS	son of sevenless
STAT	signal transducers and activators of transcription 5
TBST	tris-buffered saline with tween-20
TKp	thymadine kinase promoter
WAP	whey albumin protein
WAT	white adipose tissue
WM	whole mount
WT	wild type

CHAPTER ONE:
INTRODUCTION

The growth hormone and insulin-like growth factor (GH-IGF-I) system plays essential roles in postnatal growth, development, and metabolism. For example, Lupu *et al.* (2001) estimated that GH and IGF-I alone account for 14% and 35% of postnatal growth, respectively whereas their overlapping actions account for 34% of postnatal growth. The overlapping actions represent GH actions mediated via its stimulation of IGF-I synthesis. GH stimulation of IGF-I synthesis occurs in extra-hepatic tissues such as muscle and in liver (Mathews *et al.* 1986; Murphy *et al.* 1987). The IGF-I produced by extra-hepatic tissue remains near its cellular site of production and represents the autocrine/paracrine arm of the IGF-I system (Le Roith *et al.* 2001). These IGF-I molecules are usually bound to one of six IGF binding proteins (IGFBPs) (Jones & Clemmons 1995; Stewart & Rotwein 1996). Liver-derived IGF-I, on the other hand, is secreted in plasma and corresponds to the endocrine arm of the IGF-I system. Circulating IGF-I is bound in a 150 kDa ternary complex composed of one molecule each of IGF-I, IGFBP-3 or -5, and the acid labile subunit (ALS), a protein produced predominantly by the liver (Baxter 1988; Twigg & Baxter 1998).

Effects of GH are mediated through the growth hormone receptor (GHR). Binding of GH to its receptor leads to activation of JAK2. This is followed by JAK2 dependent activation of various signaling cascades (Lanning & Carter-Su 2006). The growth promoting effects of GH are mediated predominantly by the signal transducer activator of transcription (Stat) 5a and 5b proteins (Waters *et al.* 2006). Genetic mouse models have been created in which each individual Stat5 gene is ablated (Liu *et al.* 1997; Udy *et al.* 1997). These models show that Stat5a is absolutely required for proper mammary gland development during late pregnancy and lactation, but Stat5a

appears to play no role in regulation of growth (Liu *et al.* 1997). On the other hand, Stat5b plays important roles in regulating sexually dimorphic growth rates and male specific hepatic gene expression (Udy *et al.* 1997). So far, no studies have ever directly assessed whether growth effects of exogenous GH were also lost in Stat5 deficient mice. Chronic administration of GH has been used to evaluate the responsiveness of various GH/IGF-I mutant models to exogenous GH (Liu & LeRoith 1999; Liu *et al.* 2000b; Fielder *et al.* 1996). Therefore, the objective of the work described in Chapter 3 was to test whether exogenous GH could stimulate not only overall growth of $Stat5^{\Delta N}$ mice but also other GH-dependent responses such as organ growth and insulin resistance.

As mentioned above, ALS is responsible for formation of ternary complexes and the development of the circulating IGF-I reservoir (Baxter 1988; Twigg & Baxter 1998). So far, ALS has been postulated to function exclusively as a component of the circulating IGF-I system. Additional studies have established that IGF-I deficiency associated with lack of ALS has functional impacts. First, null ALS mice suffer a 13-20% growth deficit after birth (Ueki *et al.* 2000). Bone length is shorter and bone metabolism is impaired in null ALS mice (Yakar *et al.* 2002). Null ALS mice have normal plasma glucose and insulin concentrations (Ueki *et al.* 2000) but are protected from GH-mediated insulin resistance (Haluzik *et al.* 2003). These studies demonstrate a functional role for ALS in postnatal growth and metabolism, but the role of ALS in mammary gland development has not been studied.

The mammary gland undergoes extensive morphological and biochemical changes during postnatal life. These dynamic changes are under strict hormonal control by sex steroid hormones and various growth factors (Richert *et al.* 2000). GH, IGF-I, and IGFBPs are involved in mammary development. A role for ALS, either through its ability to modulate plasma IGF-I or through local effects, has never been

considered. Therefore, the objective of the work described in Chapter 4 was to evaluate the role of ALS in mammary gland development using the null ALS mouse model.

CHAPTER TWO:

LITERATURE REVIEW

INTRODUCTION

The somatotropic axis is one of the major hormonal systems regulating growth, development, and metabolism (Le Roith *et al.* 2001). Growth hormone (GH) can act directly on target tissues, or it can act indirectly by stimulating insulin-like growth factor (IGF-I) production in liver and extra-hepatic tissues. Liver derived IGF-I is secreted in plasma and represents the endocrine arm of the IGF system whereas extra-hepatic IGF-I production represents the autocrine/paracrine arm (Le Roith *et al.* 2001). In circulation and the extracellular space, IGF-I is bound to one of six insulin-like growth factor binding proteins (IGFBPs). Before birth, IGF-I circulates in a binary complex in which IGFBP-2 is the predominant IGFBP (Jones & Clemmons 1995). Upon induction of acid labile subunit (ALS) synthesis after birth, circulating IGF-I is bound in a 150 kDa ternary complex composed of one molecule each of IGF-I, IGFBP-3 or –5, and ALS (Baxter 1988; Twigg & Baxter 1998). A second IGF protein, IGF-II, exists but is not regulated by GH and plays no role in mediation of GH effects. Therefore, IGF-II will not be discussed extensively in the following pages.

In the first part of this review, the components of the IGF system will be described. These include IGF-I and IGF-II, their receptors and binding proteins, and the ALS. Growth hormone is the most important regulator of IGF-I and ALS expression, and its effects on the IGF-I system are mediated predominantly via the signal transducers and activators of transcription 5 (Stat5) proteins (Woelfle & Rotwein 2004). Therefore, the second section will provide an overview of growth hormone receptor signaling with emphasis on Stat5 and the molecular mechanisms whereby Stat5 regulates IGF-I and ALS gene expression. The final section covers the

functional role of the somatotropic axis in postnatal growth, carbohydrate metabolism, and mammary development.

COMPONENTS OF THE IGF SYSTEM

The insulin-like growth factors and their receptors

IGF-I and IGF-II (IGFs) are insulin-like peptides of 70 and 67 amino acids, respectively (Humbel 1990; Daughaday & Rotwein 1989). IGF-I and IGF-II are synthesized by many tissues and are regulated by many different factors. IGF-II expression in the rodent is high during fetal life but in contrast to most other species, decreases to undetectable levels after birth (Stempien *et al.* 1986; Graham *et al.* 1986; Brown *et al.* 1986), resulting in virtually no circulating IGF-II in adult rodents (Moses *et al.* 1980). IGF-I levels are reciprocal to IGF-II levels: IGF-I levels are low during fetal life and increase after birth (Daughaday *et al.* 1982; Singh *et al.* 1991; Hwang *et al.* 2008). In the adult mouse, the primary source of circulating IGF-I is the liver, accounting for approximately 75% of plasma IGF-I (Yakar *et al.* 1999; Sjogren *et al.* 1999).

Three types of receptors are recognized by the IGFs. The IGF-I receptor (IGF-IR) binds IGF-I with greatest affinity, followed by IGF-II and then insulin. The IGF-IR has 100-1000 fold higher affinity for IGF-I than insulin and a 2-15 fold higher affinity for IGF-I than IGF-II (Jones & Clemmons 1995). The IGF-II receptor (IGF-IIR) binds IGF-II with greater affinity than IGF-I and does not bind insulin. The insulin receptor (IR) binds insulin with highest affinity, followed by IGF-II and then IGF-I (Humbel 1990). The biological effects of IGFs are mediated through the IGF-IR while the IGF-IIR removes excess IGF-II from circulation (O'Dell & Day 1998).

The IGF-IR and insulin receptor are structurally related and share 50% amino acid sequence identity. Both receptors are heterotetramers composed of two α and two β subunits linked by disulfide bonds. The extracellular ligand-binding domain is

formed by the α subunits, and the transmembrane and intracellular domains are formed by the β subunits (Humbel 1990; Stewart & Rotwein 1996). The intracellular domain contains a tyrosine kinase and sites of tyrosine phosphorylation necessary for signaling. Two of the more important signaling cascades engaged by the activated IGF-IR are the mitogen-activated protein kinase (MAPK) pathway and phosphatidylinositol 3-kinase (PI3K) pathway via activation of insulin receptor substrate-1 (IRS-1) (Laviola *et al.* 2007).

IGF binding proteins

In circulation and the extracellular space, IGFs are bound to a family of structurally related binding proteins called IGF binding proteins (IGFBP). Currently, six different IGFBPs (named IGFBP-1 to –6) have been identified. The binding protein genes range in size from 5 kb to more than 30 kb, but all genes contain 4 conserved exons (Firth & Baxter 2002). The amino and carboxy terminal ends of these six proteins are conserved while the middle domains differ (Rechler 1993). Mutagenesis studies have demonstrated that the amino and carboxy terminal ends form a binding pocket for IGFs, and the middle region is responsible for the unique functions of the individual binding proteins (Clemmons 2001). These binding proteins have numerous functions that include, but are not limited to, extending the half-lives of IGFs, determining the bioavailability of IGFs, and modulating IGFs' biological activities. IGFBP-2, -3, and –5 are the primary IGFBPs that comprise the circulating IGF system. For these reasons, the remainder of this section will focus on IGFBP-2, -3, and –5.

IGFBP-2

The mouse IGFBP-2 gene encodes a 31 kDa protein that shares 97% homology with the rat IGFBP-2 protein (Kelley *et al.* 1996; Landwehr *et al.* 1993). IGFBP-2 contains an RGD sequence known to bind integrin-like receptors, but such a property

has yet to be described for this IGFBP (Wetterau *et al.* 1999). IGFBP-2 has a higher affinity for IGF-II than IGF-I and is thought to be particularly effective at inhibiting IGF-II actions (Firth & Baxter 2002).

Most of the circulating IGFs are bound to IGFBP-2 during fetal life and to IGFBP-3 during postnatal life. In the mouse, IGFBP-2 is detected at embryonic d10.5 (E10.5). Message levels in the liver increase significantly after birth, reach maximum levels at postnatal d3 (P3), and remain abundant thereafter (Schuller *et al.* 1994). The IGFBP-2 message also is detected in the kidney, lung, brain, spleen, testis, and ovary (Schuller *et al.* 1994). Developmental expression of hepatic IGFBP-2 differs in the rat such that it is high during fetal life but is barely detectable in adulthood (Margot *et al.* 1989).

IGFBP-3

The IGFBP-3 gene encodes a 34 kDa protein. Three glycosylation sites are present which produce circulating forms that range in size from 40 and 44 kDa (Rechler 1993). In the mouse, IGFBP-3 is detected at E11.5 in the embryo and reaches maximum levels in the liver at P7 of postnatal age. IGFBP-3 mRNA is also detected in kidney, lung, heart, spleen, and muscle (Schuller *et al.* 1994; Cerro *et al.* 1993). In the rat, IGFBP-3 mRNA is highest in the kidney but is also expressed in liver, stomach, placenta, and uterus (Albiston & Herington 1992). In the liver, IGFBP-3 has been localized to the nonparenchymal cells and is not expressed in hepatocytes (Chin *et al.* 1994; Scharf *et al.* 1996).

After birth, IGFBP-3 is the most abundant IGFBP in circulation with its concentration surpassing that of any other IGFBP by ~10-fold (Baxter 1994). Furthermore, IGFBP-3 has the highest binding affinity for IGF-I (Rechler 1993) such that over 75% of circulating IGF-I is bound to IGFBP-3 (Rajaram *et al.* 1997).

IGFBP-5

The IGFBP-5 gene encodes a 29 kDa protein. Variation in glycosylation results in the appearance of IGFBP-5 as a triplet of 29-34 kDa when analyzed by Western ligand blot (James *et al.* 1993; Wetterau *et al.* 1999; Schneider *et al.* 2002). It is highly conserved across human, rat, and mouse (97%) (Kou *et al.* 1994). IGFBP-5 is detected in the E11.5 old mouse embryo (Schuller *et al.* 1994). In the adult mouse, IGFBP-5 mRNA is detected at high levels in the kidney, uterus, and skeletal muscle and at lower levels in the lung, heart, and brain, but expression is completely absent in the liver (James *et al.* 1993; Shimasaki *et al.* 1991; Schuller *et al.* 1994) (Kou *et al.* 1994).

The acid labile subunit and ternary complex formation

ALS plays a crucial role in the circulating IGF system as it is responsible for formation of the ternary complex. Purified human ALS migrates as a doublet with a molecular mass of 84-86 kDa by SDS-PAGE analysis. N-glycanase treatment decreased the molecular mass to 60-64 kDa demonstrating that serum ALS is glycosylated (Baxter *et al.* 1989; Dai & Baxter 1992).

In rat, baboon, sheep, and pig, ALS mRNA expression has only been detected in the liver by Northern analysis (Dai & Baxter 1994; Delhanty & Baxter 1996; Rhoads *et al.* 2000; Lee *et al.* 2001). In contrast, ALS expression was detected in the liver, gonadal fat, and kidney of both male and female mice (Giesy 2004).

Expression of ALS is barely detectable by Northern analysis in the liver of rats between birth and P10 of age. Expression is induced around P21 of age and reaches maximal levels by P42 (Dai & Baxter 1994). In contrast to the rat, hepatic ALS mRNA was easily detected at P1 of age in the mouse (Giesy 2004). By in situ hybridization, a more dramatic increase in hepatic ALS expression was observed between birth and P20 of age in the rat (Chin *et al.* 1994). At one week of age,

circulating ALS concentrations are ~1000 ng/mL. Levels increase 5-fold by 8 weeks of age and decline slightly with increasing age (Hwang *et al.* 2008).

The ALS protein is most prevalent in plasma (Baxter & Dai 1994). Based on the mRNA data described above, most of circulating ALS is thought to be synthesized by liver. After birth, ALS recruits IGF-I into ternary complexes composed of one molecule each IGF-I, IGFBP-3 or –5, and ALS (Baxter 2000). The prevalent ternary complex is one where the IGFBP moiety is IGFBP-3. Appearance of ALS and formation of the ternary complex are thought to be important steps in the development of the endocrine IGF-I system. ALS associates with the binary complex of IGF-I and IGFBP-3 or –5. ALS binds only binary complexes as it has virtually no affinity for either IGF-I or IGFBP alone (Baxter *et al.* 1989). ALS circulates in 2-3 molar excess over IGF-I and IGFBP-3, driving 75% of circulating IGF-I into ternary complexes (Baxter 1990). Only 10% of IGFBP-3 is found in its free form in circulation (Baxter *et al.* 2002). In humans, ~55% of circulating IGFBP-5 is bound to IGF-I and ALS (Twigg & Baxter 1998; Baxter *et al.* 2002). These IGFBP-5 ternary complexes are not as abundant as IGFBP-3 complexes because circulating levels of IGFBP-5 are only 10% of IGFBP-3 levels (Baxter *et al.* 2002; Baxter 1988).

Free IGF-I has a half-life of 10-12 minutes. The half-life of IGF-I is extended to 20-30 minutes when in binary complexes and to 12-15 hours when in ternary complexes (Zapf *et al.* 1986; Guler *et al.* 1989). The dramatic increase in IGF-I half-life when in a ternary complex stems from the inability of ALS to cross the endothelial barrier (Binoux & Hossenlopp 1988).

GROWTH HORMONE REGULATION OF THE IGF SYSTEM

Effects of GH are mediated through the growth hormone receptor (GHR). Signaling is initiated when GH sequentially recruits two GHR monomers. This dimerization event causes a conformational change, aligning two Janus kinase 2

(JAK2) molecules (Dominici *et al.* 2005). These tyrosine kinases activate one another via transphosphorylation and phosphorylate tyrosine residues on the GHR. The phosphorylated residues on both molecules serve as docking sites for downstream signaling mediators (Lanning & Carter-Su 2006). Upon JAK2 activation, GHR signaling can proceed through three main pathways: signal transducers and activators of transcription (Stat) pathway, mitogen-activated protein kinase (MAPK) pathway, and phosphatidylinositol 3-kinase (PI3K) pathway. More recently, GH has been shown to activate the tyrosine kinase Src independent of JAK2 activation (Lanning & Carter-Su 2006; Brooks *et al.* 2008). Termination of JAK/Stat signaling in the GHR pathway is mediated by three families of proteins: the suppressors of cytokine signaling (SOCS), the SH2-containing phosphatases [SHP, also known as phosphotyrosine phosphatase (PTP)], and the protein inhibitors of activated Stats (PIAS) (Wormald & Hilton 2004). A more detailed overview of the GH signaling pathway is given below.

GH Signaling pathways

GH activation of the Stat proteins has been studied extensively (Herrington *et al.* 2000). GH activates Stat5 predominantly and to a lesser extent, Stat1 and Stat3 (Hosui & Hennighausen 2008). Upon activation of JAK2, Stat proteins are recruited to phosphorylated tyrosine residues on the GHR via their SH2 domains, followed by JAK2 phosphorylation of specific tyrosine residues on Stat proteins. The Stat proteins can then homo- or heterodimerize, translocate to the nucleus, bind specific DNA sequences, and activate transcription (Herrington *et al.* 2000).

To activate the MAPK pathway, Shc, an SH2 domain containing adapter protein, is recruited to the receptor and phosphorylated. Phosphorylated Shc binds growth factor receptor binding protein-2 (Grb2) and the guanine nucleotide exchange factor, Son of Sevenless (SOS). The assembly of this complex brings SOS in close

proximity to the membrane and enables activation of the small GTP-binding protein, Ras (Piwien-Pilipuk *et al.* 2002). Ras then activates the serine/threonine kinase, Raf, which activates the tyrosine/serine/threonine kinase, MEK, and MEK specifically activates ERK1 and 2. ERKs can phosphorylate many different proteins, including cytoskeletal targets, cytosolic proteins, and nuclear proteins (Carter-Su *et al.* 2000). The MAPK pathway has been implicated in GH-stimulation of c-fos, egr-1, and junB transcription (Piwien-Pilipuk *et al.* 2002).

The final pathway that I will describe is GH-activation of PI3K. GH stimulates JAK2 phosphorylation of insulin receptor substrates (IRS) -1 and -2 which allows IRS proteins to interact with PI3K. PI3K is composed of two subunits, the regulatory subunit p85α and the catalytic subunit p110. IRS binds to p85 which relieves the basal inhibition of p110 and recruits the heterodimer to its substrate at the plasma membrane (Engelman *et al.* 2006). Activation of PI3K converts lipid second messengers, phosphatidylinositol-3,4-bisphosphate (PIP2) to phosphatidylinositol-3,4,5-triphosphate (PIP3) (Hirsch *et al.* 2007). These lipid messengers bind to the pleckstrin homology (PH) domain of 3-phosphoinositide-dependent kinase-1 (PDK-1) and the serine/threonine kinase Akt (also known as protein kinase B). Akt can activate various processes including stimulating glycogen synthesis, glycolysis, and cell survival via inhibition of pro-apoptotic factors (Piwien-Pilipuk *et al.* 2002)

Inhibitors of GH signaling

Several mechanisms limit GH signaling. The SHP and PIAS proteins are constitutively expressed and attenuate GH signaling by dephosphorylating JAK2 and GHR and repressing Stat activity, respectively (Wormald & Hilton 2004). The SOCS family of proteins is an inducible inhibitor of the GH pathway and can interfere directly with the signaling cascade and can target the receptor for proteasomal degradation (Wormald & Hilton 2004).

Three different phosphatases, SHP1, PTP1b, and PTP-H1 are involved in down regulation of GHR signaling. GH activates SHP1, resulting in nuclear translocation. In the nucleus, SHP-1 binds Stat5b and attenuates its activity. SHP1 also binds JAK2 and controls the duration of JAK2 phosphorylation (Flores-Morales *et al.* 2006). PTP1b can interact with GHR and/or JAK2 in a GH-dependent manner and dephosphorylates residues on both molecules. In addition, PTP-H1 can dephosphorylate the GHR (Flores-Morales *et al.* 2006). The PIAS family is composed of 4 members: PIAS1, PIAS3, PIASx, and PIASy (Wormald & Hilton 2004). PIAS1 and PIAS3 bind Stat1 and Stat3, respectively, to inhibit DNA association. The mechanism by which PIASx and PIASy inhibit Stat proteins is unknown, but neither PIAS prevents Stats from associating with DNA (Wormald & Hilton 2004). It is not known whether the PIAS proteins are involved in down-regulation of GHR signaling.

The SOCS family contains eight known proteins, SOCS1 -7 and cytokine-inducible SH2 domain containing protein (CIS), but only SOCS1-3 and CIS are induced by GH (Flores-Morales *et al.* 2006). SOCS1 can bind JAK2 and block its kinase activity as well as regulate proteasomal degradation of activated JAK2 (Ungureanu *et al.* 2002). SOCS2 and CIS bind GHR and compete with Stat5 for binding to the receptor (Ram & Waxman 1999). The mechanism for SOCS3 down regulation of GHR signaling is thought to involve SOCS3 binding to the GHR and inhibiting JAK2 kinase activity. Moreover, GH regulation of SOCS1, SOCS2, and CIS is mediated via Stat5b (Woelfle & Rotwein 2004).

The Stat proteins

A major portion of the actions of GH are mediated via the IGF-I system. Current evidence indicates GH relies predominantly on Stat proteins, particularly Stat5, to alter the activity of the IGF-I system (Woelfle *et al.* 2005). Therefore, this

section provides a brief overview of the Stat proteins with an emphasis on Stat5 and its regulation of the IGF-I system.

Seven different members of the Stat family exist, Stats 1, 2, 3, 4, 5a, 5b, and 6. Genes for Stats 1 and 4 are located on chromosome 1, Stats 2 and 6 are on chromosome 10, and Stats 3, 5a, and 5b are on chromosome 11 (Miyoshi *et al.* 2001). The Stat family members share a conserved molecular structure that consists of an N-terminal domain, followed by an α-helical coiled coil domain, a DNA-binding domain, and a linker that connects to the C-terminus. The SH2 domain is located within the C-terminus and is followed by a short region containing tyrosine residues. Activated Stat proteins bind to γ-interferon-activated sequences (GAS) and initiate transcription of target genes (Hennighausen & Robinson 2008). The Stat5 proteins have been implicated in the regulation of hepatic GH-responsive genes such as IGF-I and ALS (Woelfle & Rotwein 2004). Thus, these proteins will be described in more detail.

Genes for Stat5a and Stat5b are located on mouse chromosome 11, and their promoters are oriented head-to-head and separated by only 10 kb. The Stat5a gene is 30 kb in length, contains 20 exons, and the start codon is located in exon 3. The Stat5b gene is 50 kb in length, also contains 20 exons, but the start codon is located in exon 2. The Stat5a gene has one promoter while Stat5b has two (Miyoshi *et al.* 2001). Stat5a and Stat5b share 96% homology at the protein level and contain 793 and 786 amino acids, respectively. The greatest divergence is found in the C-terminal region where transactivation occurs (Hennighausen & Robinson 2008). Despite the similarity between these two isoforms, each has distinct functions in growth and development.

GH regulation of IGF-I and ALS via Stat5

It has been well established that GH regulates the IGF-I system, with IGF-I and ALS, being the most responsive components. Various GH deficient models have

been utilized to evaluate GH regulation of IGF-I. In the rat model, hypophysectomy dramatically decreases hepatic IGF-I expression, but expression is restored by exogenous GH treatment (Murphy *et al.* 1987; Gronowski & Rotwein 1995; Roberts, Jr. *et al.* 1987; Hynes *et al.* 1987; Rotwein *et al.* 1993; Maiter *et al.* 1988). Tissue IGF-I protein concentrations were lower in hypophysectomized rats than in normal rats. IGF-I concentrations in the liver decreased the most and were increased significantly by GH treatment (D'Ercole *et al.* 1984). Two hours after treatment of hypophysectomized rats with GH, the 7.5 kb hepatic IGF-I transcript increased 10-fold. Response peaked at 4h and returned to baseline levels by 16h (Bichell *et al.* 1992). Dwarf *lit/lit* mice have low GH serum levels. Hepatic IGF-I expression is markedly reduced in these animals, but it can be restored with administration of GH (Mathews *et al.* 1986). In GH receptor knockout mice, hepatic IGF-I mRNA expression is 1-2% of that in normal mice (Lupu *et al.* 2001).

Rotwein and coworkers demonstrated that GH effects on IGF-I mRNA occurred via stimulation of transcription (Bichell *et al.* 1992), but only recently have the molecular mechanisms been discovered. Three distinct GH response elements (GHRE) that contain paired Stat5b binding sites have been mapped within the rat IGF-I locus (Woelfle *et al.* 2003; Wang & Jiang 2005). Two pairs are located within the second intron of the IGF-I gene while the other is located 77 kb 5' to exon 1. Using chromatin immunoprecipitation (ChIP) analysis, Wang *et al.* showed that Stat5b can bind both the intronic and 5' distal sites with the IGF-I gene in a GH-dependent manner (Wang & Jiang 2005). More recently, five additional Stat5 binding sites, distributed over 3 additional chromosomal regions of the IGF-I gene, have been identified. Individually, these regions are capable of activating reporter gene expression via Stat5 binding, but a greater GH response is achieved when all five regions are activated (Eleswarapu *et al.* 2008).

GH regulation of ALS is also well understood. ALS serum levels were reduced by 75% in 10-week old GH deficient, dw/dw rats (Baxter & Dai 1994). Acromegalic humans have 2.2-fold higher plasma ALS concentration than normal individuals whereas GH deficient adults have only 30% of normal levels (Baxter 1990). In GH deficient patients, plasma ALS levels are increased with GH replacement therapy (Thoren *et al.* 1997; Labarta *et al.* 1997). In humans, acute GH treatment (single injection) had no effect on ALS mRNA or circulating levels, but a more chronic GH treatment (single injection for 5 consecutive days) increased hepatic ALS expression 85% and serum levels 1.5-fold (Olivecrona *et al.* 1999).

When primary rat hepatocytes are treated with GH, ALS production increases in a dose dependent manner with a maximum ALS response at 30 ng/mL (Dai *et al.* 1994; Scharf *et al.* 1996). At 30 ng/mL of GH, ALS mRNA levels increased by 4-fold, and ALS protein increased by 2-fold in primary hepatocytes. It was also shown that IGF-I was unable to increase serum ALS levels in hypophysectomized rats (Fielder *et al.* 1996). In hypophysectomized rats, hepatic ALS mRNA was reduced by over 90% and partially restored with GH treatment (Chin *et al.* 1994; Ooi *et al.* 1997). To confirm that GH stimulated ALS gene transcription, an ALS promoter reporter gene was transfected into rat hepatoma cells and primary rat hepatocytes. GH treatment stimulated promoter activity 3-fold (Ooi *et al.* 1997).

The molecular basis for this effect of GH has been studied using the mouse ALS promoter. Using a luciferase reporter system, Boisclair *et al.* (1996) determined that a region between nucleotides –805 to –11 of the mouse ALS promoter contained a GH responsive element. Serial deletions of the 5' region of the ALS gene narrowed the GH response region to nt –653 and nt –483. Computer analysis revealed two γ-interferon activated sequences (GAS) sites, termed ALS-GAS1 and ALS-GAS2. These GAS-like sites have been shown to mediate the effects of various cytokines,

including GH, on gene transcription (Ooi *et al.* 1998). Targeted deletion analysis revealed that ALS-GAS1 alone was required for GH activation of the mouse ALS promoter-luciferase reporter constructs. Using electrophoretic mobility shift assays (EMSAs), Stat5a and Stat5b were identified as the nuclear proteins that bind the ALS-GAS1 element after GH stimulation (Ooi *et al.* 1998).

GH regulation of IGF-I and ALS via Stat5b has been confirmed in vivo. In hypophysectomized rats infected with a control adenovirus, GH increased hepatic expression of IGF-I and ALS mRNA while infection with dominant-negative Stat5b adenovirus blocked IGF-I and ALS gene transcription. In contrast, a constitutively-active Stat5b adenovirus stimulated IGF-I and ALS expression even in the absence of GH (Woelfle & Rotwein 2004). These data illustrate that Stat5b is both necessary and sufficient for GH-induced expression of IGF-I and ALS in liver.

FUNCTIONAL ROLE OF THE GH-IGF SYSTEM

The importance of GH and IGF-I in growth, metabolism, and development has been demonstrated using various genetically engineered mouse models. Complete knockouts have provided significant insight into the role of the various components of the GH-IGF system. More sophisticated methods of gene ablation (i.e. temporally or spatially specific) have allowed for further dissection of the roles of Stat5 and IGF-I. In the next section, I will discuss the information obtained from genetically modified mouse models with respect to the role of the GH-IGF system in postnatal growth, carbohydrate metabolism, and mammary gland development.

Postnatal growth

GH receptor knockout models

The ability of the liver to respond to GH coincides with induction of hepatic GH receptor expression around 3 weeks of age in rodents. Mice that have low

circulating GH or carry mutations in the GHR are normal weight at birth but exhibit growth retardation by 3 weeks of age (Le Roith *et al.* 2001).

Null GHR model

The GHR gene was disrupted by inserting a neomycin cassette to replace the 3' end of exon 4 and a portion of intron 4/5. Exon 4 encodes part of the GH binding domain (Zhou *et al.* 1997). Body weight was similar between null GHR and wild type (WT) animals at birth, but by 4 weeks of age, null GHR weighed 45% less than WT mice. At 10 weeks of age, null GHR weighed 55% less than WT mice, and this difference was maintained through 1 year of age (Kopchick & Laron 1999). Body length and organ weights were decreased in null GHR mice. Lastly, circulating IGF-I concentration was decreased ~90% (Zhou *et al.* 1997). As described in the GHR signaling section, GH can signal through 3 distinct pathways. Thus, inactivation of the GHR eliminates all downstream receptor signaling, making it difficult to identify pathways that are critical for postnatal growth.

Knock-in GHR models

Previous studies have mapped the intracellular domains of the GHR necessary for ERK and Stat5 activation. ERK activation requires the proximal JAK2 activation domain which extends to approximately residue 391 of the GHR (Carter-Su *et al.* 2000). Stat5 signaling has been proposed to originate at Y498 and sites just proximal (Smit *et al.* 1996) or at sites distal to Y539 of the mouse GHR (Hansen *et al.* 1996). To elucidate the contribution of the various signaling pathways on postnatal growth and hepatic gene expression, Waters and coworkers (Rowland *et al.* 2005b; Rowland *et al.* 2005a) created knock-in models progressively deleting the intracellular domains of GHR.

In the knock-in 569 mutant, the GHR was truncated at proline 569 in combination with mutation of tyrosines 539 and 545 to phenylalanine (Rowland *et al.*

2005b). JAK2 and ERK activation were normal in the 569 mutants while Stat5 activation was reduced to 30% of WT. Postnatal growth rate was decreased 25% in both male and female 569 mutants. Knock-in 569 mice had reduced hepatic expression of IGF-I and ALS (65% and 55% of WT, respectively) and reduced plasma IGF-I (20% of WT) (Rowland *et al.* 2005b).

In the knock-in 391 mutant, GHR was truncated at lysine 391 (Rowland *et al.* 2005b). JAK2 and ERK activation were normal in the 391 mutants while Stat5 activation was undetectable. Postnatal growth rate was decreased 50% and 40% in male and female 391 mutants, respectively. These reductions were less than observed in the null GHR mice (58% and 50% reduction in males and females, respectively). Hepatic IGF-I and ALS expression was decreased to less than 10% of WT for both genes, whereas circulating IGF-I was less than 10%. These results suggest that the growth promoting effects of GH depends primarily on Stat5 signaling while ERK plays a lesser role.

Stat5 mutant models

Upon initiation of the work described in this dissertation, three null Stat5 were described, null Stat5a, null Stat5b, and what was thought to be null Stat5a/b. A number of tissue-specific knockouts have been described since. These models have been created to dissect the functions of Stat5a and Stat5b. Models relevant to growth will be discussed in the following section.

Null Stat5 models

Targeted disruption of the Stat5a gene was achieved by replacing the promoter sequence, the first non-coding exon, and the first two protein coding exons with a neomyocin cassette (Liu *et al.* 1997). Offspring from heterozygous crosses segregated in the expected ratio of 1:2:1. Homozygous Stat5a deficient mice appeared to develop

normally and were similar to heterozygous or WT animals with respect to size, activity, and fertility.

The Stat5b gene was disrupted by inserting a neomycin cassette at a *Bam*HI site that disrupts the codon for amino acid 181 (Udy *et al.* 1997). Null Stat5b pups were normal size at birth, but by 4-5 weeks of age, body weight gain was reduced 27% in male but not female mice. The growth curves of null Stat5b males overlapped with those of WT and null Stat5b females. Circulating GH was elevated in 3 of 6 male mutant mice with no changes observed in female mice. Plasma IGF-I was decreased 30% in mutant mice, irrespective of sex (Udy *et al.* 1997). Overall, data in Stat5a and Stat5b null mice suggest that GH-stimulated postnatal growth is mediated through Stat5b.

Stat5b is the major mediator responsible for the effects of pulsatile GH secretion on sexually dimorphic growth and hepatic gene expression. Male mice grow at a faster rate than females, and many hepatic genes are regulated in a sex-specific pattern (Davey *et al.* 1999). In the mouse, this sexual dimorphism is regulated, in part, by the pattern of GH secretion (Gatford *et al.* 1998). The male plasma GH pattern is characterized by discrete pulses separated by interpulses lasting at least one hour when no hormone is present. In contrast, GH secretion is more continuous in the female mouse, consisting of frequent pulses with higher interpulse concentrations (MacLeod *et al.* 1991). This profile of GH secretion also results in a sexually dimorphic pattern of hepatic Stat5 activation (Davey *et al.* 1999). In the liver, the male pattern of GH secretion stimulates phosphorylation of Stat5b resulting in expression of male-specific genes while the female pattern of secretion results in near absence of Stat5b activation (Waxman *et al.* 1995; Gebert *et al.* 1999). Consistent with that, loss of Stat5b resulted in changes in GH-regulated sexually dimorphic gene expression in the liver such that hepatic expression patterns in male null Stat5b mice were comparable to those in WT

females (Udy *et al.* 1997). These data are also consistent with absence of Stat5b having a greater impact on male than female growth.

Hypomorphic Stat5 models

In 1998, Ihle and co-workers (Teglund *et al.* 1998) attempted to knock out both *Stat5a* and *Stat5b* by inserting neomyocin- and hygromyocin cassettes into the first coding exon of the respective genes. These mice were believed to be true knockouts, but it has since been established that this particular model expresses N-terminally deleted Stat5a and 5b proteins ($Stat5a^{\Delta N}$ and $Stat5b^{\Delta N}$). The corresponding mRNAs retain in-frame start codons at amino acid position 103 or 137, with the ATG at position 137 predominantly used (Kornfeld *et al.* 2008). Despite expression of N-truncated proteins, the growth phenotype of the individual $Stat5a^{\Delta N}$ and $Stat5b^{\Delta N}$ mutant models was essentially the same as the complete Stat5a and Stat5b mutant models described above (Liu *et al.* 1997; Udy *et al.* 1997; Teglund *et al.* 1998). $Stat5a^{\Delta N}$ and $Stat5b^{\Delta N}$ mutants were combined to create $Stat5^{\Delta N}$ mice. Mice were observed at the expected Mendelian frequency; however, one-third of the mutant pups died within 48 hours of birth. Male and female $Stat5^{\Delta N}$ mice weigh 30-40% and 20-30% less than their WT littermates and experience a significant decline in circulating IGF-I.

Recently Engblom *et al.* (2007) have shown that the transcriptional activity of Stat5 proteins in liver requires an interaction between Stat5 and the glucocorticoid receptor (GR). Upon GH treatment, $Stat5b^{\Delta N}$ binds its binding sites on the IGF-I and ALS genes, but its ability to induce transcription is reduced (Engblom *et al.* 2007). ChIP assays demonstrate that the $Stat5^{\Delta N}$ protein is able to bind target DNA. The $Stat5^{\Delta N}$ protein, however, does not associate with the GR as WT Stat5 does, which indicates that the N-terminal domain of Stat5 serves as a docking platform for GR

(Engblom *et al.* 2007). In summary, Stat5b interacts with its transcription cofactor, the glucocorticoid receptor, to activate a subset of genes that regulate growth.

Conditional Stat5 models

Presence of the Stat5a and Stat5b next to each other on chromosome 11 made it possible to ablate simultaneously both genes by inserting lox-P sites on either side of the 110 kb Stat5 locus. Heterozygous Stat5 null mice were produced by crossing Stat5 floxed females with a transgenic mouse line expressing a specific Cre transgene activated by mouse mammary tumor virus (MMTV) which resulted in Cre-mediated recombination in the germ cells (Cui *et al.* 2004). Offspring from heterozygous Stat5 crosses were examined at weaning, and only 0.5% of the weaned pups were null Stat5 as compared to the expected 25%. To determine when the lethality occurred, offspring were genotyped at E18.5 and within 12h of birth. At E18.5 the expected 25% of null Stat5 embryos were genotyped, but only 3.75% were still present within 12 hours of birth. The hematocrit of null E18.5 fetuses is significantly lower than their WT counterparts, suggesting that perinatal lethality is caused by severe anemia (Cui *et al.* 2004).

Two liver specific Stat5 null lines have been created. The first line used a Cre transgene activated by the albumin promoter ($Stat5^{AlbCre}$) (Holloway *et al.* 2007) while the second line used a Cre transgene under the control of the albumin promoter and α-fetoprotein enhancer ($Stat5^{AlfpCre}$) (Engblom *et al.* 2007). In contrast to the global Stat5 knockout, $Stat5^{AlbCre}$ mice are viable and fertile. Interestingly, $Stat5^{AlbCre}$ mice grew at the same rate as their WT counterparts despite a 50% decrease in circulating IGF-I. Alterations in expression of sexually dimorphic genes were also observed in the $Stat5^{AlbCre}$ mice, with knockout males displaying a hepatic gene profile similar to that of females (Holloway *et al.* 2007).

In contrast to the Stat5^{AlbCre} mice, growth retardation was evident at 3 weeks of age in the Stat5^{AlfpCre} mice (Engblom *et al.* 2007). The differences observed in postnatal growth between the two lines probably can be explained by the different promoters used to induce Cre expression. The albumin Cre promoter is only fully active after puberty, likely resulting in adequate Stat5 proteins in Stat5^{AlbCre} mice until postnatal growth is mostly complete. In contrast, the Alfp promoter is active perinatally leading to immediate Stat5 ablation

Muscle specific null Stat5 (Stat5^{Myf5Cre}) lines were created by crossing floxed Stat5 mice with mice expressing the Cre gene driven by the myogenic factor 5 promoter. At 8 weeks of age, female and male Stat5^{Myf5Cre} suffer a 12% and 20% decline in body weight, respectively, as compared to their WT counterparts. X-ray analysis reveals that Stat5^{Myf5Cre} mice have smaller skeletons. When corrected for total body weight, percent lean and percent fat mass were similar in WT and Stat5^{Myf5Cre} mice. Muscle IGF-I mRNA and circulating IGF-I were decreased 60% and 15%, respectively, in Stat5^{Myf5Cre} mice while GH levels were unchanged.

IGF-I and ALS mutant models

GH effects on the IGF system are mediated predominantly via Stat5 regulation of IGF-I and ALS (Woelfle & Rotwein 2004). The growth phenotypes observed in GHR and Stat5 mutant models could be attributed, at least in part, to down-regulation of IGF-I and ALS. Therefore, the effects of IGF-I and ALS mutations on postnatal growth are described below.

Null IGF-I models

Various null IGF-I models have been developed using distinct gene targeting techniques (Baker *et al.* 1993; Liu *et al.* 1993; Powell-Braxton *et al.* 1993). The growth phenotypes are similar among these different models (Liu *et al.* 2000a). Null IGF-I mice are 40% smaller at birth, and most die soon after birth. A significant

number of mutants do survive in a mixed background of MF1 and 129/sv, and these, at maturity, weigh only 30% of WT animals (Liu *et al.* 1998). Global IGF-I knockouts, however, are inadequate to assess the relative role of endocrine vs. autocrine/paracrine IGF-I on growth.

Conditional IGF-I and ALS mutant models

To ascertain the role of endocrine IGF-I in postnatal growth, mice lacking IGF-I specifically in the liver [LID (liver IGF-I deficient)] were created. Two liver deficient models with similar phenotypes were created independently (Yakar *et al.* 1999; Sjogren *et al.* 1999). In one model, exon 4 of the IGF-I genes was flanked by loxP sites, and floxed animals were crossed with mice carrying Cre-recombinase regulated by the albumin promoter (Yakar *et al.* 1999). In the second model, the floxed IGF-I mice were crossed with a Cre line driven by an inducible interferon promoter which eliminated IGF-I expression in both liver and spleen (Sjogren *et al.* 1999). Despite a 70% decrease in circulating IGF-I, LID mice did not display a growth phenotype. LID mice also have significantly elevated levels of GH due to lack of negative feedback by circulating IGF-I (Yakar *et al.* 1999).

For several years, these results led researchers to believe that endocrine IGF-I did not play a role in postnatal growth. It has now been established that significant levels of circulating IGF-I are present in younger LID mice as the albumin promoter is not fully activated until ~4 weeks of age (Tang *et al.* 2005). Using an alternative approach, rat IGF-I was expressed specifically in the liver of null IGF-I mice. In this model, endocrine IGF-I was able to completely restore postnatal growth in null IGF-I mice which again suggests that endocrine IGF-I does indeed play a critical role in postnatal growth (Wu *et al.* 2008).

Targeted deletion of the ALS gene in mice was achieved by replacing the coding regions of exon 1, intron 1, and ~1300 bp of exon 2 with a neomycin cassette

(Ueki *et al.* 2000). Mice lacking the ALS gene (ALSKO) suffered a 13-20% growth deficit. In null ALS animals, circulating IGF-I and IGFBP-3 were decreased by 67% and 90%, respectively (Ueki *et al.* 2000). These changes were attributed to increase plasma turnover as hepatic mRNA levels of IGF-I and IGFBP-3 were unchanged.

When the liver deficient IGF-I model was crossed with the ALSKO model (LID+ALSKO), IGF-I levels were reduced more than 80%, and postnatal growth was decreased by 30% (Yakar *et al.* 2002). The exact contribution of endocrine IGF to postnatal growth remains unknown, but it appears that a threshold level of circulating IGF-I is required.

Differences in postnatal growth are quantified in a variety of ways. Growth may reflect changes in body weight, body composition, or bone length. GH and IGF-I are important regulators of bone growth and remodeling throughout life (Giustina *et al.* 2008). GH can act directly on bone cells to stimulate proliferation in the growth plate, or it can act indirectly via upregulation of IGF-I expression in liver and bone (Ohlsson *et al.* 2000). Local effects of IGF-I can also be independent of GH, and these effects are responsible for stimulation of osteoblasts and bone formation (Giustina *et al.* 2008). The role of endocrine IGF-I in bone growth and remodeling has been evaluated in the LID, ALSKO, and LID+ALSKO models. Femoral bone length was significantly shorter in these three models as compared to controls. Mutant mice also suffered reduced bone mineral density and bone volume. Exogenous IGF-I treatment was able to increase femoral length and restore the height of the growth plate in each of the three models (Yakar *et al.* 2002). Thus, endocrine IGF-I is essential for normal bone growth.

Carbohydrate Metabolism

GH models

Growth hormone is an important modulator of insulin sensitivity. GH stimulates pancreatic cell growth and insulin production and secretion (Liu *et al.* 2004). GHR mutant mice have increased insulin sensitivity while transgenic mice overexpressing GH are hyperinsulinemic and insulin resistant. In null GHR mice, blood glucose and serum insulin concentrations are decreased 40% and 80%, respectively, suggesting a state of hypersensitivity to insulin (Dominici *et al.* 2000). Evaluation of the insulin signaling pathway showed that liver insulin receptor (IR) concentrations are increased along with increased IR phosphorylation in null GHR mice. Despite low serum insulin concentrations, activation of the downstream IR signaling cascade (i.e. phosphorylation of IRS-1 and Shc and activation of PI3K) was similar to WT controls (Dominici *et al.* 2000). The observed hypoinsulinemia in null GHR mice is a consequence of altered pancreatic islet structure and function (Liu *et al.* 2004). Decreased cell proliferation and cell growth are responsible for the reduction in pancreatic cell mass in null GHR mice. Furthermore, pancreatic insulin mRNA expression was reduced, leading to decreased insulin production.

As expected, elevated GH levels yield the opposite effect on indices of carbohydrate metabolism. In transgenic mice over-expressing bovine growth hormone (bGH-TG), plasma insulin levels were increased nearly 5-fold while plasma glucose was normal (Dominici *et al.* 1999a). Insulin receptor concentration was decreased while IR, IRS-1, and PI3K activity were maximally stimulated under basal conditions in both liver and muscle of bGH-TG mice. Exogenous insulin treatment increased IR and IRS-I phosphorylation and PI3K activity in liver and muscle of WT mice while no additional stimulation was observed in bGH-TG (Dominici *et al.* 1999b; Dominici *et al.* 1999a). Thus, the bGH-TG mice were insensitive to insulin treatment.

IGF-I and ALS models

Carbohydrate metabolism has been studied in the LID mice. In this model, the lack of negative feedback by circulating IGF-I increased circulating GH concentrations from 2.8 to 17.8 ng/mL in LID mice (Yakar *et al.* 2001). Insulin levels were increased 4-fold, and LID mice were less sensitive to exogenous insulin. In LID mice, insulin-stimulated IR and IRS-1 phosphorylation was normal in liver and adipose tissue but impaired in muscle. Thus, the insulin insensitivity in LID mice is muscle specific. Treatment of LID mice with exogenous IGF-I reduced plasma GH and improved insulin sensitivity (Yakar *et al.* 2001).

To determine if this improvement was due to increased IGF-I or reduced GH, LID mice were crossed with GH-antagonist (GHa) transgenic mice (Yakar *et al.* 2004). GHa mice were generated by introducing a point mutation in the GH gene which prevents proper dimerization of the GHR, blocking GH action (Chen *et al.* 1991). When insulin sensitivity was evaluated using the hyperinsulinemic-euglycemic clamp technique, LID mice exhibited impaired insulin sensitivity in muscle, liver, and adipose tissue. Insulin sensitivity was improved in LID+GHa mice, suggesting that elevated GH levels are the major cause of insulin resistance in LID mice (Yakar *et al.* 2004).

Insulin sensitivity is also dependent on IGF-I availability. When LID mice are crossed with the ALSKO mice (LID+ALSKO), circulating IGF-I concentrations are reduced to only ~15% of WT, and GH levels increase above those seen in LID mice (Haluzik *et al.* 2003). Yet, LID+ALSKO mice have improved whole body insulin responsiveness (Haluzik *et al.* 2003). In this case, improved insulin action was caused by an increase in plasma concentration of free IGF-I, a potent insulin sensitizer in skeletal muscle and adipose tissue.

Recent studies have identified a mechanism involving PI3K whereby GH antagonizes insulin signaling. PI3K is a heterodimer composed of the p85 subunit and the catalytic subunit p110. The p85 subunit serves two functions. First, it provides a binding domain for IRS proteins, and second, it regulates the activity of the p110 catalytic subunit (Dominici *et al.* 2005). Increased expression of p85α increases the pool of free p85α which competes with the p85-p110 heterodimer for binding sites on IRS-1. As a result, PI3K activity decreases when free p85α is in excess (Biddinger & Kahn 2006). Excess GH induced p85α expression in skeletal muscle. Muscle p85α mRNA was increased in skeletal muscle of LID mice, but normalized when LID mice were treated with a GH antagonist. Moreover, GH was unable to induce insulin resistance in p85α heterozygous mice (Barbour *et al.* 2005).

A similar mechanism of GH induced insulin resistance has been demonstrated in white adipose tissue (WAT). Chronic GH over-expression increased p85α mRNA and protein expression in WAT while p85α mRNA was decreased in GH-deficient *lit/lit* mice. Furthermore, PI3K activity was decreased when GH is in excess and increased when GH is deficient (Del Rincon *et al.* 2007). These results suggest that one mechanism whereby GH induces insulin resistance in skeletal muscle and WAT is by increasing the amount of free p85α monomers, which in turn, leads to reduced PI3K activity.

Stat5 models

GH is required for β-cell proliferation and stimulation of insulin expression and secretion (Liu *et al.* 2004). The Stat5 proteins are activated by GH in insulin-producing INS-1 cells and in cultured rat islets (Friedrichsen *et al.* 2001). These observations suggest that some of the effects of GH on insulin secretion are mediated via Stat5.

In mice lacking hepatic Stat5 ($Stat5^{AlbCre}$), plasma IGF-I was reduced by 50%, and GH levels were significantly elevated. In 10 week old $Stat5^{AlbCre}$ mice, the levels of glucose, triglycerides and free fatty acids (FFA) were similar to WT, but insulin levels were significantly elevated (Cui *et al.* 2007). Glucose clearance was impaired and insulin sensitivity was reduced in $Stat5^{AlbCre}$ mice. By 17 months of age, serum glucose, insulin, and triglyceride levels were all increased in $Stat5^{AlbCre}$ mice. Furthermore, mutant mice were glucose intolerant and were severely insulin resistant (Cui *et al.* 2007).

Carbohydrate metabolism also was examined in mice lacking Stat5 in muscle ($Stat5^{Myf5Cre}$). In contrast to the hepatic Stat5 mutant, GH levels were not increased in $Stat5^{Myf5Cre}$ mice (Klover & Hennighausen 2007). Moreover, serum glucose, insulin and FFA were not different between $Stat5^{Myf5Cre}$ mice and controls, but triglyceride levels were significantly elevated. Glucose clearance was impaired in $Stat5^{Myf5Cre}$ mice while insulin sensitivity was maintained (Klover & Hennighausen 2007).

Pancreatic specific null Stat5 mice ($Stat5^{Pdx1Cre}$) were created by crossing floxed Stat5 mice with mice expressing Cre driven by the pancreatic and duodenal homeobox 1 (Pdx1) promoter (Lee *et al.* 2007). $Stat5^{Pdx1Cre}$ mice are the same size as WT mice and have normal pancreatic development. Glucose homeostasis was evaluated over a 15 month period in WT and mutant mice. Circulating insulin, glucose, and glucagon were similar between WT and $Stat5^{Pdx1Cre}$ mice as was pancreatic insulin mRNA and protein expression. Mild glucose intolerance was observed in aged or pregnant $Stat5^{Pdx1Cre}$ mice (Lee *et al.* 2007). These results demonstrate that Stat5 is not required for pancreatic development but may be necessary when β-cell proliferation is needed to maintain glucose homeostasis.

Mammary gland development

The mammary gland undergoes extensive morphological and biochemical changes during postnatal life. These changes are specific to the virgin state, pregnancy, lactation, and involution. During the first phase, the ducts elongate to fill the mammary fat pad (Hovey *et al.* 2002). Development during pregnancy is characterized by further branching of the ducts and alveolar differentiation. During lactation, the alveoli expand to completely fill the gland, and active milk secretion is established (Brisken 2002). Upon weaning, the lactating gland undergoes involution whereby remodeling returns the gland to its pre-pregnancy state (Lamote *et al.* 2004). These dynamic changes are under strict hormonal control by various steroid and peptide hormones (Richert *et al.* 2000). In the next few pages, I will discuss changes during each phase with a focus on the roles played by the GH-IGF-I system.

Virgin State

At birth, the mammary gland consists only of a few rudimentary ducts. The rudimentary ductal structure remains inactive until approximately 3 weeks of age when the ovaries begin secreting estrogen (Hovey *et al.* 2002). The growing ducts of the pubertal animal have club-shaped structures at their tips, called terminal end buds (TEBs). They are composed of two cell types: the outer cap cells that give rise to basal cells and the body cells that give rise to luminal cells (Howlin *et al.* 2006). The TEBs are the primary epithelial structures and are the sites of ductal elongation and branching in the mammary gland. At regular intervals, some TEBs invaginate to form two TEBs, both of which continue to grow, forming a branched structure. This continues until the entire fat pad is filled with a simple ductal tree (Brisken 2002).

The GH-IGF-I axis plays a critical role in mammary ductal elongation (Kleinberg 1997; Kleinberg *et al.* 2000; Hadsell *et al.* 2002). GHR is expressed in the stromal compartment of the mammary gland. In the pubertal, virgin animal, IGF-I,

and IGF-IR expression is detected in the TEBs, and IGF-I is also expressed in the stroma surrounding the TEBs (Richert & Wood 1999). In post pubertal mice, IGF-IR mRNA was also detected in the ductal epithelial cells. IGFBP-3 and -5 are expressed in the TEBs and ductal epithelium (Wood *et al.* 2000).

GH binds GHR in the stromal compartment of the mammary gland, upregulating IGF-I expression. IGF-I then binds to its receptor on epithelial cells to promote ductal development and TEB formation (Kleinberg *et al.* 2000). Ruan and colleagues (Ruan *et al.* 1992) demonstrated that IGF-I can substitute for GH mediated mammary gland development in hypophysectomized rats. Consistent with these data, null GHR mice have impaired ductal outgrowth and limited side-branching (Gallego *et al.* 2001).

In mice lacking either IGF-I or IGF-IR, TEB formation and ductal growth was diminished as a result of decreased cellular proliferation (Ruan & Kleinberg 1999; Bonnette & Hadsell 2001). Administration of a GH antagonist decreased hepatic mRNA expression and circulating IGF-I levels in virgin female mice and delayed mammary ductal growth. This delay was associated with a decrease in TEB numbers and reduced branching of the ductal tree (Divisova *et al.* 2006). Taken together, these data suggest that GH acts indirectly on the mammary gland by upregulating local IGF-I expression. In addition, estrogen enhances both GH-induced expression of IGF-I mRNA in the mammary stroma and the stimulatory effect of IGF-I on mammary development (Ruan *et al.* 1995).

Pregnancy and lactation

Massive proliferation of ductal branches and formation of alveolar buds occur in early pregnancy (Brisken 2002). During the second half of pregnancy, alveolar buds expand into alveoli which progressively differentiate into milk secreting structures (Brisken & Rajaram 2006). By early lactation, over 70% of the gland is

occupied by the secreting epithelium, leaving ~30% of the gland occupied by adipocytes. Once lactation is established, the alveoli expand to completely fill the gland (Richert *et al.* 2000).

The precise roles of GH and the IGF-I system in regulating mammary development during pregnancy and lactation are largely unknown. In mid-pregnancy, IGF-I mRNA expression is detected in the stromal cells immediately surrounding the ducts. In late pregnancy, IGF-I and IGF-IR mRNA are widely expressed in ductal and alveolar epithelium (Richert & Wood 1999). During pregnancy, IGFBP-3 expression is detected in the outer layer of epithelial cells and decreases during lactation. IGFBP-5 expression is detected in the stromal compartment surrounding the primary ductal tree and lobulo-alveolar structures during pregnancy. Expression decreases by lactation d2 and remains low during lactation (Allar & Wood 2004).

Reduced stromal IGF-I impaired alveolar bud development in early pregnancy (Loladze *et al.* 2006). By mid-pregnancy, the mammary gland had a hyperplastic phenotype characterized by alveoli lacking a defined lumen and increased nuclei per alveolus Reduced epithelial expression of IGF-I mRNA in late pregnancy had little effect on mammary development (Loladze *et al.* 2006).

Stat5 proteins are critical for mammary development during pregnancy. Both GH and prolactin activate Stat5 in the mammary gland (Gallego *et al.* 2001). Null Stat5a females were fertile and gave birth to live pups, but they were unable to nurse their young (Liu *et al.* 1997). Further investigation of mammary development revealed that mutant females failed to develop lobulo-alveolar structures, and expression of the milk proteins α-lactalbumin and whey acid protein (WAP) was decreased (Liu *et al.* 1997; Teglund *et al.* 1998). Interestingly, Stat5b protein levels were decreased in null Stat5a mice and were unable to compensate for the loss of Stat5a (Liu *et al.* 1997).

Null Stat5b mice consistently aborted between d8 – d17 of pregnancy. Administration of progesterone maintained pregnancy in null Stat5b females, but nevertheless, they appeared to have impaired mammary gland development because dams were unable to successfully nurse their pups (Udy *et al.* 1997). Female $Stat5^{\Delta N}$ mice had impaired corpora lutea development and were infertile. As a result of the infertility, mammary gland development during pregnancy and lactation could not be evaluated (Teglund *et al.* 1998).

Mammary specific deletion of both Stat5a and 5b was performed using two different Cre systems. In the first case, mammary Stat5 expression was ablated before pregnancy by stimulating mammary Cre expression with the MMTV promoter (Cui *et al.* 2004). All dams were unable to nurse their pups. Loss of Stat5 did not affect ductal outgrowth or primary and secondary branching. However, lobulo-alveolar structures failed to form, demonstrating that proliferation of mammary secretory epithelium requires Stat5 (Cui *et al.* 2004).

To determine whether Stat5 was necessary for the survival of the fully differentiated mammary epithelium, Stat5 was eliminated in the mammary during late pregnancy after lobulo-alveolar development occurred, using Cre driven by a WAP promoter ($Stat5^{WAPCre}$). These dams were able to nurse their litters, but histological evaluation of the glands revealed decreased alveolar density. Those mammary epithelial cells that lacked Stat5 de-differentiated and were eliminated via apoptosis (Cui *et al.* 2004).

Involution

Removal of milk from the mammary gland is necessary for the maintenance of lactation (Stein *et al.* 2007). Therefore, the lactating gland involutes to its pre-pregnancy form upon weaning. The process of involution involves apoptosis of the mammary epithelial cells and structural remodeling of the gland (Lamote *et al.* 2004).

In rodents, this stage is typically studied using forced weaning, where the dam is allowed to lactate for 8-12 days and then the pups are removed (Richert *et al.* 2000). The first phase of involution is characterized by an accumulation of milk in alveoli and minimal cell death. During this early stage, involution is reversible and lactation can be re-established if pups are returned within 2 days of removal (Lamote *et al.* 2004). As involution proceeds, the epithelial cells of the alveoli undergo apoptosis. By day 4 of involution, the alveoli begin to collapse, the basement membrane is degraded, and macrophages invade. By this time, fat-filled adipocytes reappear. By d21, the gland has returned to its pre-pregnancy state (Richert *et al.* 2000).

Involution is thought to be facilitated by attenuation of IGF-I signaling. This attenuation appears to be dependent on the induction of mammary IGFBP-5 synthesis. On day 2 of involution, IGFBP-5 concentration in milk increased 50-fold in the rat (Tonner *et al.* 1997). In primary mammary epithelial cultures, IGFBP-5 inhibited IGF-I mediated cell proliferation (Marshman *et al.* 2003). Similar results were obtained in vivo using a transgenic mouse model that overexpressed IGFBP-5 specifically in the mammary (Tonner *et al.* 2002). During the first 10 days of lactation, mammary cell number and milk synthesis were both decreased, and mammary cell proliferation was impaired. The concentration of pro-apoptotic factors, caspase-3 and plasmin, increased while pro-survival factors, Bcl-2 and Bcl-$_{XL}$, decreased. Mammary development was rescued when animals were treated with a form of IGF-I that has low affinity for IGFBP-5 (Tonner *et al.* 2002). Finally, involution was evaluated in null IGFBP-5 mice. In this model, involution was delayed after forced weaning. Appearance of apoptotic cells and the reappearance of adipocytes were both retarded in mutant mice (Ning *et al.* 2007). Reciprocally, overexpression of IGF-I in the mammary glands of lactating mice delayed the involution process (Neuenschwander *et al.* 1996).

SUMMARY

The functional importance of the GH-IGF-I system on postnatal growth, carbohydrate metabolism, and mammary development has been reviewed above. GH can act directly on target tissues, or it can act indirectly by stimulating IGF-I production. The IGF-I mediating effects can arise locally or can be produced in the liver. Effects of GH are mediated through the GH receptor. Binding of GH to its receptor leads to activation of JAK2. This is followed by JAK2 dependent activation of various signaling cascades (Lanning & Carter-Su 2006). The downstream mediation of the growth promoting effects of GH have been attributed predominantly to the Stat5a and 5b proteins (Waters *et al.* 2006).

Genetic mouse models have been created in which each individual Stat5 gene is ablated (Liu *et al.* 1997; Udy *et al.* 1997). These models show that Stat5a is absolutely required for proper mammary gland development during late pregnancy and lactation, but Stat5a appears to play no role in regulation of growth (Liu *et al.* 1997). On the other hand, Stat5b plays important roles in regulating sexually dimorphic growth rates and male specific hepatic gene expression (Udy *et al.* 1997). Stat5b has also been shown to mediate the positive effects of GH on hepatic production of major components of the circulating IGF-I system, namely, IGF-I and ALS (Woelfle & Rotwein 2004). So far, no studies have ever directly assessed whether growth effects of exogenous GH were also lost in Stat5 deficient mice. Chronic administration of GH has been used to evaluate the responsiveness of various GH/IGF-I mutant models to exogenous GH (Liu & LeRoith 1999; Liu *et al.* 2000b; Fielder *et al.* 1996). Therefore, the objective of Chapter 3 was to test whether exogenous GH could stimulate not only overall growth of $Stat5^{\Delta N}$ mice but also other GH-dependent responses such as organ growth and insulin resistance.

In the case of most tissues, IGF-I remains near its cellular site of production and represents the autocrine/paracrine arm of the IGF-I system (Le Roith *et al.* 2001). These IGF-I molecules are usually bound to one of six IGF binding proteins (Jones & Clemmons 1995; Stewart & Rotwein 1996). Liver-derived IGF-I, on the other hand, is secreted in plasma and represents the endocrine arm of the IGF-I system. In postnatal animals, circulating IGF-I is bound in a 150 kDa ternary complex composed of one molecule each of IGF-I, IGFBP-3 or -5, and ALS (Baxter 1988; Twigg & Baxter 1998).

ALS is thought to function exclusively as a component of the circulating IGF-I system. It is responsible for formation of ternary complexes in circulation, building a reservoir of circulating IGF-I, and preventing its insulin-like effects (Zapf *et al.* 1995). Characterization of the null ALS mutant revealed a functional role for ALS in postnatal growth and metabolism (Ueki *et al.* 2000; Haluzik *et al.* 2003), but the role of ALS in mammary gland development has not been studied.

The mammary gland undergoes extensive morphological and biochemical changes during postnatal life. These dynamic changes are under strict hormonal control by sex steroid hormones and various growth factors (Richert *et al.* 2000). GH, IGF-I, and IGFBPs play critical roles during all phases of postnatal mammary gland development. GH-induced expression of IGF-I in the mammary fat pad stimulates ductal elongation in the virgin state (Walden *et al.* 1998). IGF-I is also important in early pregnancy, promoting proliferation of ductal branches and formation of alveolar buds (Loladze *et al.* 2006). Furthermore, involution is thought to be facilitated by attenuation of IGF-I signaling, and this attenuation appears to be dependent on the induction of mammary IGFBP-5 synthesis (Flint *et al.* 2003).

The only known function of ALS is to bind binary complexes of IGF-I and IGFBP-3 or -5 in plasma and to give rise to a substantial plasma IGF-I reservoir. IGF-

I, IGFBP-3, and -5 are expressed in the mammary gland, but whether ALS synthesis occurs remains unknown. Similarly, the possibility that ALS has a functional role on mammary gland development has not been examined. Therefore, the objective of Chapter 4 was to evaluate the role of ALS in mammary gland development using the null ALS mouse model.

CHAPTER THREE:

EFFECT OF CHRONIC GROWTH HORMONE TREATMENT IN STAT5$^{\Delta N}$ MICE

INTRODUCTION

Growth hormone (GH) plays an essential role in the promotion of growth, development, and metabolism during postnatal life (Le Roith *et al.* 2001). GH exerts these positive effects by acting directly on target tissues and indirectly by stimulating the synthesis of insulin-like growth factor (IGF-I) in liver and other tissues (Le Roith *et al.* 2001). Effects of GH are mediated through the growth hormone receptor (GHR). Binding of GH to its receptor leads to activation of Janus kinase 2 (JAK2). This is followed by JAK2 dependent activation of various signaling cascades (Lanning & Carter-Su 2006). The downstream mediation of the growth promoting effects of GH have been attributed predominantly to the signal transducers and activators of transcription (Stat) 5a and 5b proteins (Waters *et al.* 2006).

Null mutations for each of the Stat5 isoforms alone or in combination have been developed. The single mutant models have demonstrated that Stat5a is important in mammary development (Liu *et al.* 1997) while Stat5b is necessary for sexually dimorphic body growth rates and for male specific hepatic gene expression (Udy *et al.* 1997). Stat5b has also been shown to mediate the positive effects of GH on hepatic production of major components of the circulating IGF-I system, namely, IGF-I and ALS (Woelfle & Rotwein 2004). Moreover, plasma IGF-I concentrations are lower in mice lacking Stat5b (Udy *et al.* 1997). It is unknown to what extent extra-hepatic GH-stimulated IGF-I production also depends on this mechanism. It is also unknown whether other actions of GH, such as induction of insulin resistance, depend on the presence of Stat5.

Therefore, our aim was to test whether exogenous GH could stimulate growth, development, and insulin resistance in Stat5 mutant mice. For this study, we used the mouse model developed by Ihle and colleagues (Teglund *et al.* 1998), which combine hypomorphic mutations for both Stat5a and 5b ($Stat5^{\Delta N}$). $Stat5^{\Delta N}$ mice are viable after birth unlike mice missing both Stat5a and 5b. Moreover, $Stat5^{\Delta N}$ mice recapitulate the major defects seen in the mice harboring single null Stat5 mutations (i.e., impaired mammary development and growth) (Teglund *et al.* 1998).

MATERIALS AND METHODS

$Stat5^{\Delta N}$ mice and genotyping analysis

Experimental procedures involving live animals were conducted with the approval of the Cornell University Institutional Animal Care and Use committee. The facility was kept at constant temperature (~22°C) and humidity (~65%) with controlled lighting (14 h light/10 h dark cycle). All animals were offered water and fed a standard rodent chow (Harlan Tekland 8640 containing 22% protein, 5% fat, Harlan, Madison, WI) *ad libitum* unless otherwise noted. Mice that express N-terminally deleted Stat5a and Stat5b ($Stat5^{\Delta N}$) proteins were studied. Heterozygous breeding pairs were used to generate offspring for all experiments. This mating strategy was used because $Stat5^{\Delta N}$ mice are infertile (Teglund *et al.* 1998).

At weaning, tail biopsies were taken to determine genotypes. DNA was isolated using the HotSHOT method (Truett *et al.* 2000). Briefly, tail biopsies (~4 mm) were incubated at 95°C for 1 h in 100 μL hydrolysis solution (25 mM NaOH, 0.2 mM EDTA, pH 12). Samples were neutralized with an equal volume of 40 mM Tris-HCl, pH 5.0. Two μL of neutralized solution were amplified in a final volume of 20 μL containing 1X Taq PCR buffer (10 mM Tris-HCl, 50 mM KCl, 0.1% Triton x-100 and 1.2 mM $MgCl_2$), 0.2 mM dNTPs and 0.625 units of Taq polymerase (Promega, Madison, WI). The *Stat5a* and *Stat5b* genes are located adjacent to one another on

mouse chromosome 11, and the transcriptional start sites are located within 10 kb of each other (Hennighausen & Robinson 2008). Because of their close proximity, these genes behave as a single 110 kb locus, and thus a single PCR amplifying the *Stat5b* gene was performed. Primer sequences for the Stat5b locus were from Teglund et al. (1998). For genotyping, forward primers F-11 (5'- TCA AAC ACA CCT CAA TTA GTC C -3') and TKp (5'- GCA AAA CCA CAC TGC TCG AC -3') were used with the reverse primer R8 (5'- GGA GAT CTG CTG GCT GAA AG -3'). Final primer concentrations were 0.25 μM for each. The reaction was first denatured at 94°C for 10 minutes, followed by 29 cycles of 94°C for 1 minute, 55°C for 30 seconds, and 72°C for 1 minute with a 5 second extension per cycle. A last cycle was performed identically except that the 72°C step lasted 7 minutes. This combination of primers yielded bands of 321 bp for the wild type (WT) Stat5b allele and 132 bp for the $Stat5^{\Delta N}$ allele. Products were visualized by agarose gel electrophoresis.

GH activation of truncated Stat5

Wild type and $Stat5^{\Delta N}$ male mice (n=5 animals/genotype) were given a single intra-peritoneal injection of saline or recombinant bovine GH [GH, 4 μg/g body weight (BW)]. Mice were sacrificed 15 minutes later by carbon dioxide asphyxiation. Liver, gonadal fat pad, and gastrocnemius muscle were dissected and snap-frozen immediately in liquid nitrogen.

Western immunoblot analysis

Total cellular extracts were prepared by homogenizing tissues (100 mg liver and muscle, 200 mg adipose) in 1 mL lysis buffer (10 mM Tris, 1.0% Triton x-100, 150 mM NaCl, 1 mM EGTA, 1 mM sodium orthovanadate, 1 mM sodium pyrophosphate, 10 mM sodium fluoride, 10 μg/mL leupeptin, 1 mM phenyl methyl sulfonyl fluoride). Homogenates were clarified twice by centrifugation (10,000 g for 20 minutes at 4°C).

The protein content of the extracts was measured by the BCA protein assay (Pierce, Rockford, IL). Thirty-five μg of protein were electrophoresed on 10% sodium dodecyl sulphate (SDS) polyacrylamide gels and transferred overnight to nitrocellulose membranes (Schleider, and Schuell Inc., Keene, NH). The membranes were blocked for 1h at room temperature with Tris-buffered saline supplemented with Tween-20 (TBST, 0.05 M Tris pH 7.4, 0.2 M NaCl, 0.1% Tween-20) containing 5% w/v non fat dried skim milk. Membranes were incubated with primary antibodies specific for STAT5 phosphorylated on tyrosine 694 (pY^{694} STAT5, Cell Signaling Technology, Inc., Beverly, MA) and total Stat5 (Santa Cruz, Santa Cruz, CA). Primary antibodies were diluted in blocking solution (pSTAT5, 1:500 and total Stat5, 1:2000). Following incubation, membranes were washed five times (5 min each) in TBST, then incubated with HRP-conjugated goat-anti rabbit secondary antibody (KPL, Gaithersburg, MD) at a 1:5000 dilution in blocking solution for 1 h at room temperature. Signals were detected with LumiGlo chemiluminescence reagents (KPL) and autoradiography.

Chronic GH treatment of $Stat5^{\Delta N}$

A total of 29 WT and 31 $Stat5^{\Delta N}$ mice were studied. Mice were randomly allocated to receive twice daily subcutaneous injections of saline or recombinant bovine GH (GH, 3 μg/g BW/injection). Treatments started on postnatal day 35 and continued for 4 weeks. On a daily basis, animals were weighed and injected at 0900h and injected again at 2100h. On the last day of treatment, animals were injected at 0900h and food was removed. The animals were euthanized 4h later by carbon dioxide asphyxiation. Blood was collected immediately by cardiac puncture, and processed to plasma by the addition of heparin (60 U/ml). Nose to anus length was measured using digital calipers. Liver, kidney, spleen, gonadal fat pad, and gastrocnemius muscle were dissected, blotted dry, weighed, and snap-frozen

immediately in liquid nitrogen. Plasma and tissues were stored at –20°C and -80°C, respectively.

Analysis of IGF-I, insulin, and glucose in plasma

Plasma IGF-I concentrations were measured using a rat IGF-I double antibody radioimmunoassay (RIA) purchased from Beckman Coulter (Webster, Texas). Analysis was performed as recommended by the manufacturer using 25 μL plasma for acid-ethanol extraction. The range of the standard was 150-4500 ng/mL.

Plasma insulin concentrations were measured using a two-day disequilibrium rat insulin RIA (Sensitive Rat Insulin RIA kit, Linco Research, Inc., St. Louis, MO). The range of the standard was 0.02-1.0 ng/mL.

Plasma glucose concentrations were measured by the glucose oxidase method using reagents from Sigma (St. Louis, MO). The assay was performed in duplicate using 2 μL of plasma. Absorbance was read at 450 nm using a microplate reader (VERSAmax, Molecular Devices Corp., Sunnyvale, CA) driven by the SOFTmax PRO software (Molecular Devices).

Northern blot analysis

For Northern analysis, total RNA was extracted from liver by affinity chromatography according to manufacturer recommendations (RNeasy® Mini Kit, Qiagen Inc., Valencia, CA). The concentration of total RNA was determined by measuring absorbance at 260 nm, and RNA quality was assessed on formaldehyde agarose gels by staining with Sybr Green II stain (Molecular Probes, Eugene, OR).

Total RNA (10 μg) was electrophoresed on a 1% denaturing agarose gel containing 0.66 M formaldehyde, 1X MOPS (0.04 M 3-N-Morpholino-propanesulfonic acid, 0.05 M sodium acetate, 0.001 M EDTA, pH 8.0). Electrophoresis was performed for 2 h at 80 V in 1X MOPS. Total RNA was transferred onto a nylon membrane (GeneScreen™, NEN® Research Products) by

capillary transfer in 10X SSPE (1X SSPE = 0.18 M NaCl, 1 mM EDTA, pH 8.0; 1 mM sodium phosphate). Membranes were irradiated in a UV crosslinker at 120 mJ/cm^2, dried for 1 h at 60°C, and stored at -20°C until hybridization.

To detect ALS and IGF-I mRNA in liver, membranes were prehybridized at 50°C in a solution of 50% formamide/dextran sulfate, 5X SSPE, 10X Denhardt's [1X Denhardt's = 0.02% bovine serum albumin (BSA), 0.02% ficoll 400, 0.02% polyvinylpyrrolidone (MW 40,000)], 100 mg/ml salmon sperm DNA, and 1% SDS. The ALS probe used was a 750 bp DNA fragment corresponding to nt +163 to nt +915 of the mouse ALS cDNA (numbering relative to $A_{+1}TG$) (Ueki *et al.* 2000), and the IGF-I probe was a 406 bp fragment corresponding to nt -22 to +384 of the rat IGF-I DNA (numbering relative to $A_{+1}TG$). The probes were labeled with [α-^{32}P] dCTP (3000 Ci/mmol) by random priming (Prime-It, Stratagene, La Jolla, CA). After a 2 h prehybridization, the DNA probes (~1 x 10^6 dpm/ml) were added and the hybridization continued overnight. After hybridization, membranes were washed twice for 30 minutes in a solution of 2X SSPE/0.2% SDS at room temperature, and twice for 15 minutes in a solution of 0.1X SSPE at 60°C.

The 18S ribosomal RNA was detected with a low specificity labeled oligonucleotide (Deindl 2001). The oligo sequence is 5'-CGG AAC TAC GAC GGT ATC TG-3' and was labeled with [γ-^{32}P] dATP (3000 Ci/mmol) using T4 polynucleotide kinase (Promega, Madison, WI). Hybridizations were conducted at 42°C in a solution of 50% formamide/dextran sulfate, 5X SSPE, 10X Denhardt's, 1% SDS. Hybridizations were performed with the labeled probe (~2 x 10^6 dpm/ml) mixed with a 10-fold molar excess of unlabelled oligonucleotide. Membranes were washed three times each with 2X SSPE/0.2% SDS at 45°C.

For visualization of ALS, IGF-I, and 18S signals, membranes were exposed to x-ray film (Fuji Medical Systems USA, Inc., Stanford, CT). Signals were quantified

by phosphoimaging using a FUJIX BIO-IMAGING ANALYSER BAS1000 (Fuji Photo Film Co., Ltd.).

Real-time PCR Analysis

For real-time PCR assays, liver (20 mg), gonadal fat (150 mg), and gastrocnemius muscle (30 mg) were homogenized in 1 mL Qiazol reagent (Qiagen Inc., Valencia, CA). Total RNA was purified by affinity chromatography, combined with an on-column RNase-free DNase treatment (Qiagen). RNA concentration and quality were assessed by RNA Nano LabChip Kit (Agilent Technologies, Palo Alto, CA).

Real-time SYBR green PCR assays were used to measure transcript abundance of p85α regulatory subunit of phosphotidylinositol 3-kinase (PI3K) and 18S in liver using the primers listed in Table 3.1. Real-time SYBR green PCR was also used to measure IGF-I, PI3K, and 18S in gonadal fat pad and gastrocnemius muscle. Briefly, total RNA (2 μg) was reverse-transcribed in a 20 μL volume using the High Capacity cDNA Reverse Transcription Kit (Applied Biosystems, Foster City, CA) according to the manufacturer's recommendation. PCRs were performed in duplicate in a 25 μL volume using Power SYBR Mix (Applied Biosystems). Reactions contained 500 mM of each primer and diluted cDNA (25 ng except 2.5 ng for 18S). For each tissue, data were analyzed using a relative standard curve generated using serial two-fold dilutions of cDNA prepared and pooled for the respective tissue. Unknown sample expression was then determined from the standard curve. 18S expression was used as a covariate in the statistical analysis.

GH induced insulin resistance

To test whether Stat5 plays a role in GH induced insulin resistance, 18 week old WT and Stat5$^{\Delta N}$ male mice (n = 5-7 per genotype) were used in a cross-over design with 3.5 d periods separated by a 2 wk interval. Treatments were twice daily

Table 3.1. Real time PCR primers.

Gene[1]	Primer[2]	Sequence[3]
IGF-I	F	CAG TTC GTG TGT GGA CCG AG
	R	GCT CCG GAA GCA ACA CTC AT
PI3K	F	TCA TCA GTG TTG GCT TAC GCT
	R	TTG TTG GCT ACA GTA GTG GGC
18S	F	GTG GGC CTG CGG CTT AAT
	R	GCC AGA GTC TCG TTC GTT ATC

[1]Primers were designed to measure the abundance of the acid labile subunit (ALS), insulin-like growth factor I (IGF-I), the p85a regulatory subunit of phosphotidylinositol 3-kinase (PI3K), and 18S ribosomal RNA (18S)

[2]F, forward; R, reverse.

[3]Primer sequences are shown in the 5' to 3' orientation.

subcutaneous injections of saline or recombinant bovine GH (GH, 3 μg/g BW/injection). After the final injection at 0900h, feed was removed and an insulin tolerance test (ITT) was performed 6 h later. Blood samples were obtained by nicking the dorsal tail artery. The time 0 blood sample was taken followed by an intraperitoneal injection of human insulin (0.6 U/kg BW, Humulin® R, Eli Lilly and Company, Indianapolis, IN). Blood was collected 30, 60, and 90 min after insulin injection. Glucose measurements were performed with an Ascensia Contour glucometer (Bayer Health Care, Tarrytwon, NY).

The response area to insulin was calculated from the time of challenge to 90 min post-challenge. Response areas were calculated as percent drop from baseline (time 0 = 100%). Area under the response curve was calculated using cubic spline interpolation and the trapezoidal rule with the EXPAND procedure in SAS (SAS Institute, Cary NC).

Statistical analyses

Analyses were performed using SAS statistical software (SAS Institute, Cary, NC). For growth data (weight gain, lengths, and organ weights), data were separated by sex to avoid a 3-way interaction (sex x genotype x treatment). Data were analyzed using the MIXED procedure of SAS (SAS Institute) for body weight, length, and organ data. The model included fixed effects of covariate (initial body weight), genotype, treatment, and the interaction of genotype and treatment. For all other data, the model included genotype, treatment, and the interaction of genotype and treatment. For analysis of real-time PCR data, the 18S value was used as the covariate. For all analyses, the effect of genotype (Geno) was assessed by comparing saline-treated WT and $Stat5^{\Delta N}$ mice. The interaction of genotype and treatment (Geno x Trt) was used to determine whether GH effects varied across genotype. Statistical significance was set to $P<0.05$ for main effects and $P<0.10$ for the interaction.

RESULTS

Expression and activation of truncated Stat5

Presence of truncated Stat5 has been evaluated in liver, but not in muscle or adipose tissue (Engblom *et al.* 2007). First, we surveyed liver, adipose tissue, and muscle for expression of truncated Stat5 protein and determined if Stat5$^{\Delta N}$ could be activated by GH. Male mice were treated with a single injection of GH and sacrificed 15 minutes later. Total and phospho-Stat5 were measured by Western blot in liver, gastrocnemius muscle and gonadal adipose tissue. In WT mice, Stat5 was easily detected in all three tissues and was robustly phosphorylated in response to GH (Figure 3.1). In Stat5$^{\Delta N}$ mice, truncated Stat5 was present in all three tissues but its abundance was substantially less than WT in liver and adipose tissue. GH was able to activate Stat5$^{\Delta N}$ in all three tissues.

Effect of GH treatment on body weight gain, linear growth, and organ weights

In order to assess the role of Stat5 in GH-stimulated growth, we treated WT and Stat5$^{\Delta N}$ mice with exogenous GH for four weeks starting at d35 of age. Body weights were recorded daily and cumulative weight gain calculated by difference from body weight at d35. At the start of treatment, female and male Stat5$^{\Delta N}$ weighed 25% and 32% less than their WT counterparts (Stat5$^{\Delta N}$ vs. WT female, 13.0 vs. 17.4g; Stat5$^{\Delta N}$ vs. WT male, 14.8 vs. 21.7g, $P<0.05$). The body weight gain curves show that female Stat5$^{\Delta N}$ and WT mice had similar growth patterns over the treatment period. Nevertheless, by the end of treatment, saline-treated Stat5$^{\Delta N}$ mice grew less than their WT counterparts (Figure 3.2C; Geno, $P<0.05$).

The body weight gain curve of the saline-treated Stat5$^{\Delta N}$ males was obviously less steep than their WT counterparts. In fact, their body weight gain curve was nearly super-imposable over that of saline-treated WT and Stat5$^{\Delta N}$ females (Figures 3.2A &

Figure 3.1. Effect of acute GH treatment on activation of Stat5 protein in wild type and Stat5a/b N-terminal deletion mutant (Stat5$^{\Delta N}$) mice. Male wild type (WT) and Stat5$^{\Delta N}$ mice were treated with GH (GH, 4 µg/g BW) or an equivalent volume of saline (saline) (n = 3-5 for each genotype by treatment combination). Mice were sacrificed 15 minutes after injection. Protein extracts were prepared from liver, gastrocnemius muscle, and gonadal adipose tissue and analyzed by Western immunoblotting for phospho (pY Stat5) and total Stat5. Representative blots are shown.

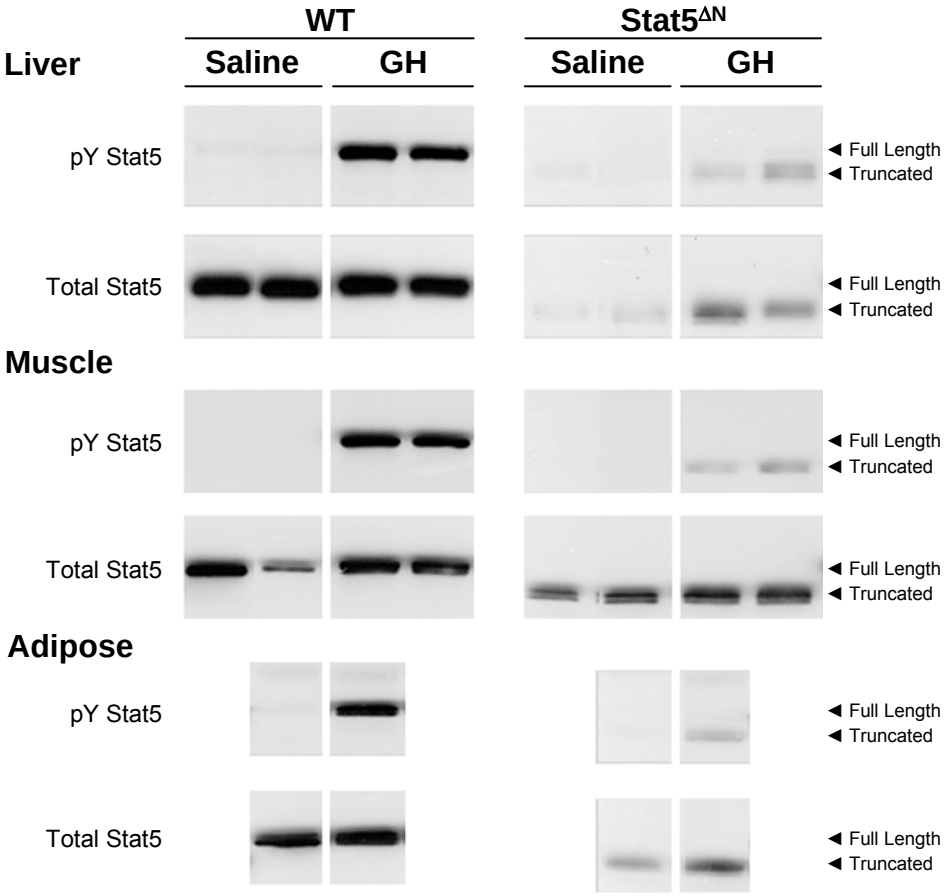
WT
Stat5ΔN
Liver
Saline
GH
Saline
GH
pY Stat5
◄ Full Length
◄ Truncated
Total Stat5
◄ Full Length
◄ Truncated
Muscle
pY Stat5
◄ Full Length
◄ Truncated
Total Stat5
◄ Full Length
◄ Truncated
Adipose
pY Stat5
◄ Full Length
◄ Truncated
Total Stat5
◄ Full Length
◄ Truncated

Figure 3.2. Effect of chronic GH treatment on body weight gain in female wild type and Stat5a/b N-terminal deletion mutant (Stat5$^{\Delta N}$) mice. Female wild type (WT) and Stat5$^{\Delta N}$ mice were treated twice daily with GH (GH, 3 µg/g BW/injection) or an equivalent volume of saline (saline) from day 35 to 63 of age. Body weights were recorded daily throughout the treatment period. A: Weight gain was calculated for each day as the difference from body weight at the start of treatment. B: Weight gain achieved over the first week of treatment. C: Weight gain achieved over the entire treatment period. Each line or bar represents the average of 6-8 mice. The significant effects of genotype (Geno) and the interaction between genotype and treatment (Geno x Trt) are reported.

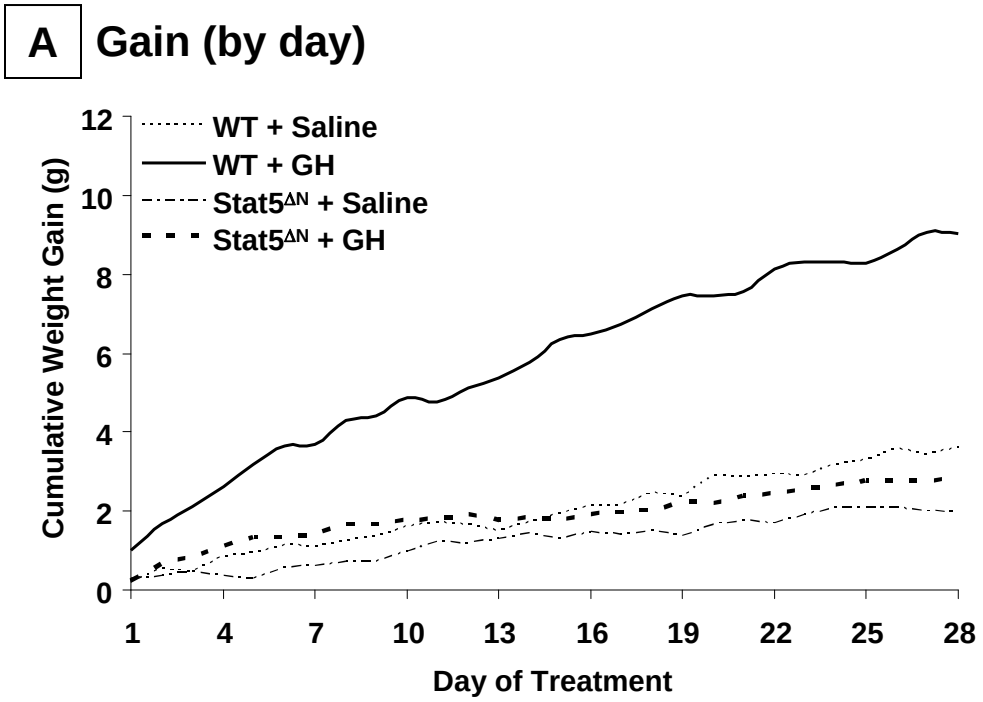
A
Gain (by day)
WT + Saline
WT + GH
Stat5ΔN + Saline
Stat5ΔN + GH
Cumulative Weight Gain (g)
Day of Treatment
0
2
4
6
8
10
12
1
4
7
10
13
16
19
22
25
28

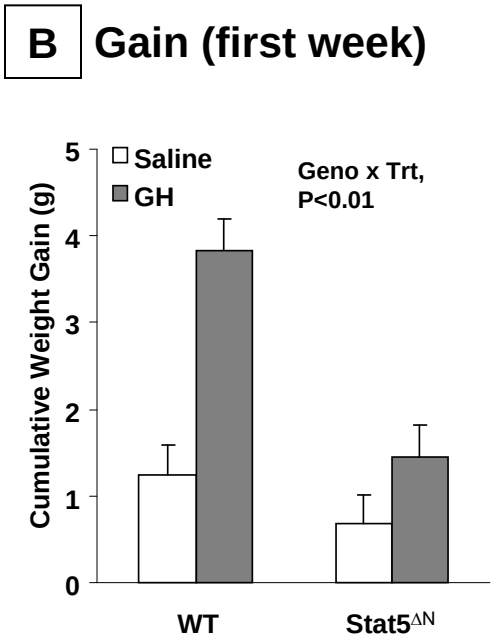
B
Gain (first week)
Saline
GH
Geno x Trt,
P<0.01
Cumulative Weight Gain (g)
0
1
2
3
4
5
WT
Stat5ΔN

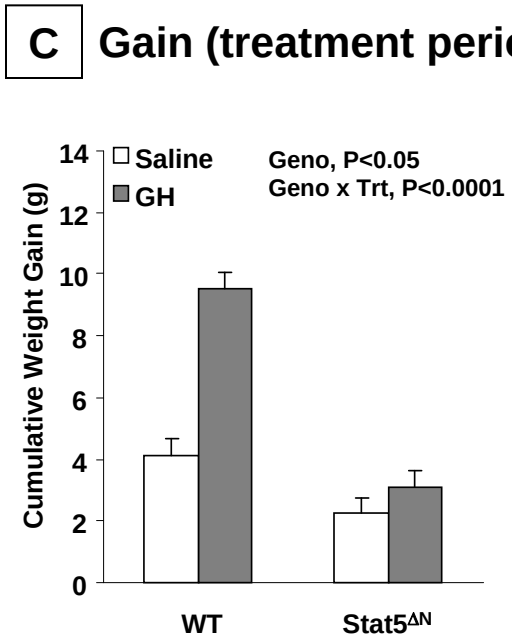
C
Gain (treatment period)
Saline
GH
Geno, P<0.05
Geno x Trt, P<0.0001
Cumulative Weight Gain (g)
0
2
4
6
8
10
12
14
WT
Stat5ΔN

3.3A). Accordingly, body weight gain in Stat5$^{\Delta N}$ males over the whole period was substantially less than saline-treated WT mice (Figure 3.3C; Geno, P<0.05).

GH increased the gain of female WT mice by 210% after 1 week and by 130% over the entire treatment period, but these positive effects were completely absent in Stat5$^{\Delta N}$ females (Figures 3.2B & 3.2C; Geno x Trt, P<0.01 or less). GH appeared somewhat less effective in stimulating body weight gain in WT males (compare Figure 3.2C to 3.3C), but again, its positive effects were not observed in Stat5$^{\Delta N}$ males (Figures 3.3B & 3.3C, Geno x Trt, P<0.07 or less).

Body length measurements were taken at the end of treatment. Body and femoral length were both decreased in male and female Stat5$^{\Delta N}$ mice (Figures 3.4A & 3.4B; Geno, P<0.001 or less). GH increased body length in WT mice but had no effect in Stat5$^{\Delta N}$ mice, irrespective of sex (Figures 3.4A & 3.4B; Geno x Trt, P<0.06 or less). A similar effect of GH on femoral length was also seen (Figure 3.4B; Geno x Trt, P≤0.05).

Organ weights were measured at the end of the study (Tables 3.2 & 3.3). The absolute organ weights of WT mice were significantly greater than those of Stat5$^{\Delta N}$ mice (Geno, P<0.05 or less). These results were consistent between both sexes except that the liver weights were similar in female WT and Stat5$^{\Delta N}$ mice. With the exception of muscle, GH treatment increased absolute organ weight of all tissues in WT but not in Stat5$^{\Delta N}$ mice (Geno x Trt, P<0.07 or less).

Because of the significant differences in final body weight among the treatment groups, organ weights were normalized to final body weight. Stat5$^{\Delta N}$ mice had heavier livers than WT mice but had lighter muscles (Tables 3.2 &3.3; Geno, P<0.05 or less). Stat5$^{\Delta N}$ mice also tended to have a lighter gonadal fat depot (P<0.09 or less). The genotype x treatment interactions occurred only in male muscle (increased only in WT, P<0.03) and female gonadal fat (reduced only in WT, P<0.08).

Figure 3.3. Effect of chronic GH treatment on body weight gain in male wild type and Stat5a/b N-terminal deletion mutant (Stat5$^{\Delta N}$) mice. Male wild type (WT) and Stat5$^{\Delta N}$ mice were treated twice daily with GH (GH, 3 µg/g BW/injection) or an equivalent volume of saline (saline) from day 35 to 63 of age. Body weights were recorded daily throughout the treatment period. A: Weight gain was calculated for each day as the difference from body weight at the start of treatment. B: Weight gain achieved over the first week of treatment. C: Weight gain achieved over the entire treatment period. Each line or bar represents the average of 6-8 mice. The significant effects of genotype (Geno) and the interaction between genotype and treatment (Geno x Trt) are reported.

A Gain (by day)

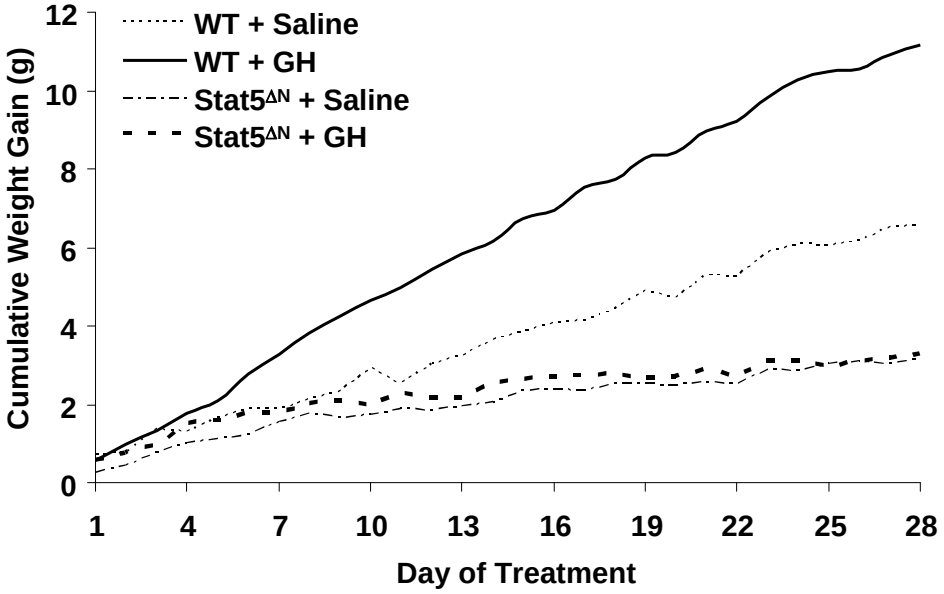

B Gain (first week)

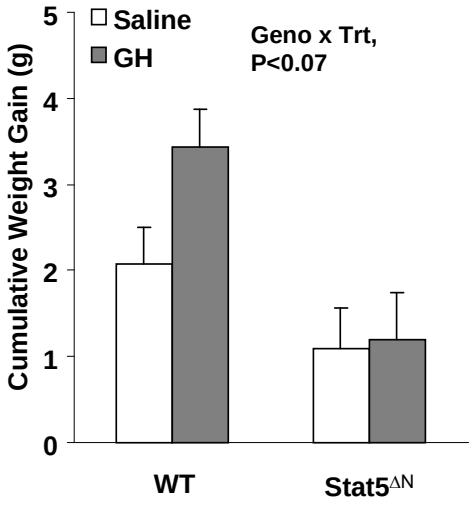

C Gain (treatment period)

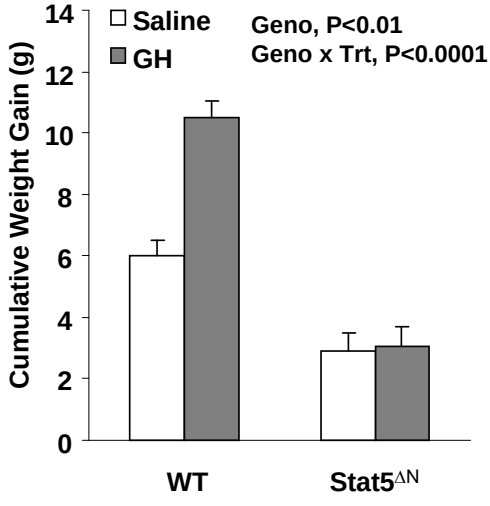

Figure 3.4. Effect of chronic GH treatment on cumulative body length and femoral length in wild type and Stat5a/b N-terminal deletion mutant (Stat5$^{\Delta N}$) mice. Wild type (WT) and Stat5$^{\Delta N}$ mice were treated twice daily with GH (GH, 3 µg/g BW/injection) or an equivalent volume of saline (saline) from 35 to 63 d of age. A: Body length (nose to anus) measurements taken at the end of treatment are shown for male and female mice. B: Femoral length measurements taken at the end of treatment are shown for male and female mice Each bar represents the mean ± SE of 6-8 mice. The significant effects of genotype (Geno) and the interaction between genotype and treatment (Geno x Trt) are reported.

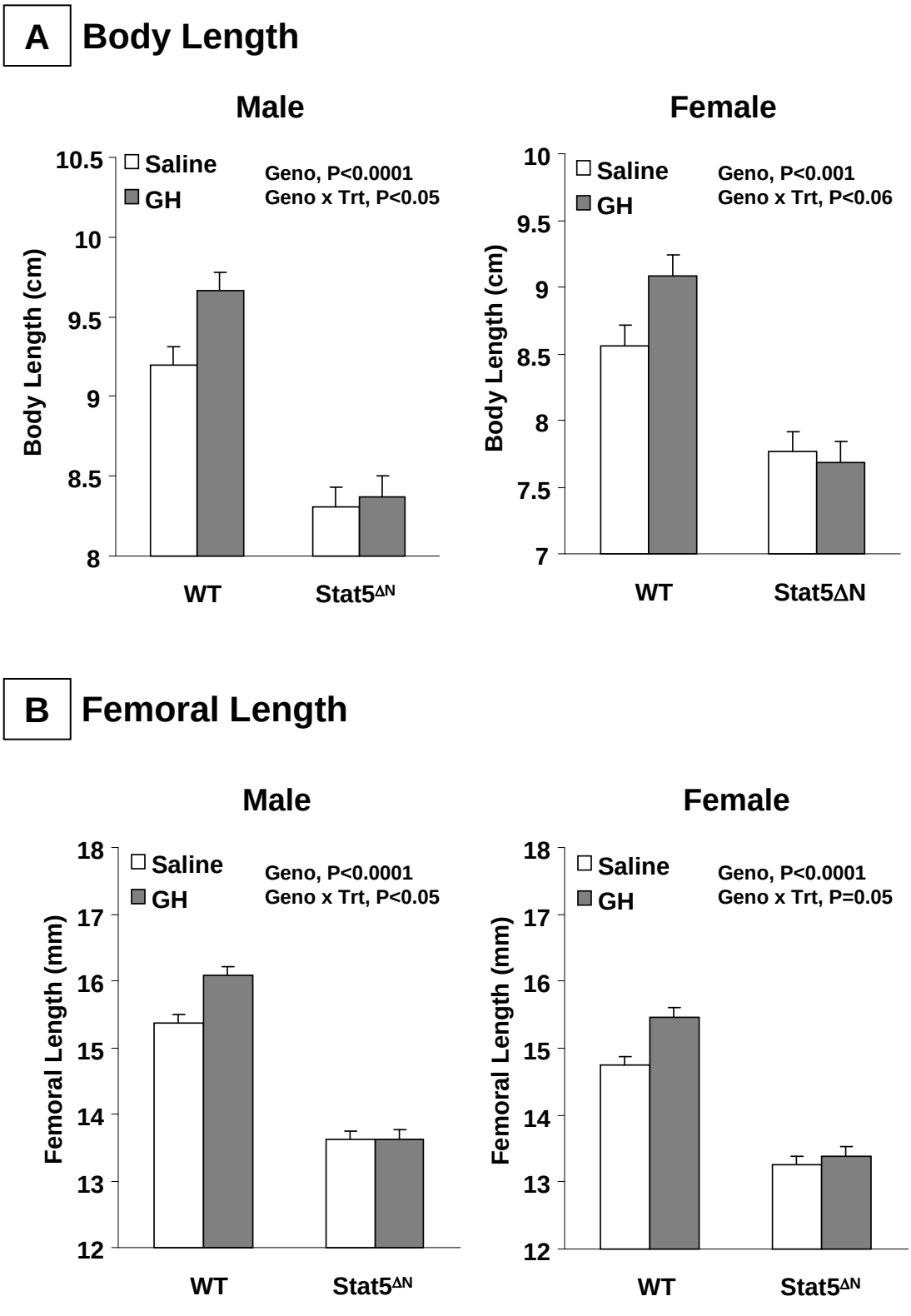
A
Body Length
Male
Female
Saline
GH
Geno, P<0.0001
Geno x Trt, P<0.05
Geno, P<0.001
Geno x Trt, P<0.06
Body Length (cm)
10.5
10
9.5
9
8.5
8
7.5
7
WT
Stat5ΔN
B
Femoral Length
Geno, P<0.0001
Geno x Trt, P<0.05
Geno, P<0.0001
Geno x Trt, P=0.05
Femoral Length (mm)
18
17
16
15
14
13
12

Table 3.2. Effect of chronic GH treatment on organ weight in wild type and STAT5$^{\Delta N}$ male mice.

	WT[1]		Stat5$^{\Delta N1}$			Significance[2]	
	Saline	GH	Saline	GH	SEM	Geno	Geno x Trt
Absolute weight (g)							
Liver	1.15	1.45	1.00	0.92	0.04	0.02	0.01
Kidney	0.34	0.38	0.23	0.22	0.01	0.01	0.03
Gonadal Fat	0.27	0.39	0.15	0.15	0.02	0.01	0.02
Muscle	0.24	0.25	0.15	0.15	0.01	0.01	NS
Normalized weight (% body weight)							
Liver	4.58	4.83	5.71	5.50	0.17	0.01	NS
Kidney	1.33	1.26	1.30	1.32	0.05	NS	NS
Gonadal Fat	1.09	1.29	0.85	0.89	0.09	0.07	NS
Muscle	0.96	0.84	0.88	0.89	0.03	0.05	0.03

[1]Male wild type (WT) and Stat5a/b N-terminal deletion mutant (Stat5$^{\Delta N}$) mice were treated twice daily with GH (GH, 3 µg/g BW/injection) or an equivalent volume of saline (saline) from day 35 to 63 of age. N = 6-8 mice for each treatment.

[2]Significance level for the effect of genotype (Geno, saline-treated WT vs Stat5$^{\Delta N}$) and the interaction between genotype and treatment (Geno x Trt); NS, non-significant (P>0.05 for main effects and P>0.10 for the interaction).

Table 3.3. Effect of chronic GH treatment on organ weight in wild type and STAT5$^{\Delta N}$ female mice.

	WT[1]		Stat5$^{\Delta N1}$			Significance[2]	
	Saline	GH	Saline	GH	SEM	Geno	Geno x Trt
Absolute weight (g)							
Liver	0.92	1.21	0.95	0.96	0.06	NS	0.02
Kidney	0.24	0.26	0.18	0.18	0.01	0.01	0.07
Gonadal Fat	0.14	0.23	0.08	0.07	0.02	0.01	0.01
Muscle	0.18	0.25	0.12	0.13	0.01	0.01	0.01
Normalized weight (% body weight)							
Liver	4.60	4.80	6.23	6.12	0.27	0.01	NS
Kidney	1.18	1.04	1.17	1.13	0.03	NS	NS
Gondadal Fat	0.71	0.92	0.51	0.43	0.08	0.09	0.08
Muscle	0.88	1.00	0.79	0.84	0.02	0.02	NS

[1]Female wild type (WT) and Stat5a/b N-terminal deletion mutant (Stat5$^{\Delta N}$) mice were treated twice daily with GH (GH, 3 µg/g BW/injection) or an equivalent volume of saline (saline) from day 35 to 63 of age. N = 6-8 mice for each treatment.

[2]Significance level for the effect of genotype (Geno, saline-treated WT vs Stat5$^{\Delta N}$) and the interaction between genotype and treatment (Geno x Trt); NS, non-significant (P>0.05 for main effects and P>0.10 for the interaction).

Effect of GH treatment on indices of IGF-I expression

Circulating IGF-I levels tended to be reduced in male Stat5$^{\Delta N}$ by 29% and were significantly reduced by 34% in female Stat5$^{\Delta N}$ (Figure 3.5; Geno, P<0.001). GH treatment increased IGF-I levels by 73% and 88% in male and female WT mice, respectively but was completely ineffective at increasing circulating levels in Stat5$^{\Delta N}$ mice (Figure 3.5; Geno x Trt, P<0.05 or less).

Liver is the predominant source of circulating IGF-I, and changes in plasma IGF-I are generally accounted by changes in hepatic IGF-I expression (Le Roith *et al.* 2001). To determine if this mechanism accounted for lack of GH-stimulated plasma IGF-I, IGF-I expression was analyzed in liver. Given that the lack of GH effect was seen in both sexes and that the effect of Stat5$^{\Delta N}$ was more pronounced in males, this was done only in male mice. Expression of the 7.5 kb IGF-I transcript was decreased 65% in Stat5$^{\Delta N}$ male mice (Figure 3.6A; Geno, P<0.001). GH treatment increased the expression of the 7.5 kb IGF-I transcript in WT liver but had no effect in Stat5$^{\Delta N}$ liver (Figure 3.6A; Geno x Trt, P<0.05).

We also assessed hepatic expression of the ALS gene. Like IGF-I, ALS is produced predominantly in liver in a GH-dependent manner. Stat5$^{\Delta N}$ mice expressed lower levels of the ALS transcript as compared to saline-treated WT (Figure 3.6B; Geno P<0.01). Hepatic ALS expression increased in response to GH treatment in WT mice only (Figure 3.6B; Geno x Trt, P<0.05).

Finally, we asked whether GH induction of IGF-I expression was also impaired in extra-hepatic tissues of Stat5$^{\Delta N}$. The Stat5$^{\Delta N}$ mutation decreased IGF-I expression in the muscle and the gonadal fat pad (Figure 3.7, Geno, P<0.05 or less). GH treatment increased expression of IGF-I in the gastrocnemius muscle and gonadal fat pad of WT male mice, but had absolutely no effect in Stat5$^{\Delta N}$ mice (Figure 3.7, Geno x Trt, P<0.05 or less).

Figure 3.5. Effect of chronic GH treatment on plasma IGF-I in wild type and Stat5a/b N-terminal deletion mutant (Stat5$^{\Delta N}$) mice. Wild type (WT) and Stat5$^{\Delta N}$ mice were treated twice daily with GH (GH, 3 µg/g BW/injection) or an equivalent volume of saline (saline) from 35 to 63 d of age. Plasma was obtained on the last day of treatment and analyzed for IGF-I by RIA. Circulating IGF-I levels are shown for male and female mice. Each bar represents the mean ± SE of 5 mice. The significant effects of genotype (Geno) and the interaction between genotype and treatment (Geno x Trt) are reported.

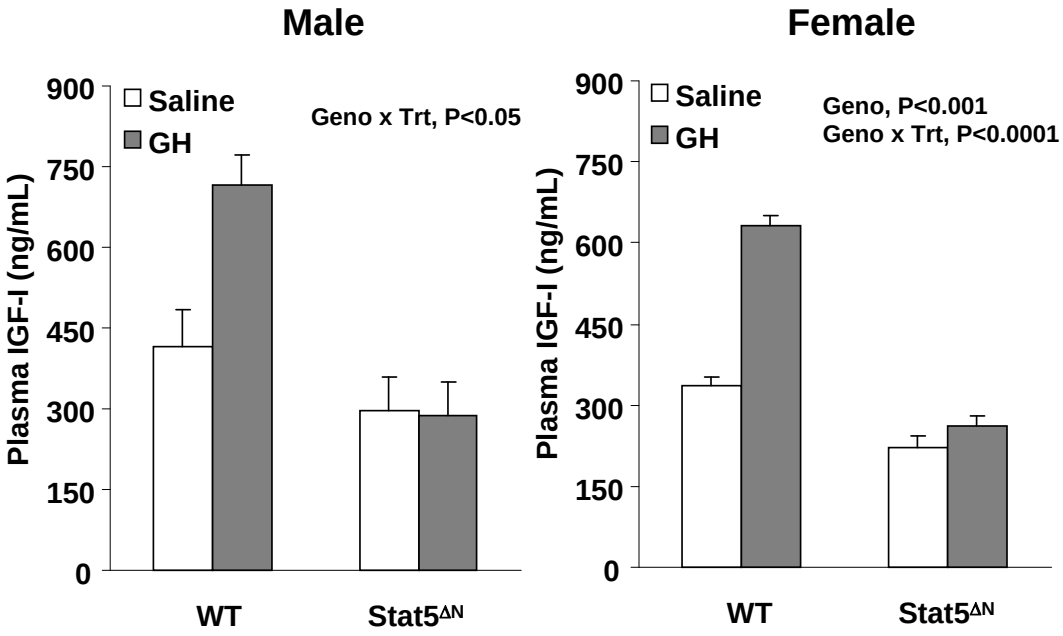
Male
Female
Saline
GH
Geno x Trt, P<0.05
Geno, P<0.001
Geno x Trt, P<0.0001
Plasma IGF-I (ng/mL)
900
750
600
450
300
150
0
WT
Stat5ΔN

Figure 3.6. Effect of chronic GH treatment on hepatic IGF-I and ALS mRNA in wild type and Stat5a/b N-terminal deletion mutant (Stat5$^{\Delta N}$) mice. Wild type (WT) and Stat5$^{\Delta N}$ mice were treated twice daily with GH (GH, 3 µg/g BW/injection) or an equivalent volume of saline (saline) from 35 to 63 d of age. Total RNA was isolated from liver of male mice and analyzed by Northern blotting for expression of IGF-I, ALS, and 18S. A. *Left:* Northern blot analysis of IGF-I gene expression. *Right:* Each bar represents the mean ± SE (n=5) of the 7.5 kb IGF-I signal (normalized to 18S). The significant effects of genotype (Geno) and the interaction between genotype and treatment (Geno x Trt) are reported. B. *Left:* Northern blot analysis of ALS gene expression. *Right:* Each bar represents the mean ± SE (n=5) of the ALS signal (normalized to 18S). The significant effects of genotype (Geno) and the interaction between genotype and treatment (Geno x Trt) are reported.

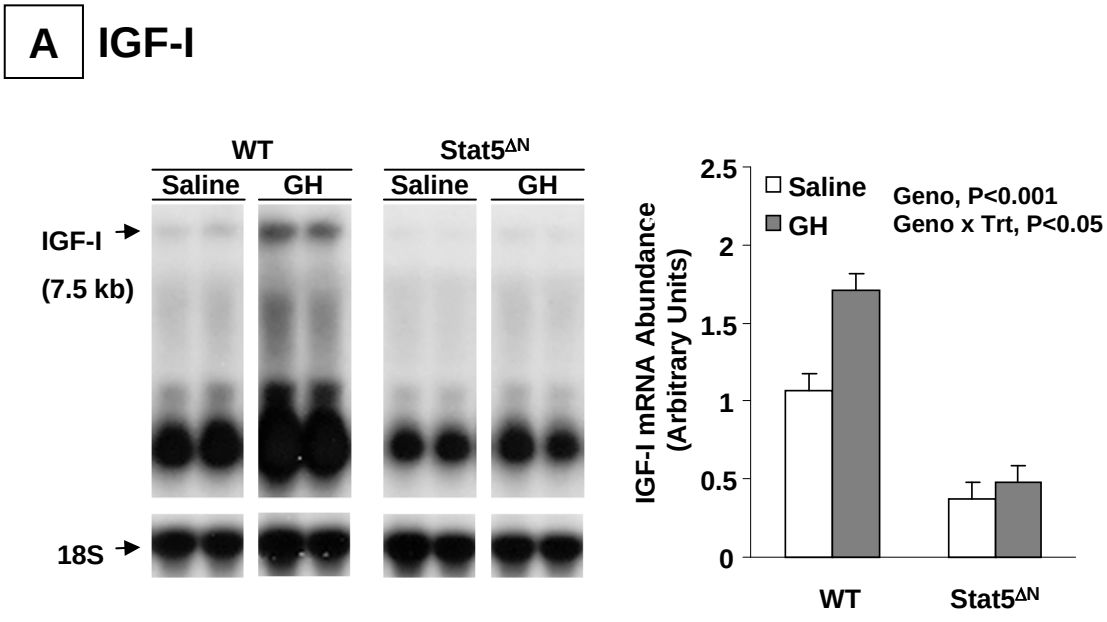
A
IGF-I
WT
Stat5ΔN
Saline
GH
Saline
GH
IGF-I
(7.5 kb)
18S
IGF-I mRNA Abundance
(Arbitrary Units)
2.5
2
1.5
1
0.5
0
Saline
GH
Geno, P<0.001
Geno x Trt, P<0.05
WT
Stat5ΔN

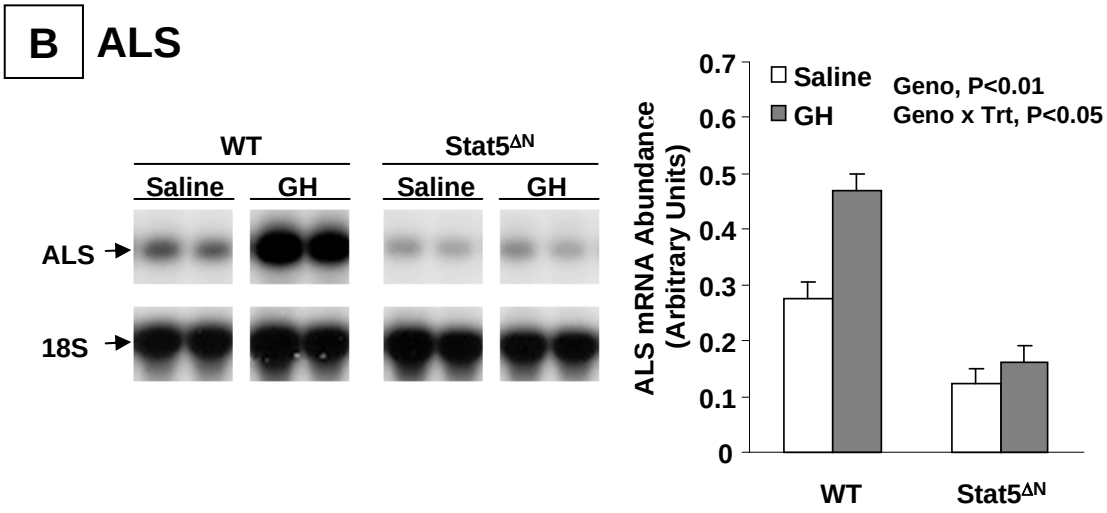
B
ALS
WT
Stat5ΔN
Saline
GH
Saline
GH
ALS
18S
ALS mRNA Abundance
(Arbitrary Units)
0.7
0.6
0.5
0.4
0.3
0.2
0.1
0
Saline
GH
Geno, P<0.01
Geno x Trt, P<0.05
WT
Stat5ΔN

Figure 3.7. Effect of chronic GH treatment on IGF-I mRNA expression in muscle and adipose tissue in wild type and Stat5a/b N-terminal deletion mutant (Stat5$^{\Delta N}$) mice. Wild type (WT) Stat5$^{\Delta N}$ mice were treated twice daily with GH (GH, 3 µg/g BW/injection) or an equivalent volume of saline (saline) from 35 to 63 d of age. Total RNA was isolated from the gastrocnemius muscle and gonadal adipose tissue of male mice. IGF-I mRNA abundance was measured using quantitative real time PCR. Each bar represents the mean ± SE of 6-8 mice. The significant effects of genotype (Geno) and the interaction between genotype and treatment (Geno x Trt) are reported.

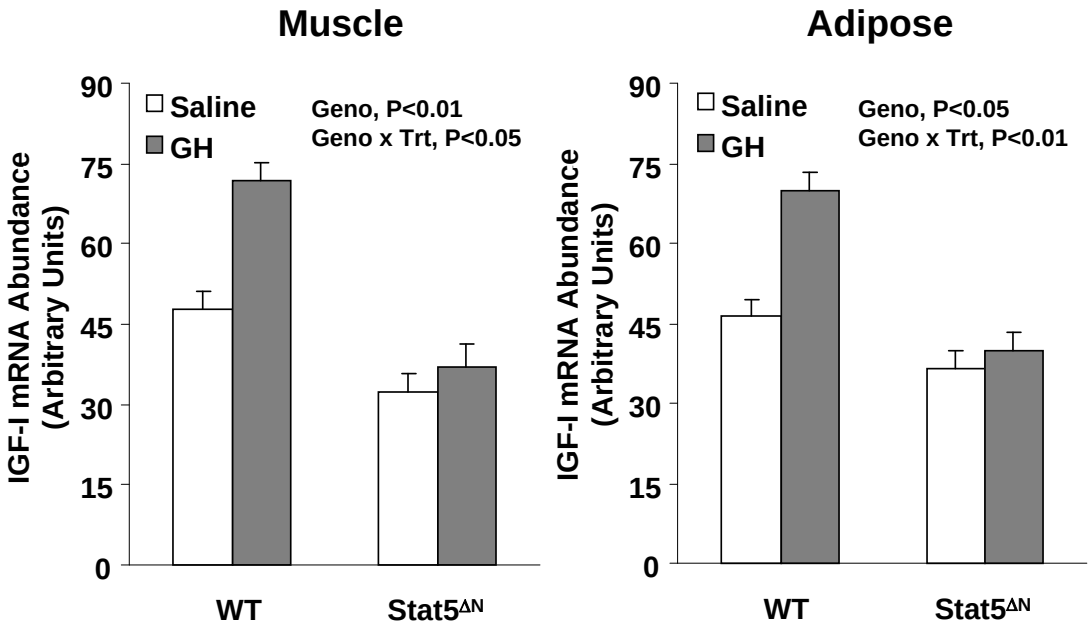
Muscle
Adipose
IGF-I mRNA Abundance (Arbitrary Units)
90
75
60
45
30
15
0
Saline
GH
Geno, P<0.01
Geno x Trt, P<0.05
Geno, P<0.05
Geno x Trt, P<0.01
WT
Stat5ΔN

Effect of GH treatment on carbohydrate metabolism

Chronic elevation of GH leads to insulin resistance (Dominici *et al.* 1999b), but whether this effect of GH requires Stat5 is unknown. As an initial step to examine this issue, plasma was obtained at the end of the treatment period and analyzed for glucose and insulin. In female mice, genotype did not affect plasma glucose or insulin (Table 3.4). In male mice, plasma glucose was also similar between genotypes, but genotype impacted insulin levels. Stat5$^{\Delta N}$ males had lower plasma insulin levels than their WT counterparts (Table 3.4, Geno, $P<0.01$).

To assess more directly the role of Stat5 in GH-induced insulin resistance, insulin tolerance tests were performed on WT and Stat5$^{\Delta N}$ male mice. At 30 minutes after insulin injection, blood glucose in WT saline-treated animals decreased ~30%, and a similar decline was seen in Stat5$^{\Delta N}$ mice, irrespective of treatment. In GH-treated WT mice, however, plasma glucose dropped only 15% (Figure 3.8A). At 90 minutes post insulin injection, plasma glucose levels were still suppressed in WT saline-treated and both saline- and GH-treated Stat5$^{\Delta N}$ mice while levels had returned to baseline in GH-treated WT mice (Figure 3.8A). To quantify insulin responsiveness, area under the glucose response curve (AUC) was calculated and analyzed. GH treatment significantly reduced AUC in WT mice but had no effect in Stat5$^{\Delta N}$ mice (Figure 3.8B; Geno x Trt, $P<0.01$). Overall, these data demonstrate that GH induced insulin resistance in WT mice while GH-treated Stat5$^{\Delta N}$ mice remained insulin sensitive.

GH-dependent insulin resistance has recently been linked to induction of the regulatory subunit of PI3K, p85α (Barbour *et al.* 2005). This raises the possibility that GH is unable to induce p85α in Stat5$^{\Delta N}$ mice, and therefore may explain why these mice are more insulin responsive when treated with GH. To evaluate this possibility, we measured expression of p85α in liver, gonadal fat pad, and gastrocnemius muscle

Table 3.4. Effect of chronic GH treatment on plasma insulin and glucose in wild type and STAT5$^{\Delta N}$ mice.

	WT[1]		Stat5$^{\Delta N1}$			Significance Level[2]	
	Saline	GH	Saline	GH	SEM	Geno	Geno x Trt
Male							
Insulin (ng/mL)	0.39	0.52	0.26	0.35	0.03	0.01	NS
Glucose (mg/dL)	210	247	263	236	23	NS	NS
Female							
Insulin (ng/mL)	0.36	0.39	0.38	0.31	0.04	NS	NS
Glucose (mg/dL)	198	237	238	222	24	NS	NS

[1]Wild type (WT) and Stat5a/b N-terminal deletion mutant (Stat5$^{\Delta N}$) mice were treated twice daily with GH (GH, 3 µg/g BW/injection) or an equivalent volume of saline (saline) from day 35 to 63 of age. N = 5 mice for each treatment.

[2]Significance level for the effect of genotype (Geno, WT versus Stat5$^{\Delta N}$), treatment (Trt, saline versus GH), and their interaction (Geno x Trt); NS, non-significant (P>0.05 for main effects and P>0.10 for the interaction).

Figure 3.8. Effect of GH treatment on insulin sensitivity in wild type and Stat5a/b N-terminal deletion mutant (Stat5$^{\Delta N}$) mice. Wild type (WT) Stat5$^{\Delta N}$ male mice were treated twice daily with GH (GH, 3 µg/g BW/injection) or an equivalent volume of saline (saline) for 3.5 days. The basal concentration of blood glucose was measured at time 0, immediately before administration of insulin (0.6 mU/g BW). Blood glucose was measured again at 30, 60, and 90 minutes after insulin injection. A: Response to insulin is expressed as percent of basal glucose. Each point represents the mean ± SE of 5-6 mice. B: Area under the glucose response curve was calculated for each group using the trapezoid method. Each bar represents the mean ± SE of 5-6 mice. The significant effects of genotype (Geno) and the interaction between genotype and treatment (Geno x Trt) are reported.

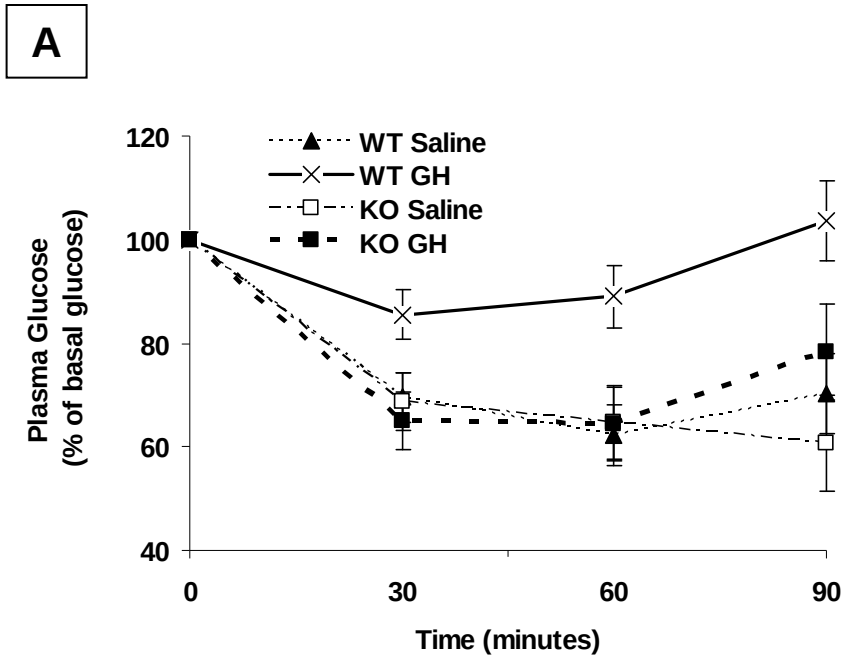
A
120
100
80
60
40
Plasma Glucose
(% of basal glucose)
WT Saline
WT GH
KO Saline
KO GH
0
30
60
90
Time (minutes)

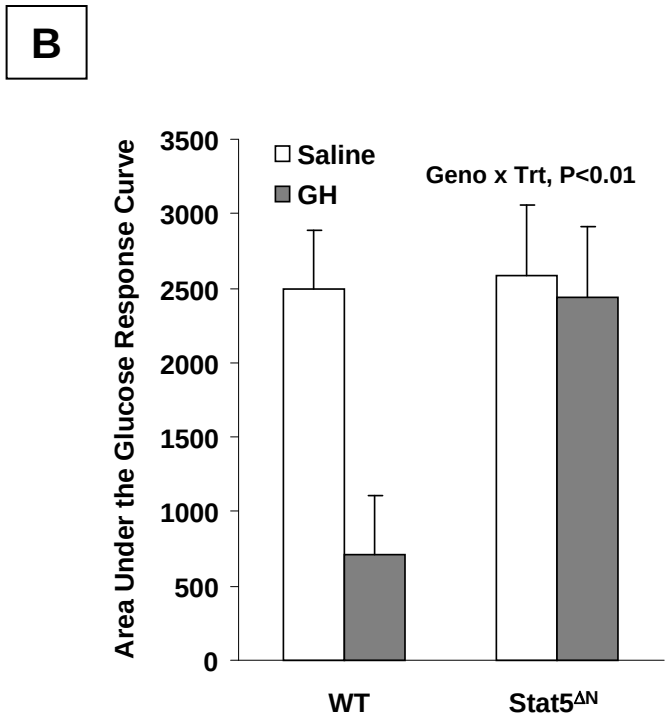
B
3500
3000
2500
2000
1500
1000
500
0
Area Under the Glucose Response Curve
Saline
GH
Geno x Trt, P<0.01
WT
Stat5ΔN

of both WT and Stat5$^{\Delta N}$ male mice treated for a 4 week period with GH or saline. Basal levels of p85α expression were similar between saline treated WT and Stat5$^{\Delta N}$ male mice for all tissues (Figure 3.9, Geno, P>0.05). In WT mice, exogenous GH increased or tended to increase p85α expression in liver, muscle, and gonadal fat but had no effect in Stat5$^{\Delta N}$ mice (Figure 3.9, Geno x Trt P=0.15 or less).

DISCUSSION

Studies performed over the last 15 years have characterized the molecular events involved in GH signaling and have identified the Stat5 proteins as central to its transcriptional effects (Hosui & Hennighausen 2008). The Stat5 proteins consist of two isoforms, Stat5a and Stat5b, each encoded by its own gene (Liu *et al.* 1995). Genetic mouse models have been created in which each individual Stat5 gene has been ablated (Liu *et al.* 1997; Udy *et al.* 1997). These models show that Stat5a is absolutely required for proper mammary gland development during late pregnancy and lactation, but Stat5a appears to play no role in growth (Liu *et al.* 1997). On the other hand, Stat5b plays important roles in regulating sexually dimorphic growth rates and hepatic gene transcription (Udy *et al.* 1997). Loss of Stat5b in male mice decreased body weight gain 27%, and knockout males grew at a rate similar to WT and Stat5b mutant females (Udy *et al.* 1997).

In 1998, Teglund *et al.* (1998) attempted to knock out both *Stat5a* and *Stat5b* by inserting a neomyocin- and hygromyocin cassette into the first coding exon of the respective genes. Their Stat5a mutant model had a similar phenotype as that described by Liu *et al.* (1997), with impaired mammary gland development but normal growth. Moreover, their Stat5b mutant model was characterized by a male specific deficit in postnatal growth similar to that described by Udy *et al.* (1997). When both mutations were combined (Stat5$^{\Delta N}$), male mice had a postnatal growth deficit similar to that reported in the original Stat5b mutant. Interestingly, female Stat5$^{\Delta N}$ mice not only had

Figure 3.9. Effect of chronic GH treatment on p85α subunit of PI3K mRNA expression in liver, muscle, and adipose tissue in wild type and Stat5a/b N-terminal deletion mutant (Stat5$^{\Delta N}$) mice. Wild type (WT) and Stat5$^{\Delta N}$ mice were treated twice daily with GH (GH, 3 µg/g BW/injection) or an equivalent volume of saline (saline) from 35 to 63 d of age. Total RNA was isolated from liver, gastrocnemius muscle, and the gonadal adipose tissue of male mice. And analyzed for mRNA abundance of the p85α isoform was measured by quantitative real time PCR. Each bar represents the mean ± SE of 6-8 mice. The effects of genotype (Geno) and the interaction between genotype and treatment (Geno x Trt) are reported.

Liver

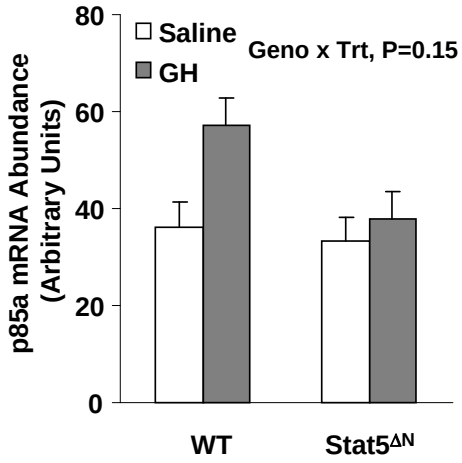

Muscle

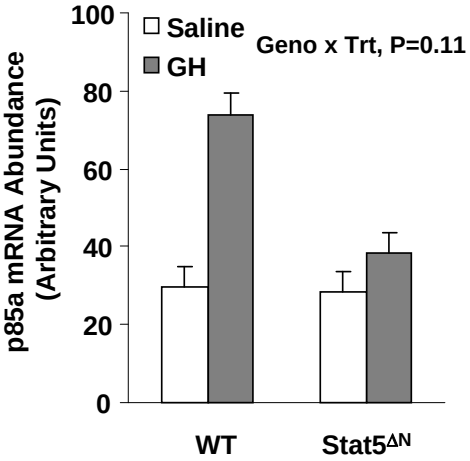

Adipose

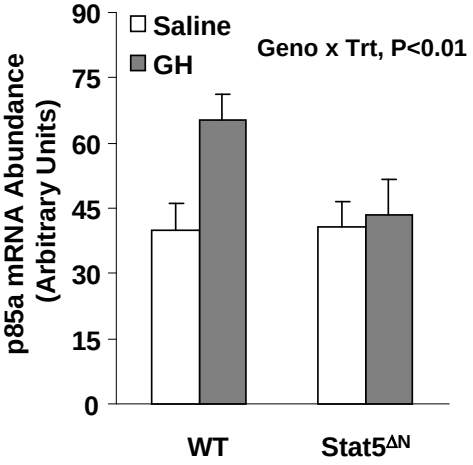

impaired mammary development but also suffered a growth deficit (Teglund *et al.* 1998).

Stat5$^{\Delta N}$ mice were believed to be true knockouts, but it has since been established that this strategy led to the synthesis of Stat5 proteins with N-terminal deletions (Riedlinger *et al.* 2002). This is because the mutation strategy for both Stat5a and Stat5b targeted the naturally used start codon but left intact Kozak sequences and in-frame ATGs at amino acid position 103 and 137. The ATG at position 137 is predominantly used in translation of the truncated proteins (Kornfeld *et al.* 2008). Truncated Stat5 proteins were identified in liver of Stat5$^{\Delta N}$ mice (Engblom *et al.* 2007). We now show that truncated Stat5 proteins are also present in muscle and gonadal adipose of Stat5$^{\Delta N}$ mice. Truncated Stat5 proteins are significantly less abundant than Stat5 proteins in liver, muscle, and adipose tissue in WT mice but can be phosphorylated in response to GH.

Stat5$^{\Delta N}$ mice remain a valid model to study GH-dependent effects mediated by Stat5 even if they express truncated proteins. First, total Stat5 ablation is not an option as shown by the perinatal lethality seen in total Stat5 knockouts (Cui *et al.* 2004). Second, the phosphorylated truncated Stat5 proteins are able to bind their cognate DNA element but are transcriptionally inactive for most Stat5-dependent growth-related promoters in liver (Engblom *et al.* 2007). The reason for this inactivity is that Stat5$^{\Delta N}$ proteins are lacking the N-terminal domain that is required for interaction with the glucocorticoid (GC) receptor, and this interaction is needed for transcriptional activation of most Stat5-dependent genes in liver (Engblom *et al.* 2007).

Our study confirmed that Stat5$^{\Delta N}$ mice of both sexes grew at a slower rate than WT mice (Teglund *et al.* 1998; Engblom *et al.* 2007). However, no studies have ever directly assessed whether growth effects of exogenous GH were also lost in Stat5 deficient mice. Chronic administration of GH has been used to evaluate the GH

responsiveness of various GH/IGF-I mutant models (Liu & LeRoith 1999; Liu *et al.* 2000b; Fielder *et al.* 1996). GH responsiveness appears to be dependent on developmental stage. Kasukawa *et al.* (2003) found that pubertal and post-pubertal, GH-deficient *lit/lit* mice treated with GH had greater body weight gain and increased circulating IGF-I levels as compared to those animals treated during the pre-pubertal period. For these reasons, we treated WT and Stat5$^{\Delta N}$ mice with exogenous GH for four weeks between days 35 and 63 of age. In response to exogenous GH treatment, WT male and female mice grew at a greater rate than their saline-treated counterparts; Stat5$^{\Delta N}$ mice, however, completely failed to respond to GH treatment. Similarly, GH treatment increased body and femoral length only in WT mice.

The GH-IGF-I system is one of the major hormonal systems regulating postnatal growth. After birth, approximately 35% of growth is mediated by the overlapping actions of GH and IGF-I (Lupu *et al.* 2001). A portion of these actions represent GH-stimulation of endocrine IGF-I which is nearly completely liver-derived (Yakar *et al.* 1999). The molecular mechanism whereby GH-dependent Stat5 activation stimulates hepatic IGF-I transcription has only been elucidated recently. Three distinct GH response elements (GHRE) that contain paired Stat5b binding sites have been mapped within the rat IGF-I locus (Woelfle *et al.* 2003; Wang & Jiang 2005). More recently, five additional Stat5 binding sites, located in 3 new chromosomal regions, have been identified. Individually, these regions are able to activate reporter gene expression via Stat5 binding, but a greater GH response is achieved when all five regions are present (Eleswarapu *et al.* 2008). This mechanism has been confirmed in vivo. In hypophysectomized rats infected with a control adenovirus, GH increased hepatic expression of IGF-I mRNA while infection with dominant-negative Stat5b adenovirus blocked IGF-I gene transcription. In contrast, a constitutively-active Stat5b adenovirus stimulated IGF-I expression even in the

absence of GH (Woelfle *et al.* 2004). These data illustrate that Stat5b is both necessary and sufficient for GH-induced expression of IGF-I in liver. Our data confirm these observations because GH was completely unable to increase hepatic IGF-I mRNA and plasma IGF-I in Stat5$^{\Delta N}$ mice. This also is consistent with data presented by Engblom *et al.* that glucocorticoid receptor interactions are critical for the ability of Stat5 to stimulate hepatic transcription of the IGF-I and ALS genes (Engblom *et al.* 2007).

The second portion of the overlapping GH-IGF-I effects are carried out by the autocrine/paracrine IGF-I system and represent GH stimulation of extra-hepatic IGF-I synthesis (Mathews *et al.* 1986; Murphy *et al.* 1987). Whether this stimulation was also dependent on Stat5 was unknown. Thus, we evaluated basal and GH-stimulated IGF-I mRNA expression in muscle and adipose. Similar to the pattern of hepatic IGF-I mRNA expression, we showed that basal IGF-I expression levels in Stat5$^{\Delta N}$ mice are also decreased. Consistent with this, muscle specific ablation of Stat5 decreased IGF-I mRNA expression in that tissue as well (Klover & Hennighausen 2007). More specifically, we show that GH stimulated IGF-I expression in both tissues in WT mice while it failed to do so in Stat5$^{\Delta N}$ mice. This finding also suggests that the interaction of GR and Stat5 is required for GH-stimulated IGF-I gene expression not only in liver, but also in extra-hepatic tissues.

Excessive levels of GH alter organ growth proportionally for heart and spleen, but disproportionally increase the growth of liver and muscle (Le Roith *et al.* 2001). Indeed, we observed that exogenous GH induced a disproportional fractional liver growth in mice (Ueki 2006). We intended to use these indices as a second measure of GH action in Stat5$^{\Delta N}$ mice. The effect of GH on liver was of particular interest because liver has no IGF-I receptors (Werner *et al.* 1989), and thus could be used as an index of the growth effects of GH that are independent of IGF-I. Lupu *et al.* (2001)

have shown that these IGF-I independent effects of GH account for ~14% of postnatal growth. Overall, our results suggest that Stat5 is also required for GH effects that are independent of IGF-I. Specifically, GH did not stimulate fractional liver weight and did not lead to a genotype x treatment interaction. It is true that the fractional liver weight of Stat5$^{\Delta N}$ mice was increased. Similar observations were made in null Stat5b and liver-specific null Stat5 mice (Udy *et al.* 1997; Cui *et al.* 2007). As is the case for Stat5$^{\Delta N}$, both of these models have lower plasma IGF-I and presumably excessive GH secretion. However, failure of exogenous GH to stimulate fractional liver weight in WT mice suggests that liver hypertrophy in saline-treated Stat5$^{\Delta N}$ mice is not because of direct GH effects.

The final GH-dependent endpoint we examined was insulin resistance. Chronic elevation of GH leads to hyperinsulinemia and insulin resistance (Dominici *et al.* 1999a). Given that tissue specific Stat5 knockout models have altered glucose tolerance and insulin sensitivity, we evaluated the role of truncated Stat5 in GH-induced insulin resistance. Exogenous GH induced insulin resistance only in the WT mice while GH-treated Stat5$^{\Delta N}$ mice maintained normal insulin sensitivity. These results suggest that GH-induced insulin resistant state is also dependent on a Stat5 function.

Recent studies have identified a mechanism involving PI3K whereby GH antagonizes insulin signaling (Barbour *et al.* 2005). PI3K is a heterodimer composed of the p85 subunit and the catalytic subunit p110. The p85 subunit provides a binding domain for IRS proteins and regulates the activity of the p110 catalytic subunit (Dominici *et al.* 2005). Increased expression of p85α increases the pool of free p85α which competes with the p85-p110 heterodimer for binding sites on IRS-1. As a result, PI3K activity decreases when free p85α is in excess (Biddinger & Kahn 2006). In muscle, GH-stimulated increase in p85α resulted in decreased PI3K activity and

subsequent insulin resistance (Biddinger & Kahn 2006). Moreover, reduced p85α expression prevented GH-induced insulin resistance (Barbour *et al.* 2005). A similar mechanism of GH-stimulated p85α expression has been described in white adipose tissue (WAT) as well (Del Rincon *et al.* 2007). Consistent with this mechanism, we showed that exogenous GH treatment in WT male mice stimulated p85α mRNA expression in liver, muscle, and gonadal fat. More importantly, we show for the first time that Stat5 upregulated p85α expression in a GH-dependent manner because this effect was lost in liver, muscle, and fat of $Stat5^{\Delta N}$ mice. Interestingly, another Stat protein, Stat3 regulates expression of the two other regulatory isoforms of PI3K, p50α and p55α but has no effect on p85α (Abell *et al.* 2005).

In conclusion, the N-terminal domain of Stat5 is absolutely necessary to mediate the effects of exogenous GH. $Stat5^{\Delta N}$ mice fail to grow in response to GH treatment, likely due to the inability to stimulate IGF-I in liver and other tissues. Lack of a GH effect on liver growth suggests that growth effects mediated by GH alone are also lost. Finally, a functional Stat5 protein is required for GH-induced insulin resistance. $Stat5^{\Delta N}$ mice remain insulin sensitive even when treated with exogenous GH, possibly due to the inability of GH to stimulate p85α expression.

CHAPTER FOUR:
ROLE OF THE ACID LABILE SUBUNIT IN MOUSE MAMMARY GLAND DEVELOPMENT

INTRODUCTION

The somatotropic axis plays an important role in growth and development (Le Roith *et al.* 2001). Growth hormone (GH) can act directly on target tissues, or it can act by stimulating tissue production of insulin-like growth factor (IGF-I). In the case of most tissues, IGF-I remains near its cellular site of production and represents the autocrine/paracrine arm of the IGF-I system (Le Roith *et al.* 2001). These IGF-I molecules are usually bound to one of six IGF binding proteins (IGFBPs) (Jones & Clemmons 1995; Stewart & Rotwein 1996). Liver-derived IGF-I, on the other hand, is secreted in plasma and represents the endocrine arm of the IGF-I system. In postnatal animals, circulating IGF-I is bound in a 150 kDa ternary complex composed of one molecule each of IGF-I, IGFBP-3 or -5, and ALS (Baxter 1988; Twigg & Baxter 1998).

ALS is thought to function exclusively as a component of the circulating IGF system. It is responsible for formation of ternary complexes in circulation, building a reservoir of circulating IGF-I, and preventing its insulin-like effects (Zapf *et al.* 1995). Characterization of the null ALS mutant revealed a functional role for ALS in postnatal growth and metabolism (Ueki *et al.* 2000; Haluzik *et al.* 2003), but the role of ALS in mammary gland development has not been studied.

The mammary gland undergoes extensive morphological and biochemical changes during postnatal life. These dynamic changes are under strict hormonal control by sex steroid hormones and various growth factors (Richert *et al.* 2000). The most dramatic changes occur throughout four distinct stages: virginity, pregnancy,

lactation, and involution. During the first phase, the ducts elongate to fill the mammary fat pad (Hovey *et al.* 2002). Development during pregnancy is characterized by further branching of the ducts and alveolar differentiation. During lactation, the alveoli expand to completely fill the gland, and active milk secretion is established (Brisken 2002). Upon weaning, the lactating gland undergoes involution where extensive remodeling of the gland returns it to pre-pregnancy form (Lamote *et al.* 2004). GH, IGF-I, and IGFBPs are involved in mammary development through each of these stages. A role for ALS, either through its ability to modulate plasma IGF-I or through local effects, has never been considered. As an initial step to address this issue, we studied mammary gland development in null ALS mice.

MATERIALS AND METHODS

Animals and experimental design

Four studies were conducted to characterize ALS expression and its function during mouse mammary gland development. Experimental procedures involving live animals were conducted with the approval of the Cornell University Institutional Animal Care and Use committee. The facility was kept at constant temperature (~22°C) and humidity (~65%) with controlled lighting (14 h light/10 h dark cycle). All animals were offered water and fed a standard rodent chow (Harlan Tekland 8640 containing 22% protein, 5% fat, Harlan, Madison, WI) *ad libitum.*

ALS expression during mammary gland development

To determine the effect of physiological state on ALS expression in the mammary gland, age-matched FVB mice (d112) were studied when virgin, on d18 of pregnancy, d5 of lactation, or d2 of involution (n = 4-6/state). Mice were euthanized by carbon dioxide asphyxiation. Liver and the fourth mammary gland were dissected, snap-frozen immediately in liquid nitrogen, and stored at -80°C for extraction of total RNA.

Role of ALS in pubertal mammary gland development

Mammary development was studied in null ALS 12 mice or their WT counterparts. Mice were of a mixed background (Balb/c x 129Sv), and experimental animals were generated by crossing heterozygous male and female mice. For the study of virgin development, animals (n = 5-6 for each genotype by age combination) were sacrificed at 4, 6, and 8 wks of age. Six and 8 week old animals were collected in diestrus as mammary structures are more uniform during that stage of the estrous cycle. Stage of cycle was determined by evaluating vaginal smears stained with 0.1% methylene blue. Mice were euthanized by carbon dioxide asphyxiation, and blood was collected by cardiac puncture, processed into plasma by the addition of heparin (60 U/mL) and stored at -20°C. The uterus was dissected and weighed. The right, fourth mammary gland was fixed and embedded in paraffin while the contralateral gland was analyzed by whole mount staining.

To determine whether lack of ALS delays age at puberty, 24d old WT and null ALS mice (n = 10/genotype) were housed with proven males. Animals were checked daily for vaginal opening and presence of a copulatory plug. Body weight was measured every other day. Three days after observing a plug, animals were weighed and then euthanized by carbon dioxide asphyxiation. Blood was collected immediately by cardiac puncture, processed to plasma by the addition of heparin (60U/mL) and stored at -20°C. The uterus was dissected and weighed. Ovaries were dissected and copora lutea present at the surface of the ovary were counted using a dissecting microscope. The right, fourth mammary gland was fixed and embedded in paraffin while the contralateral gland was analyzed by whole mount staining.

Role of ALS in mammary development during pregnancy, lactation, and involution

A total of 54 wild type and null ALS (Balb/c x 129Sv) female mice were studied during pregnancy, lactation, or involution (n = 3-6 animals/genotype at each

stage of development). To obtain pregnant d8 and d18 animals, females were placed with proven males and evaluated daily for the presence of a copulatory plug, which represented d1 of pregnancy. Pregnancy was confirmed at sacrifice. To study development during lactation, the litter was normalized to 5-7 pups per dam on the day of parturition. Dams were sacrificed on d2 or d10 of lactation (d1=day of parturition).

A forced involution model was used to study mammary involution. On the day of parturition, the litter was normalized to 5-7 pups per dam, and dams were allowed to lactate for 10 days before removing the pups. Dams were euthanized 2, 4, or 6 days after pup removal by carbon dioxide asphyxiation. The right, fourth mammary gland was fixed and embedded in paraffin while the contralateral gland was analyzed by whole mount staining.

Role of ALS in GH-rescue of PRLR heterozygous mammary phenotype

PRLR heterozygous (PRLR+/-) and WT (PRLR+/+) mice on a C57Bl/6 background were obtained from The Jackson Laboratory (Bar Harbor, ME). On this background, female PRLR-/- are infertile and PRLR+/- fail to lactate, the PRLR line was propagated by crossing WT females with PRLR+/- males.

Experimental dams of interest were WT or null ALS mice harboring a single functional PRLR allele (i.e. ALS+/+/PRLR+/- or ALS-/-/PRLR+/-). These animals were generated as followed. First, PRLR+/- males were mated with WT or null ALS mice. These mice originated from the ALS 12 line backcrossed for 5 generations onto a C57Bl/6 background. F1 males of interested were recovered (either ALS+/+/PRLR+/- or ALS+/-/PRLR+/-). ALS+/+/PRLR+/- males were crossed to WT ALS mice to generate WT ALS females harboring one or two functional PRLR allele(s). ALS+/-/PRLR+/- males were crossed to null ALS mice to generate null ALS mice harboring one or two functional PRLR allele(s).

Seventy-two female mice were placed with proven male mice (n=10-16 for each of the four genotypes), and checked daily for presence of copulatory plug. The day a plug was observed was considered pregnancy d1. A first subset of mice (n = 6-8 for each of the four genotypes) was sacrificed at d14 of pregnancy. A second subset of mice (n = 8-14 for each of the four genotypes) were also sacrificed. WT or null ALS harboring one functional PRLR allele were randomly allocated to receive a daily subcutaneous injection of the vehicle, 20% polyvinylpyrrolidone (PVP), or 300 μg of bGH in 20% PVP (GH) on d14-17 of pregnancy (n = 6-8 for each genotype by treatment combination). Animals were sacrificed at d18 of pregnancy. To verify that loss of ALS does not influence mammary development in late pregnancy in this mouse strain, WT and null ALS mice harboring two functional PRLR alleles (n = 8 per genotype) were also sacrificed on d18 of pregnancy. All animals were euthanized by carbon dioxide asphyxiation, and blood was collected by cardiac puncture, processed into plasma by the addition of heparin (60 U/mL), and stored at -20°C. The fifth mammary glands and liver were dissected, snap-frozen immediately in liquid nitrogen, and stored at -80°C for extraction of total RNA. The right, fourth mammary gland was fixed and embedded in paraffin while the contralateral gland was analyzed by whole mount staining.

Genotyping analysis

DNA was isolated from tail biopsies using the HotSHOT method (Truett *et al.* 2000). Briefly, tail biopsies (~4 mm) were incubated at 95°C for 1 h in 100 μL hydrolysis solution (25 mM NaOH, 0.2 mM EDTA, pH 12). Samples were neutralized with an equal volume of 40 mM Tris-HCl, pH 5.0. Genotyping was performed by PCR using 2 μL of neutralized solution. Final volume of the PCR reaction was 20 μL and contained 1X Taq PCR buffer (10 mM Tris-HCl, 50 mM KCl, 0.1% Triton x-100 and 1.0 mM $MgCl_2$), 0.2 mM dNTPs and 0.625 units of Taq

polymerase (Promega, Madison, WI). Primer sequences and expected product sizes are given in Table 4.1. For ALS genotyping, final primer concentrations were 0.25 μM for F-Neo1 and F-ALS and 0.15 μM for R-mPrB. The reaction was first denatured at 95°C for 5 minutes. This was followed by 25 cycles of 94°C for 30 seconds, 60°C for 30 seconds, and 72°C for 1 minute with a 5 second extension per cycle. A last cycle was performed identically except that the 72°C step lasted 7 minutes. This combination of primers yielded bands of 602 bp for the WT ALS allele and 395 bp for the null ALS allele. Products were visualized by agarose gel electrophoresis.

For PRLR genotyping, final primer concentrations were 0.25 μM for F-NeoP, 0.6 μM for F-PRLR, and 0.4 μM for R-PRLR. The reaction was first denatured at 94°C for 3 minutes. This was followed by 34 cycles of 94°C for 30 seconds, 67°C for 1 minute, and 72°C for 1 minute. A last cycle was performed identically except that the 72°C lasted 2 minutes. This combination of primers yielded bands of 537 bp for the WT PRLR allele and 400 bp for the null PRLR allele. Products were visualized by agarose gel electrophoresis.

Analysis of plasma IGF-I and estradiol

Plasma IGF-I concentrations were measured using a rat IGF-I double antibody radioimmunoassay (RIA) purchased from Beckman Coulter (Webster, Texas). Analysis was performed as recommended by the manufacturer using 25 μL plasma for acid-ethanol extraction.

Plasma estradiol concentrations were measured using a RIA kit (Coat-A-Count Estradiol Kit, Siemens Medical Solutions Diagnostic, Malvern, PA). The assay was performed in duplicate using 50 μL of plasma.

Table 4.1. Nucelotide sequence of oligonucleotide primers used in PCR determination of ALS and PRLR genotype and size of the expected products.

Target Gene		Primers[1]	Product size (bp)[2]
ALS			
	Forward ALSgeno3	TGC AGC TGG GCC ACA ATC GAA TC	
	Reverse mPrB	GCA AGG AGT TAT TCC TGA GGT TG	602 (+)/395 (-)
	Forward Neo1	GAC ATA GCG TTG GCT ACC CGT GA	
PRLR			
	Forward PRLR	CAC AGT AAA TGC CAC GAA CG	
	Reverse PRLR	CCT CCC TTT CCA GAA AGC AT	537 (+)/400 (-)
	Forward NeoP	GCT TCC TCT TGC AAA ACC ACA CTG	

[1]Primer sequences shown in the 5' to 3' orientation.

[2] (+), wild type allele; (-), mutated allele

RNA isolation and Northern analysis

Total RNA from liver and mammary glands was extracted by affinity chromatography method as recommended by the manufacturer (RNeasy® Mini Kit, Qiagen Inc., Valencia, CA). The concentration of total RNA was determined by absorbance at 260 nm, and RNA quality was assessed on formaldehyde agarose gel by SYBR Green II staining (Molecular Probes, Eugene, OR).

For Northern analysis, total RNA (10 μg) was electrophoresed on a 1% denaturing agarose gel containing 0.66 M formaldehyde, 1X MOPS (0.04 M 3-N-Morpholino-propanesulfonic acid, 0.05 M sodium acetate, 0.001 M EDTA, pH 8.0). Electrophoresis was performed for 2 h at 80 V in 1X MOPS. Total RNA was transferred onto a nylon membrane (GeneScreen™, NEN® Research Products) by capillary transfer in 10X SSPE (1X SSPE = 0.18 M NaCl, 1 mM EDTA, pH 8.0; 1 mM sodium phosphate). Membranes were irradiated in a UV crosslinker at 120 mJ/cm^2, were dried for 1 h at 60°C, and stored at -20°C until hybridization.

To detect ALS mRNA, membranes were prehybridized at 50°C in a solution of 50% formamide/dextran sulfate, 5X SSPE, 10X Denhardt's [1X Denhardt's = 0.02% bovine serum albumin (BSA), 0.02% ficoll 400, 0.02% polyvinylpyrrolidone (MW 40,000)], 100 mg/ml salmon sperm DNA, and 1% SDS. The ALS probe used was a 750 bp DNA fragment corresponding to nt +163 to nt +915 of the mouse ALS cDNA (numbering relative to $A_{+1}TG$) (Ueki *et al.* 2000). The probe was labeled with [α-^{32}P] dCTP (3000 Ci/mmol) by random priming (Prime-It, Stratagene, La Jolla, CA). After a 2 h prehybridization, the DNA probe (~1 x 10^6 dpm/ml) was added and the hybridization continued overnight. After hybridization, membranes were washed twice for 30 minutes in a solution of 2X SSPE/0.2% SDS at room temperature, and twice for 15 minutes in a solution of 0.1X SSPE at 60°C.

The 18S ribosomal RNA was detected with a low specificity labeled oligonucleotide (Deindl 2001). The oligo sequence is 5'-CGG AAC TAC GAC GGT ATC TG-3' and was labeled with [γ-^{32}P] dATP (3000 Ci/mmol) using T4 polynucleotide kinase (Promega, Madison, WI). Hybridizations were conducted at 42°C in a solution of 50% formamide/dextran sulfate, 5X SSPE, 10X Denhardt's, 1% SDS. Hybridizations were performed with the labeled probe (~2 x 10^6 dpm/ml) mixed with a 10-fold molar excess of unlabelled oligonucleotide. Membranes were washed three times each with 2X SSPE/0.2% SDS at 45°C.

For visualization of ALS and 18S signals, membranes were exposed to x-ray film (Fuji Medical Systems USA, Inc., Stanford, CT). Signals were quantified by phosphoimaging using a FUJIX BIO-IMAGING ANALYSER BAS1000 (Fuji Photo Film Co., Ltd.).

Mammary gland whole mounts and histology

Whole mounts of mammary glands were performed as described by (Cui *et al.* 2004). First, individual mammary glands were spread onto a glass slide. The glands were fixed overnight in Carnoy's solution (60% ethanol, 30% chloroform, 10% acetic acid), post-fixed in 70% ethanol, rehydrated in a decreasing gradient of ethanol, and stained overnight in carmine-alum. Slides were then dehydrated in an increasing ethanol gradient, cleared in xylene overnight, and coverslips were attached using Permount (Fisher Scientific, Pittsburg, PA).

For histology, mammary tissues were fixed in 10% neutral buffered formalin overnight. Tissues were embedded in paraffin, sectioned, and stained with hematoxylin and eosin (H&E). Images of whole mounts were obtained using a dissecting microscope and digital camera. Images of histological sections were captured using bright field microscopy.

Ductal length was quantified by measuring the number of pixels between the center of the lymph node and the furthest extending duct. An image of a ruler photographed under the same magnification was used to convert pixel number to mm. In this analysis, negative numbers are obtained when the ducts have not yet reached the node and the opposite when ducts have extended beyond the node.

Immunohistochemistry

Mammary glands were fixed in 10% neutral buffered formalin overnight at 4°C, embedded in paraffin, and sectioned. The tissues were then dewaxed in xylene and rehydrated through a descending gradient of ethanol. Sections were incubated at 95°C for 20 min in 0.01M sodium citrate buffer (pH 6.0) for antigen retrieval. Tissues were permeabilized in 1X PBS +0.2% Triton X-100 for 20 minutes. Slides were washed 3 times (3 minutes each) in 1X PBS +0.1% Triton X-100 and 3 times (3 minutes each) in 1X PBS. Sections were blocked at room temperature for 1 hr in 10% normal donkey serum +1% BSA in 1X PBS, pH 7.4. Samples were first incubated with goat anti-mouse ALS (R&D Systems, Inc., Minneapolis, MN) diluted 1:500 in 1X PBS +1% BSA overnight at 4°C. Slides were washed as above then incubated with Cy3-conjugated donkey anti-goat antibody (Jackson ImmunoResearch Laboratories, Inc., West Grove, PA) diluted 1:500 in 1X PBS +1% BSA for 1 h at room temperature. Slides were washed as above. Nuclei were stained with 4´,6-diamidino-2-phenylindole [DAPI (Sigma, St. Louis, MO)]. Tissue staining was documented using an Axiovert 40 microscope (Carl Zeiss, Inc., Thornwood, NY) equipped with an AxioCam camera (Carl Zeiss, Inc.).

Statistical analyses

Analyses were performed using SAS statistical software (SAS Institute, Cary, NC). Data were analyzed using the MIXED procedure of SAS (SAS Institute). For the ALS expression data, the model included the fixed effects of stage (Stage) and

tissue (Tissue), and their interaction (Stage x Tissue). For the pubertal mammary development data, the model included the main effect of genotype (Geno). For the plasma IGF-I data at pregnancy d14, the model included the fixed effects of PRLR genotype (PRLR) and ALS genotype (Geno) and their interaction. At pregnancy d18, the model included the fixed effects of genotype (Geno) and treatment (Trt) and their interaction (Geno x Trt). Statistical significance was set to $P<0.05$ for main effects and $P<0.10$ for the interaction.

RESULTS

Expression of ALS in the mammary gland throughout development

In the mouse, we have detected ALS gene expression in the liver, gonadal fat, and kidney, and virgin mammary gland (Giesy 2004). ALS expression has not been described throughout the different phases of mammary development in any species. To do this in the mouse, we obtained the mammary gland during the virgin state, on d18 of pregnancy, on d5 of lactation, and on d2 of involution. At each developmental stage, mammary ALS expression was determined and compared to hepatic ALS expression.

The relationship between liver and mammary expression in the virgin state was different than that in the pregnant, lactating or involuting state (Figure 4.1; Tissue x State, $P<0.01$). Expression in the mammary gland was only 15% of that of liver in the virgin state (Tissue, $P<0.001$). In all other states, however, mammary ALS expression increased substantially such that it was similar to hepatic expression. Therefore, pregnancy, lactation, and involution are periods of high ALS expression in the mammary gland.

Next, we attempted to identify the mammary compartment expressing ALS using immunohistochemistry. During pregnancy, lactation, and involution, ALS immunoreactivity was detected within the ductal and/or alveolar lumens (Figure 4.2).

Figure 4.1. Effect of physiological state on the expression of the ALS gene in liver and mammary gland. FVB mice were sacrificed when virgin (112d of age) and on d18 of pregnancy, d5 of lactation, or 2 days after pup removal (involution). Liver and the 4th mammary gland were collected. *Top*: Total RNA was isolated from tissues and analyzed by Northern blotting for expression of the ALS and 18S genes. Samples from 3 representative females are shown. *Bottom*: Each bar represents the mean ± SE (n=4-6/state) of the ALS signal (normalized to 18S). The effects of tissue (Tissue), physiological state (State), and their interaction (Tissue x State) are reported.

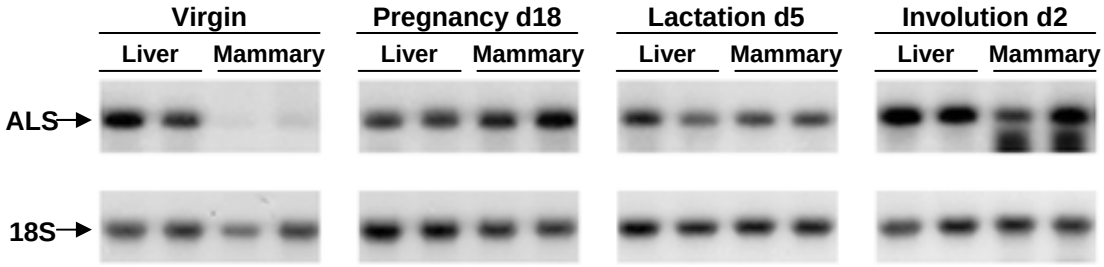
Virgin
Pregnancy d18
Lactation d5
Involution d2
Liver
Mammary
Liver
Mammary
Liver
Mammary
Liver
Mammary
ALS
18S

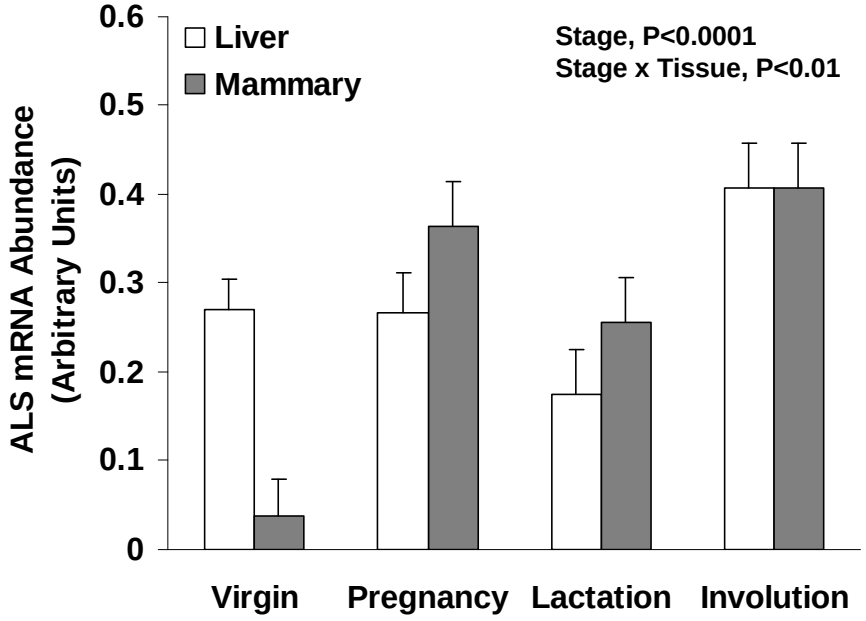
Liver
Mammary
Stage, P<0.0001
Stage x Tissue, P<0.01
ALS mRNA Abundance
(Arbitrary Units)
0.6
0.5
0.4
0.3
0.2
0.1
0
Virgin
Pregnancy
Lactation
Involution

Figure 4.2. Immunodetection of the ALS in the mammary gland. Wild type (WT) and null ALS (Null) mice were sacrificed on d18 or pregnancy, d2 of lactation, or 2 days after pup removal (involution). The 4th mammary gland was collected and analyzed for ALS protein by immunohistochemistry. Photographs for ALS staining (red) and nuclei staining (blue) are shown individually or as a merged photograph. Glands from null ALS mice served as negative controls. Representative photographs are shown.

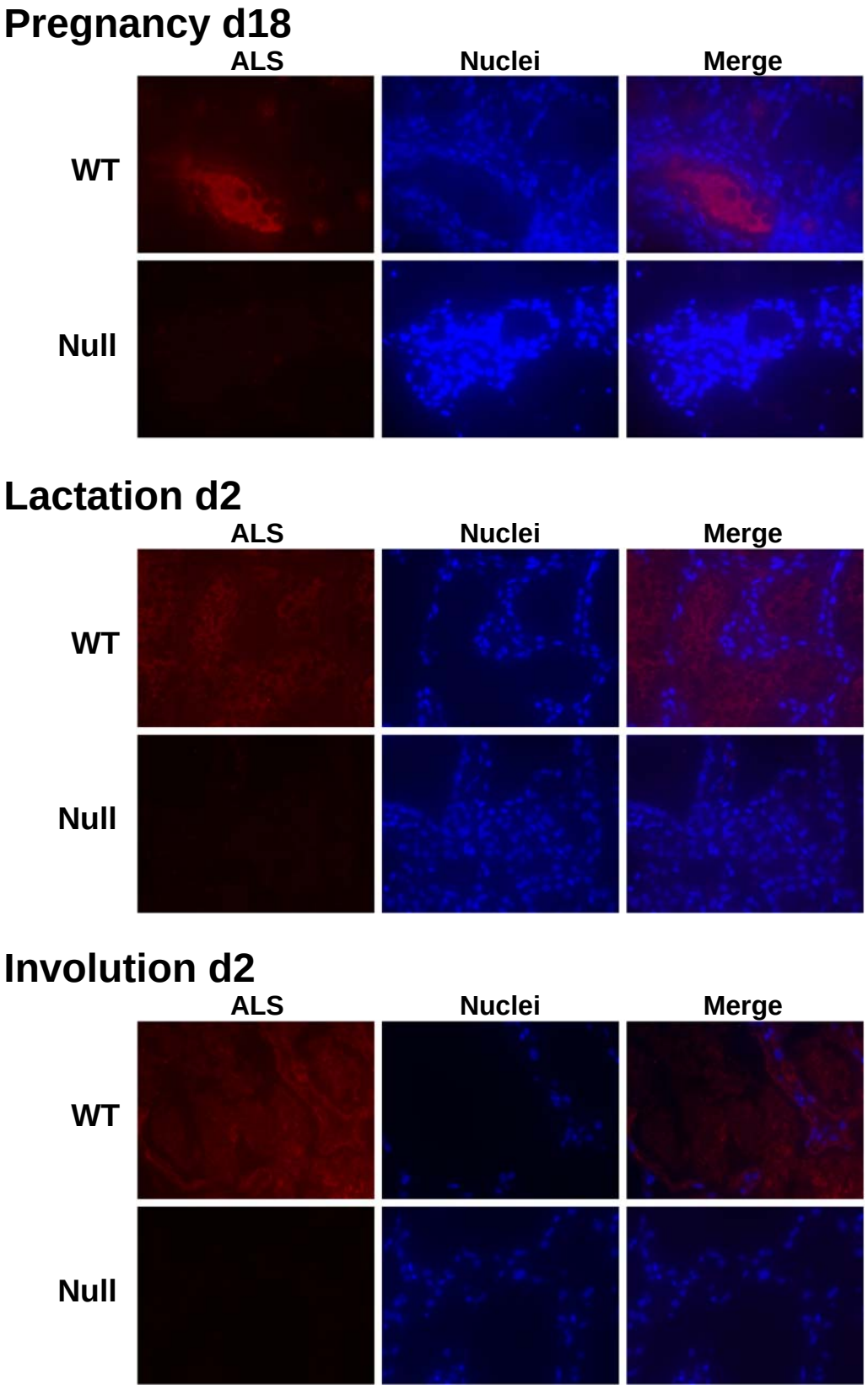
Pregnancy d18
ALS
Nuclei
Merge
WT
Null
Lactation d2
ALS
Nuclei
Merge
WT
Null
Involution d2
ALS
Nuclei
Merge
WT
Null

ALS immunoreactivity, however, was not visible in mammary epithelial cells as the signal did not localize in proximity of the stained nuclei. The antibody was specific for ALS as no signal was observed in mammary glands from null ALS mice.

Mammary development before and after puberty

To determine if ALS is important for this phase of mammary development, mammary gland whole mounts were prepared from WT and null ALS mice at 4, 6, and 8 wk of age. Ductal elongation was measured as the distance from the mammary lymph node. At 4 weeks of age, ductal extension was comparable between WT and null ALS mice (Figure 4.3; Geno, $P>0.10$). At 6 weeks of age, however, ductal extension was significantly less in null than WT mice (0.9 mm in null vs 4.4 mm in WT; Geno, $P<0.05$). At 8 weeks of age, ductal elongation tended to be greater in WT than null ALS mice (Geno, $P\leq0.10$). These results indicate that mammary ductal elongation progresses at a slower rate in the absence of ALS.

Body and uterine weights were also analyzed in these virgin animals (Table 4.2). As expected, null mice weighed significantly less than their WT counterparts at 4 and 6 weeks of age (Geno, $P<0.05$ or less). At 8 weeks of age, null mice tended to weigh less than WT mice (Geno, $P<0.09$). Absolute uterine weights were significantly lower in null mice at 4 and 8 weeks of age (Table 4.2; Geno, $P<0.05$). When expressed as a percent of body weight, uterine weight was significantly lower in null mice only at 8 weeks of age (Geno, $P<0.05$).

The mammary and uterine data suggested that some aspects of sexual maturation were proceeding more slowly in null ALS mice. Ductal elongation depends on estrogen receptor (ER) signaling even before puberty. To determine whether the slower rate of ductal extension is related to an estrogen deficit, we measured plasma estradiol levels at 4 and 6 weeks of age. Plasma estrogen levels were significantly higher in null than in WT mice at both ages (Figure 4.4A; Geno,

Figure 4.3. Mammary gland development in virgin wild type and null ALS mice. *Top:* Wild type (WT) and null ALS (Null) mice at diestrus were sacrificed at 4, 6, and 8 weeks of age (n = 5-6 for each genotype by treatment combination). The 4^{th} mammary gland was collected and analyzed by whole mount. Representative images are shown. *Bottom:* Ductal length relative to the furthest duct was measured to the center of the lymph node. Values are negative when ducts have not reached the node and positive when extended beyond. Each bar represents the mean ± SE of 5-6 mice. WT were compared to Null at each time with * $P < 0.05$, # $P \leq 0.10$.

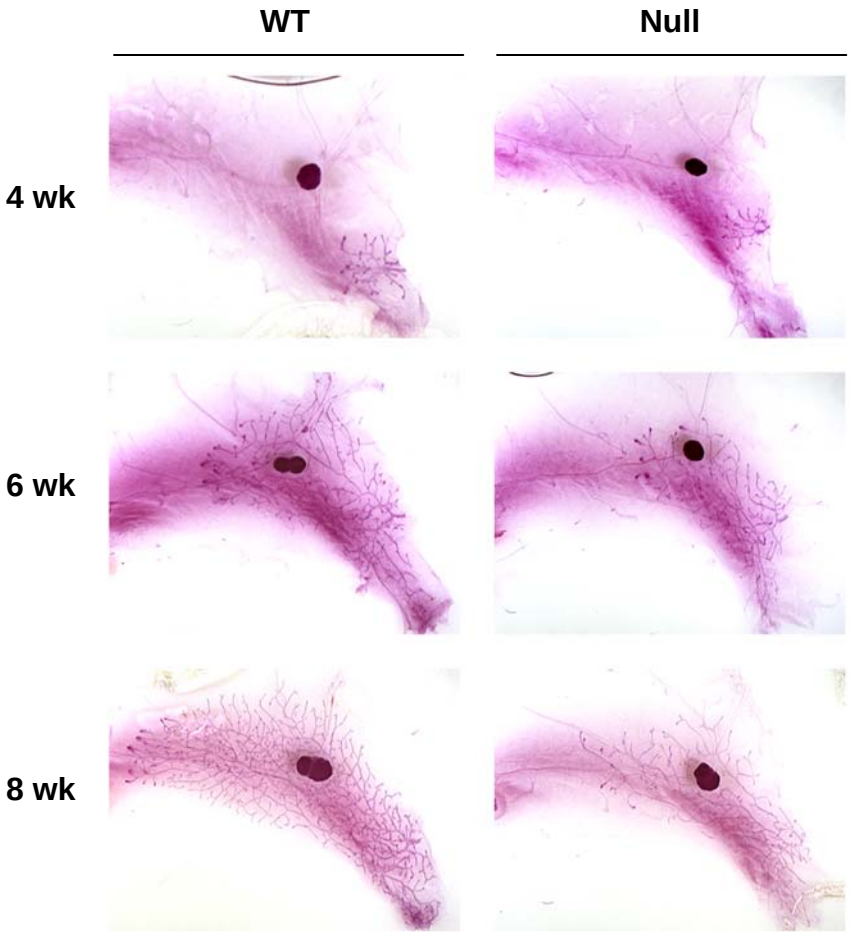
WT
Null
4 wk
6 wk
8 wk

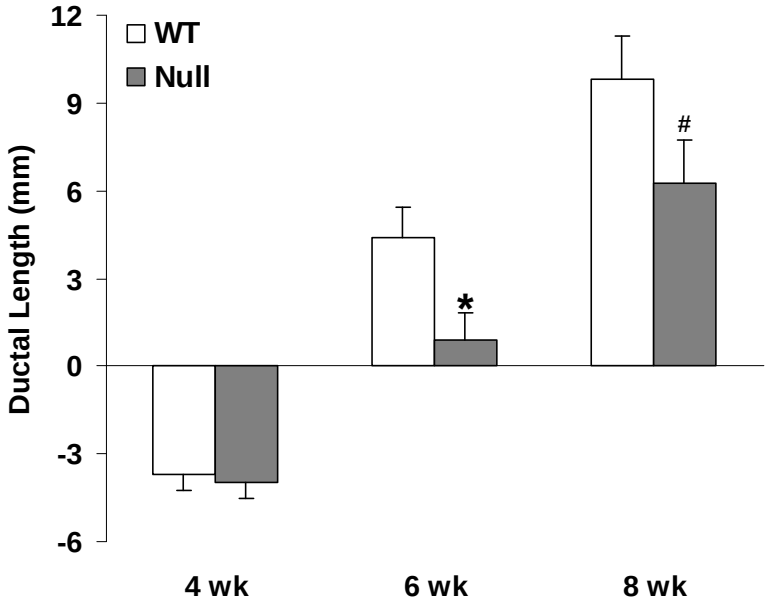
WT
Null
Ductal Length (mm)
12
9
6
3
0
-3
-6
*
#
4 wk
6 wk
8 wk

Table 4.2. Body and uterine weights of wild type and null ALS female mice during puberty.

		WT[1]	Null[1]	SEM	Significance[2]
4 weeks					
	Body weight (g)	13.06	10.41	0.50	0.01
	Uterine weight (absolute, g)	0.011	0.008	0.001	0.03
	Uterine weight (% BW)	0.08	0.07	0.01	NS
6 weeks					
	Body weight (g)	16.01	13.70	0.54	0.02
	Uterine weight (absolute, g)	0.016	0.013	0.002	NS
	Uterine weight (% BW)	0.10	0.09	0.01	NS
8 weeks					
	Body weight (g)	17.61	15.68	0.71	0.09
	Uterine weight (absolute, g)	0.047	0.029	0.004	0.02
	Uterine weight (% BW)	0.27	0.18	0.02	0.04

[1]Female wild type (WT) and null ALS (Null) mice were sacrificed at diestrus at 4, 6, or 8 weeks of age. N = 5-6 mice per genotype at each age.

[2]Significance level for the effect of genotype; NS, non significant (P>0.10).

Figure 4.4. Plasma estrogen and IGF-I levels in virgin wild type and null ALS mice. Plasma was collected from wild type (WT) and null ALS (Null) mice and analyzed by radioimmunoassay for estrogen at 4 and 6 weeks of age (A) and IGF-I at 4 weeks of age (B). Each bar represents the mean ± SE of 6 mice. The significant effect of genotype (Geno) is reported.

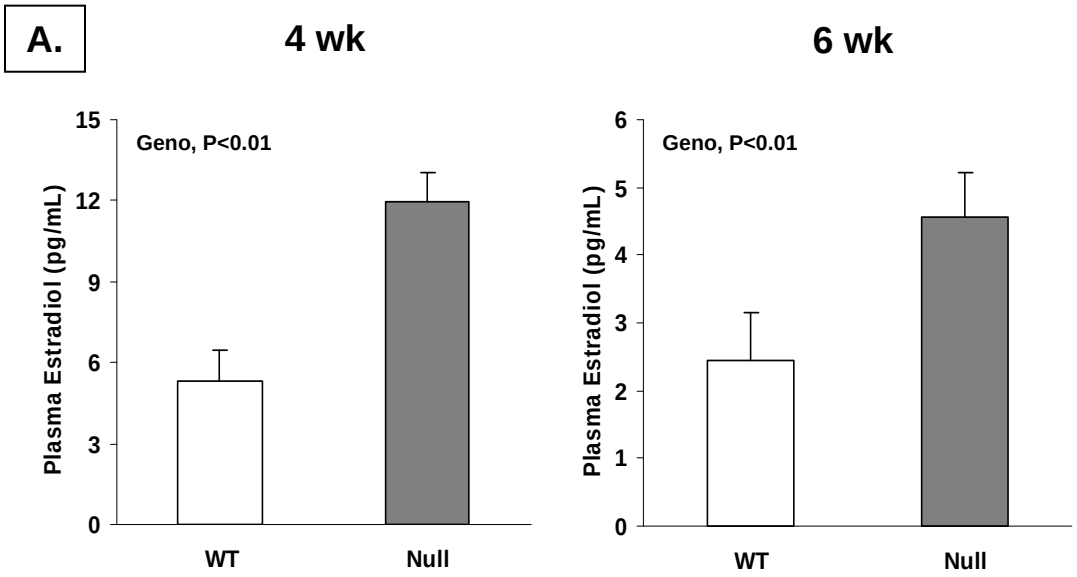
A.
4 wk
6 wk
Geno, P<0.01
Geno, P<0.01
Plasma Estradiol (pg/mL)
Plasma Estradiol (pg/mL)
15
12
9
6
3
0
6
5
4
3
2
1
0
WT
Null
WT
Null

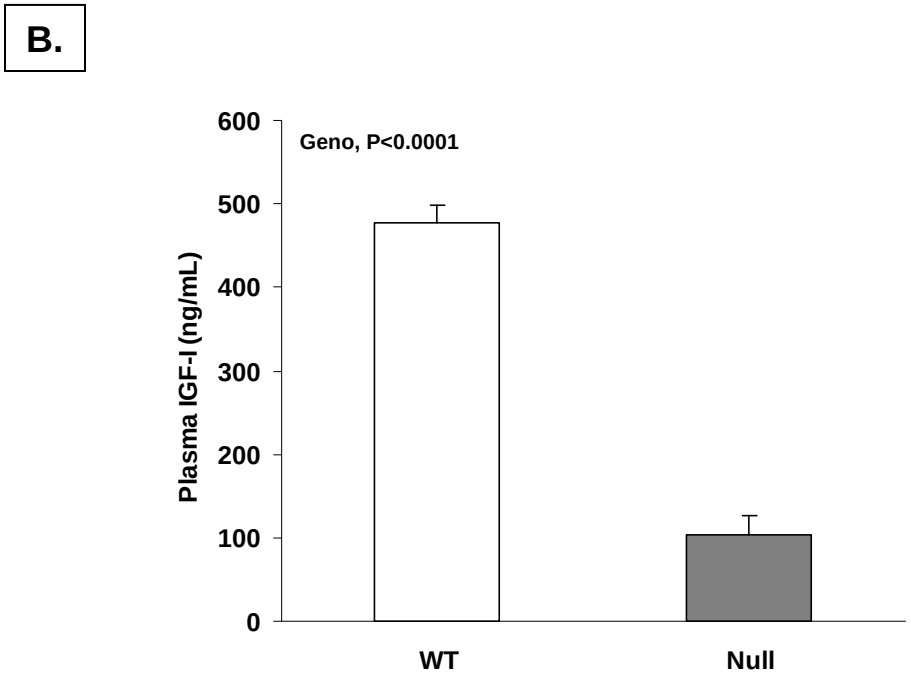
B.
Geno, P<0.0001
Plasma IGF-I (ng/mL)
600
500
400
300
200
100
0
WT
Null

P<0.01). We also measured circulating IGF-I levels at 4 weeks of age. Plasma IGF-I levels in ALS null mice were only 20% of wild type levels (Figure 4.4B; Geno, P<0.0001).

As a functional test for sexual maturation, we compared WT and null ALS mice for the timing of vaginal opening and presence of a copulatory plug when placed with a proven male starting at 24 d of age. Age at vaginal opening was similar between null and WT mice (Table 4.3; Geno, P>0.10); however, age at plug tended to be greater in null mice (41.3 d vs 37.9 d, null vs WT; Geno, P<0.07). As expected, ALS null mice weighed 15% less on day of plug (Table 4.3; Geno, P<0.01).

All mice were sacrificed 3 days later to evaluate other indices affected by sexual maturation (Table 4.3). There was no difference in absolute or percent uterine weight (Geno, P>0.10). Interestingly, null females tended to have fewer corpora lutea (CL) than WT females at the surface of their ovaries (Geno, P<0.09), suggesting that they ovulated fewer eggs. Finally, mammary ductal length was similar between WT and null ALS in this set of mice (Geno, P>0.10). Overall, these data show that lack of ALS results in delayed ductal elongation during pubertal development. In the presence of a male, null ALS animals tend to reach puberty at a slightly older age but show no impairment in ductal development by the time a plug is detected.

Mammary development during pregnancy

In order to determine the importance of ALS during pregnancy, mammary whole mounts were collected from WT and null ALS mice in early (d8) and late (d18) pregnancy. Early pregnancy is a period of rapid ductal branching and alveolar bud formation. These structures were readily observed in glands from WT mice but appeared less abundant in null ALS mice (Figure 4.5A).

Late pregnancy is characterized by near complete invasion of the mammary fat pad by the future secretory epithelium and by the presence of completely formed

Table 4.3. Indices of puberty in wild type and ALS null female mice.

	WT[1]	Null[1]	SEM	Significance[2]
Age at vaginal opening (d)	29.7	29.1	0.7	NS
Age at plug (d)	37.9	41.3	1.2	0.07
Weight at plug (g)	17.40	14.75	0.37	0.01
Weight at sacrifice (g)	18.72	15.04	0.42	0.01
Uterine weight (absolute, g)	0.067	0.061	0.004	NS
Uterine weight (% BW)	0.36	0.40	0.02	NS
Number of corpora lutea	7.6	6.3	0.5	0.09
Mammary ductal length (mm)	3.5	3.6	0.7	NS

[1]Female wild type (WT) and null ALS (Null) were placed with proven male mice at 24d of age and monitored daily. Mice were euthanized 3 days after observation of copulatory plug. N = 10 for each genotype.

[2] Significance level for the effect of genotype ($P<0.05$); NS, non significant ($P>0.10$).

Figure 4.5. Mammary gland development in wild type and null ALS mice during pregnancy. Wild type (WT) and null ALS (Null) mice were sacrificed on d8 and d18 of pregnancy (n =3 for each genotype x time combination), and the 4th mammary gland was collected. A: Whole mounts (WM) were prepared at each stage of pregnancy. Representative images are shown. Alveolar buds are marked with an arrowhead. B: On d18 of pregnancy, histological evaluation was performed with hematoxylin and eosin (H&E) staining, and slides were photographed at 2 levels of magnification (50X and 400X). Representative images are shown. Lipid droplets are marked with an arrowhead and proteinacious secretions are marked by an asterisk.

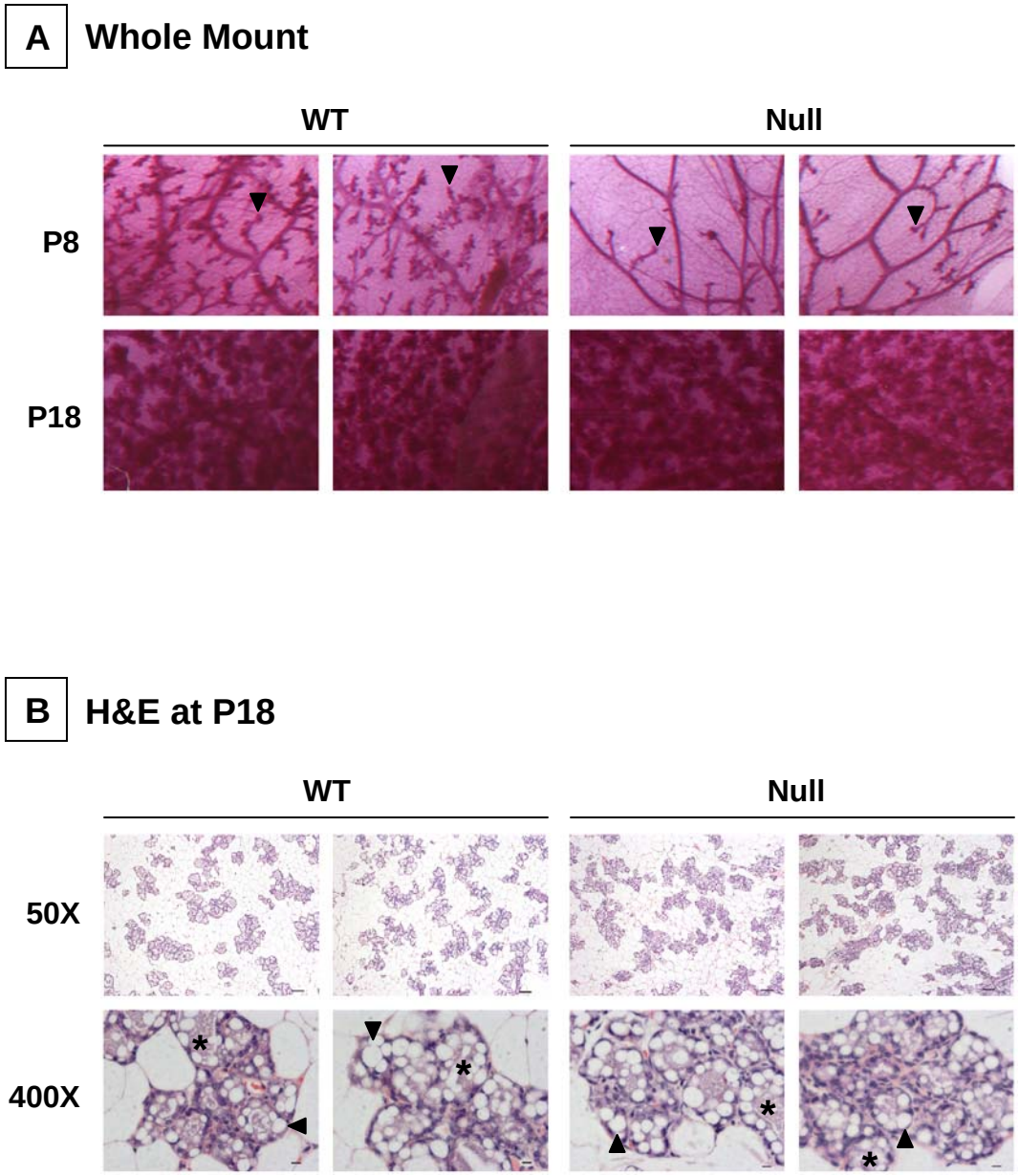
A
Whole Mount
WT
Null
P8
P18
B
H&E at P18
WT
Null
50X
400X

alveolar structures. This was seen equally well at d18 of pregnancy in both WT and null ALS mammary glands (Figure 4.5B, H&E 50X). Moreover, both WT and null ALS mammary glands appeared similarly differentiated as shown by the presence of milk fat droplets within the alveolar epithelial cells and proteinacious material within the alveolar lumen (Figure 4.5B, H&E 400X). These results suggest that ALS may promote early alveolar formation but is not essential for its completion by late pregnancy.

Next we tested the role of ALS for mammary gland development in mice heterozygous for the PRLR (PRLR +/-). These mice have a complete block in alveolar expansion starting on d14 of pregnancy. Allan *et al.* (2002) showed that exogenous GH therapy rescued this defect and speculated that a GH-dependent increase in plasma IGF-I was involved. GH, however, is unable to increase plasma IGF-I in null ALS mice (Ueki 2006). These observations prompted us to ask whether GH could still rescue the mammary defect occurring in PRLR +/- mice in the absence of ALS. WT and null ALS mice carrying a single functional PRLR allele were created. To confirm that the alveolar expansion defect occurred in these mice, mammary development was examined by whole mount at pregnancy d18. In mice carrying two functional PRLR alleles, mammary alveolar differentiation had occurred. The alveoli were filling the fat pad, and fat droplets were observed within the epithelial cells (Figure 4.6, H&E 400X). Presence of a single PRLR allele was insufficient to support full alveolar expansion in mice. This defect occurred to the same extent in null ALS mice (Figure 4.6, H&E 50X).

Next, WT and null ALS mice carrying a single functional PRLR allele were treated with exogenous GH between d14-d17 of pregnancy. At pregnancy d14, PRLR copy number did not impact plasma IGF-I, but absence of ALS reduced plasma IGF-I from 210 to 144 ng/mL (Figure 4.7A; Geno, $P<0.05$). At pregnancy d18, GH

Figure 4.6. Mammary gland development in wild type and ALS null mice carrying one or two functional copies of the PRLR gene during late pregnancy. Wild type (WT) and null ALS (Null) mice carrying two functional copies of the PRLR (PRLR +/+) or only one (PRLR +/-) were sacrificed on d18 of pregnancy (n = 6-9 per genotype). The 4th mammary gland was collected and analyzed by whole mount (WM). Histological evaluation was performed with hematoxylin and eosin (H&E) staining, and slides were photographed at 2 levels of magnification (50X and 400X). Representative images are shown. Lipid droplets are marked with an arrowhead.

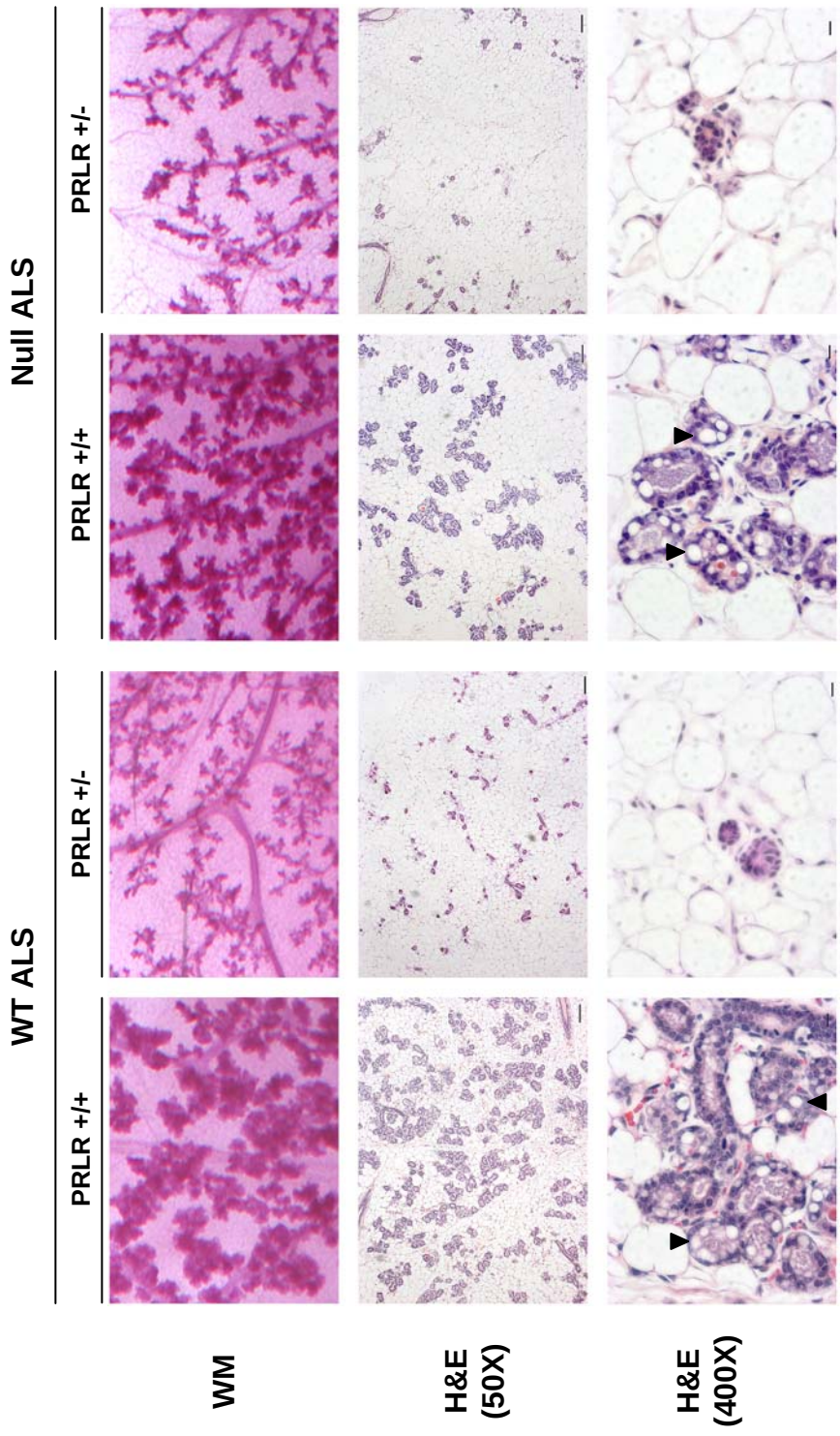
WT ALS
Null ALS
PRLR +/+
PRLR +/-
PRLR +/+
PRLR +/-
WM
H&E (50X)
H&E (400X)

Figure 4.7. Effect of PRLR copy number and ALS genotype on plasma IGF-I. A: On d14 of pregnancy, plasma was collected from mice carrying two functional copies of the PRLR (PRLR +/+) or only one (PRLR +/-) and from wild type (WT) and null ALS (Null) mice. Plasma was assayed for IGF-I by radioimmunoassay. Each bar represents the mean ± SE of 5-6 mice. The significant effect of the ALS genotype (Geno) is reported. B: Wild type (ALS WT) and null ALS (Null) mice carrying one functional copy of the PRLR gene were treated once daily with GH (GH, 300 μg/day) or an equivalent volume of vehicle [20% polyvinylpyrrolidone (PVP)] from d14-17 of pregnancy. Mice were sacrificed on d18 of pregnancy (n = 6-8 for each genotype by treatment combination). Plasma was collected and analyzed for IGF-I by radioimmunoassay. Each bar represents the mean ± SE of 5-6 mice. The effects of genotype (Geno), treatment (Trt), and their interaction (Geno x Trt) are reported.

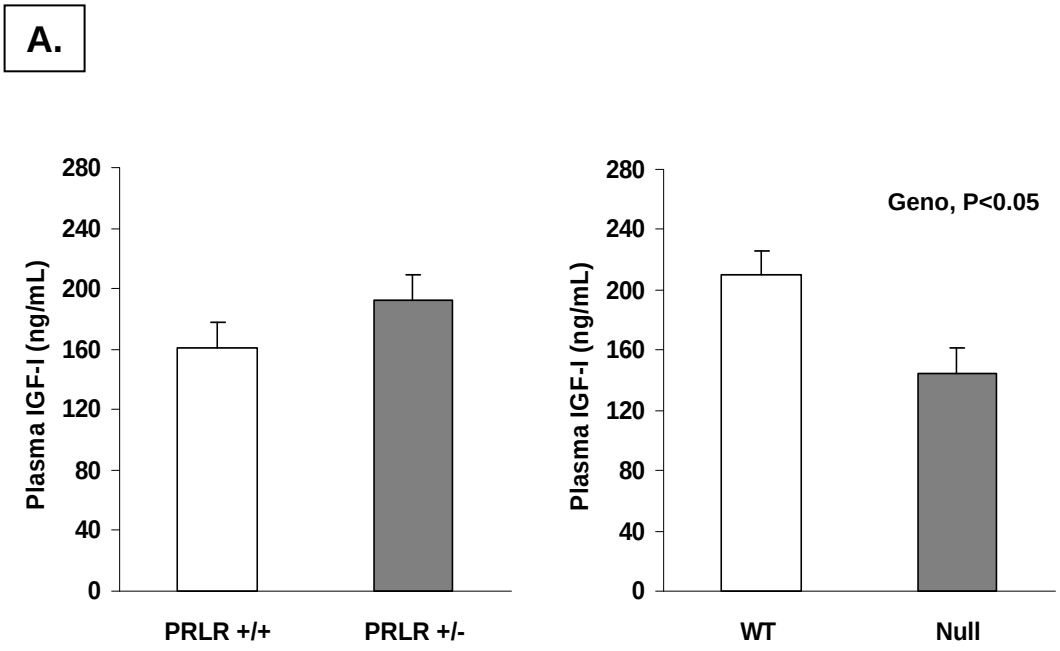
A.
Plasma IGF-I (ng/mL)
280
240
200
160
120
80
40
0
PRLR +/+
PRLR +/-
Geno, P<0.05
WT
Null

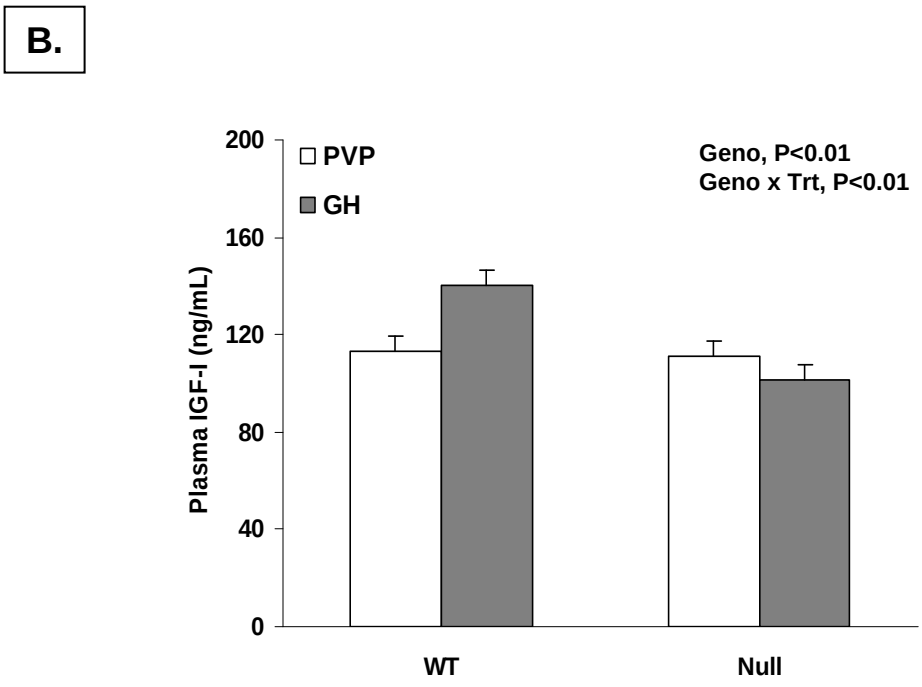
B.
Plasma IGF-I (ng/mL)
200
160
120
80
40
0
PVP
GH
Geno, P<0.01
Geno x Trt, P<0.01
WT
Null

increased plasma IGF-I 25% in WT mice but had no effect in null ALS mice (Figure 4.7B; Geno x Trt, $P<0.05$). Unexpectedly, plasma IGF-I levels were not different between null ALS and WT vehicle-treated mice. Mammary glands were also obtained at pregnancy d18 and examined by whole mount analysis. Exogenous GH treatment stimulated alveolar expansion irrespective of absence or presence of ALS (Figure 4.8, WM). This is illustrated by increased occupation of the fat pad by alveoli in GH treated animals. Irrespective of the ALS genotype, GH failed to induce the appearance of lipid droplets within the epithelial cells (Figure 4.8, H&E 400X). These data show that the ability of GH to rescue the alveolar expansion defect in PRLR +/- occurs in the absence of any change in plasma IGF-I and is completely independent of ALS.

Mammary development during lactation and involution

A coordinated balance between IGF-I and IGFBPs is necessary for survival of the epithelial cell population during lactation. To determine whether ALS may regulate this balance, mammary whole mounts were collected from WT and null ALS mice during lactation. No discernible differences were detected between the whole mounts of WT and null mice at d2 and d10 of lactation (Figure 4.9, WM). Histology of the gland appears to be normal in both genotypes with the alveoli expanding to completely fill the gland by d10 of lactation. Therefore, ALS is not required for mammary development during lactation.

Upon weaning, the lactating gland undergoes involution whereby extensive remodeling of the gland returns it to pre-pregnancy state. The process of involution involves apoptosis of the mammary epithelial cells and structural remodeling of the gland, characterized by a loss of epithelia and reappearance of lipid-filled adipocytes (Richert *et al.* 2000). This process is dependent on the induction of IGFBP-5 synthesis within the mammary gland. IGFBP-5 inactivates IGF-I to allow involution

Figure 4.8. Effect of GH treatment on mammary gland development during late pregnancy in wild type and null ALS mice carrying one functional copy of the PRLR gene. Wild type (ALS WT) and null ALS (Null) mice carrying one functional copy of the PRLR gene were treated once daily with GH (GH, 300 µg/day) or an equivalent volume of vehicle [20% polyvinylpyrrolidone (PVP)] from d14-17 of pregnancy (n = 6-8 for each genotype by treatment combination). Mice were sacrificed on d18 of pregnancy and the 4th mammary gland was collected and analyzed by whole mount (WM). Histological evaluation of mammary tissue sections was performed with hematoxylin and eosin (H&E) staining, and slides were photographed at 2 levels of magnification (50X and 400X). Representative images are shown.

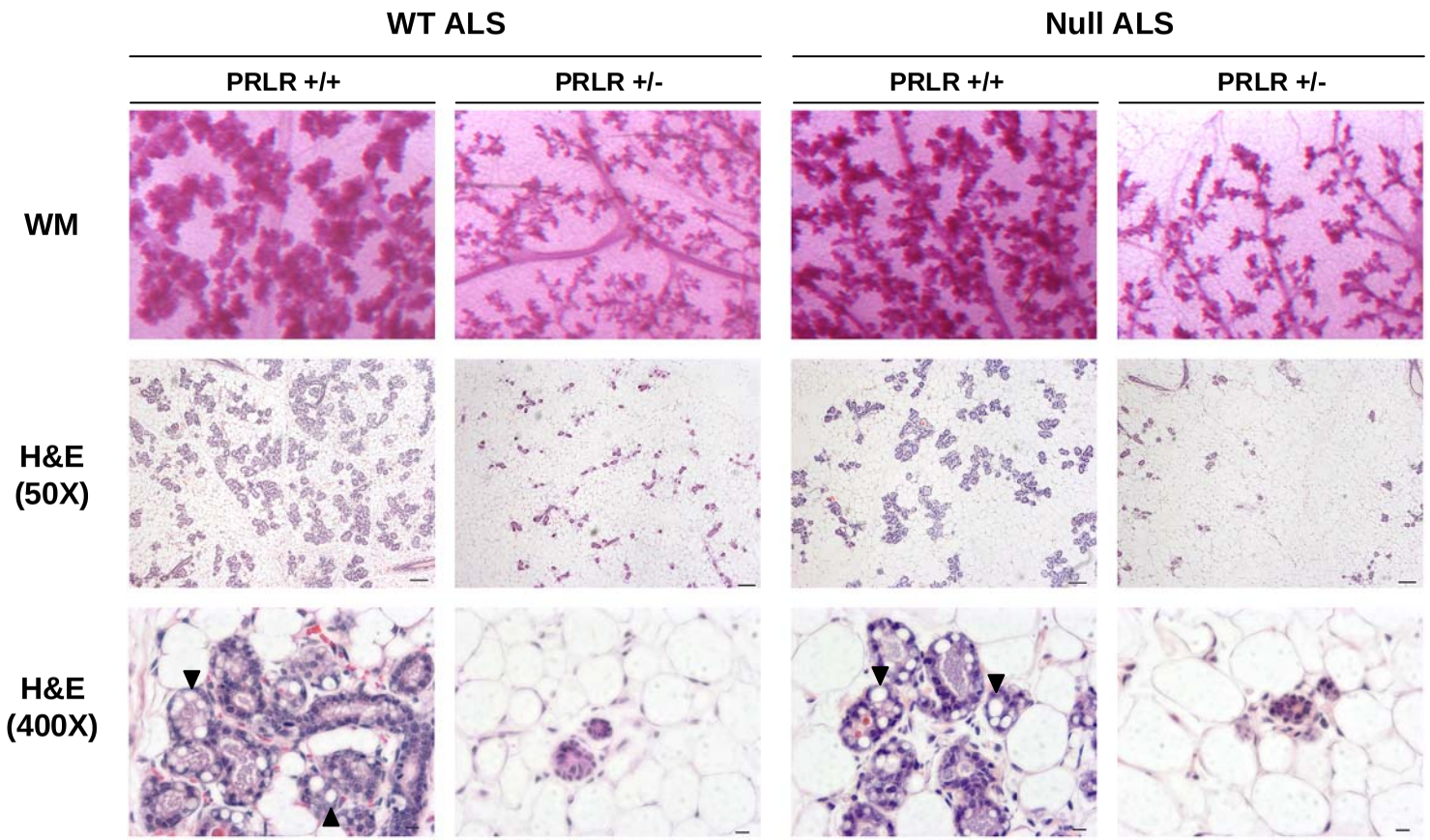
WT ALS
Null ALS
PRLR +/+
PRLR +/-
PRLR +/+
PRLR +/-
WM
H&E
(50X)
H&E
(400X)

Figure 4.9. Mammary gland development in wild type and null ALS mice during lactation. Wild type (WT) and null ALS (Null) were sacrificed on d2 or d10 of lactation (n = 3-6 for each genotype x time combination). The 4th mammary gland was collected and analyzed by whole mount (WM). Histological evaluation was performed with hematoxylin and eosin (H&E) staining, and slides were photographed at two levels of magnification (50X and 400X). Representative images are shown.

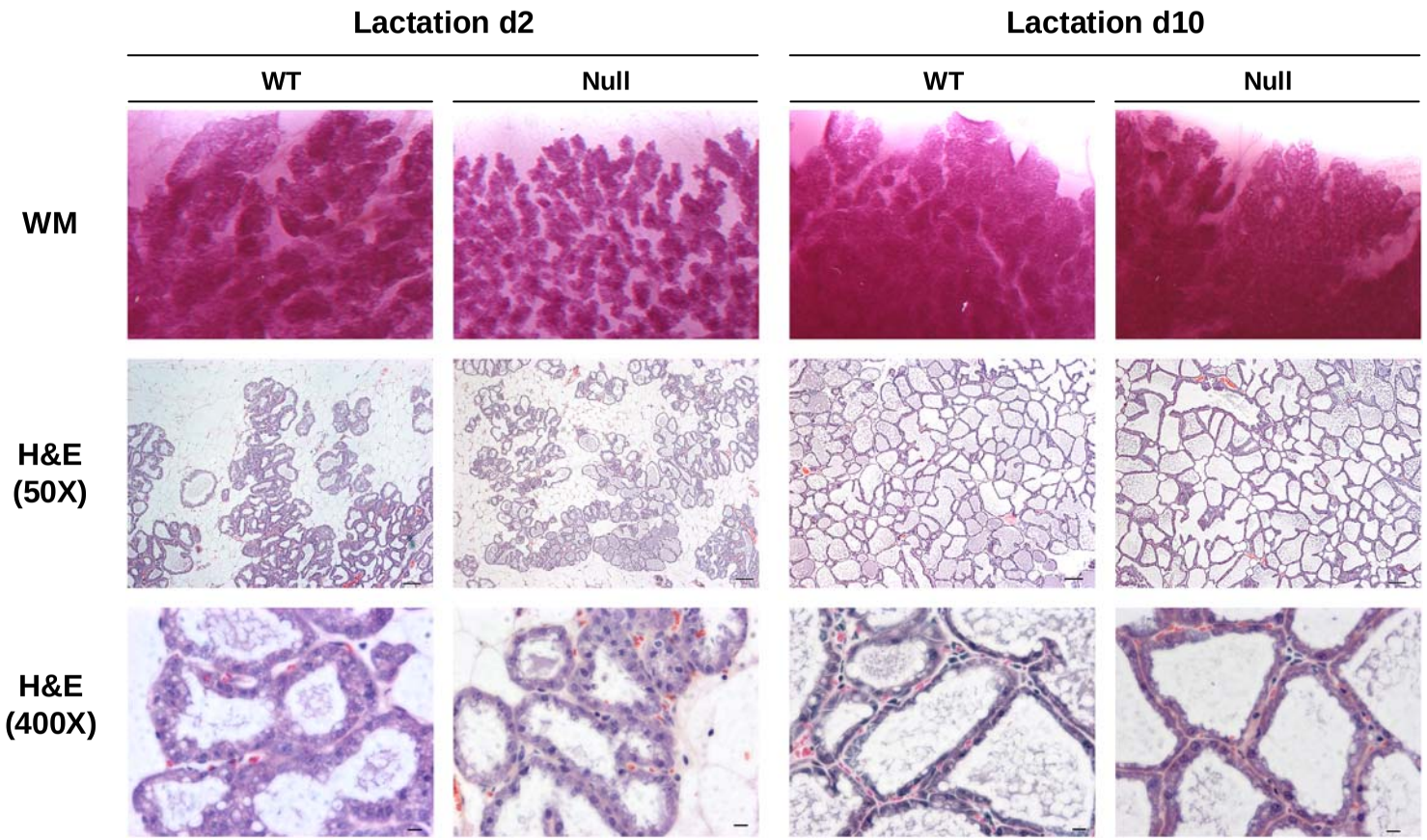
Lactation d2
Lactation d10
WT
Null
WT
Null
WM
H&E
(50X)
H&E
(400X)

to proceed (Flint *et al.* 2008). Since ALS is capable of binding binary IGF-I:IGFBP-5 complexes, we evaluated the progression of involution in null ALS and WT mice.

On d2 of involution, mammary gland morphology was similar between WT and null ALS mice. Epithelial cells occupy the majority of the gland and alveoli are intact (Figure 4.10, H&E 50X). By d4, involution appears to be delayed in null ALS mice. A greater proportion of epithelia still populates the emerging fat pad (Figure 4.10, H&E 50X) and a greater number of alveoli are intact in null ALS mice (Figure 4.10, H&E 400X). Involution is still delayed in null ALS mice at d6. In WT animals, the alveoli have collapsed while alveolar structures are still present in null ALS mice (Figure 4.10, H&E 400X). These data suggest that loss of ALS in the mammary gland delays the process of involution.

DISCUSSION

So far, ALS has been postulated to function exclusively as a component of the circulating IGF-I system. It is responsible for formation of ternary complexes and the development of the circulating IGF-I reservoir (Boisclair *et al.* 2001). Consistent with this, plasma levels of IGF-I and IGFBP-3 are reduced by 62% and 88%, respectively in null ALS mice (Ueki *et al.* 2000). Additional studies have established that IGF-I deficiency associated with lack of ALS had functional impacts. First, null ALS mice suffer a 13-20% growth deficit after birth (Ueki *et al.* 2000). Bone length is shorter and bone metabolism is impaired in null ALS mice (Yakar *et al.* 2002). Null ALS mice have normal plasma glucose and insulin concentrations (Ueki *et al.* 2000) but are protected from GH-mediated insulin resistance (Haluzik *et al.* 2003; Ueki 2006). The mammary gland is highly dependent on the GH-IGF-I system, but the functional role of ALS in mammary development has not been studied.

As an initial step to assess the role of ALS in mammary gland development, we compared mammary gland whole mounts from WT and null ALS mice during the

Figure 4.10. Mammary gland development in wild type and null ALS mice during involution. Wild type (WT) and null ALS (Null) were sacrificed on d2, d4, or d6 after pup removal (involution; n = 3-4 for each genotype x time combination). The 4^{th} mammary gland was collected and analyzed by whole mount (WM). Histological evaluation was performed with hematoxylin and eosin (H&E) staining, and slides were photographed at two levels of magnification (50X and 400X). Representative images are shown. Collapsed alveolar structures are marked with an arrowhead, and intact structures are marked with an asterisk.

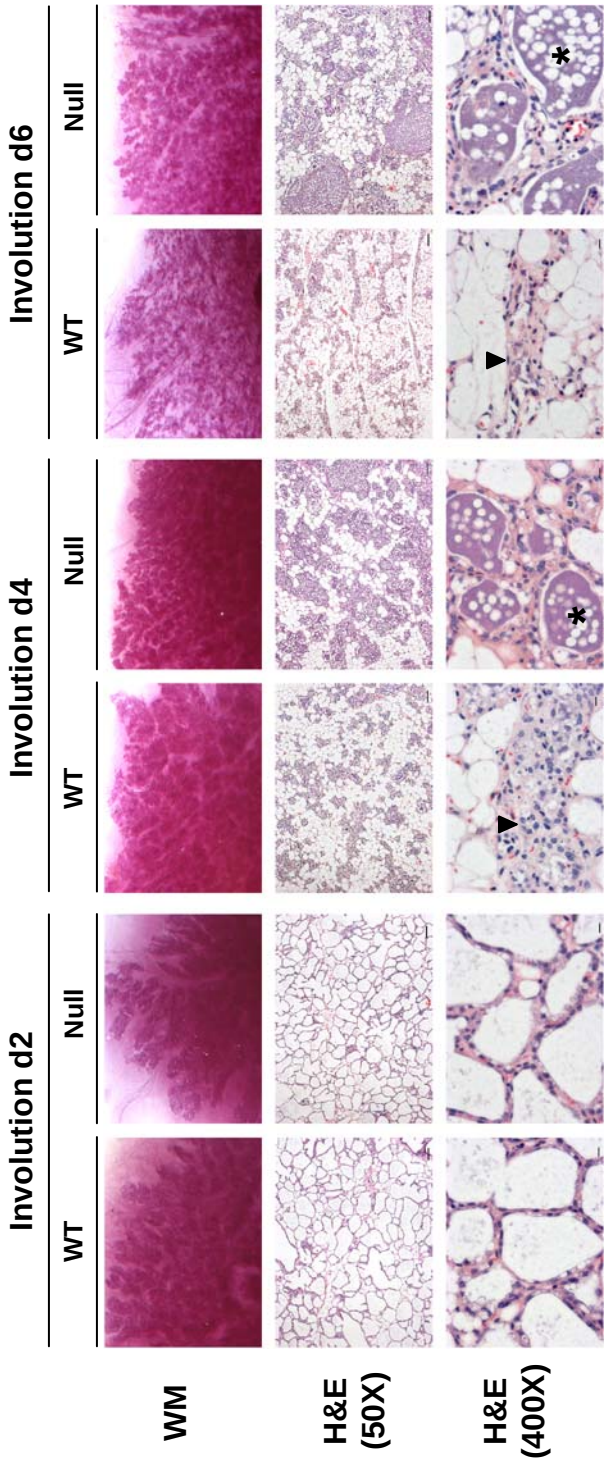
Involution d2
Involution d4
Involution d6
WT
Null
WT
Null
WT
Null
WM
H&E (50X)
H&E (400X)

period of ductal elongation, and during pregnancy, lactation, and involution. This survey suggested that absence of ALS leads to three specific mammary defects namely, delayed ductal elongation, impaired ductal branching and alveolar budding in early pregnancy, and delayed involution. Development during late pregnancy and lactation, on the other hand, appeared completely normal in null ALS mice.

Our study, however, has two significant limitations. First, we found significant ALS expression in the mammary gland at all stages examined. This observation is not a complete surprise as low levels of ALS mRNA expression have been detected in extra-hepatic tissues of a variety of species. For instance, low levels of ALS mRNA were detected in the rat renal cortex by *in situ* hybridization (Chin *et al.* 1994), in pig muscle, spleen, ovary and uterus by ribonuclease protection assay (RPA) (Lee *et al.* 2001), and in cow lung, small intestine, adipose, kidney and heart by RPA (Kim *et al.* 2006). More recently, we have reported significant levels of ALS expression in mouse adipose tissue and kidney (Giesy 2004). The level of ALS expression in the mammary gland during pregnancy, lactation, and involution is unusual in that it matches hepatic expression. We are not aware of any other non-hepatic tissue where this is the case. This observation, however, means that we are unable to attribute exclusively any of the defects identified in null ALS mice entirely to absence of ALS in plasma.

The second limitation is that the mammary gland is a heterogeneous tissue composed of epithelia, adipocytes, and connective tissue (Watson & Khaled 2008). The proportion of these compartments varies significantly throughout the different developmental stages (Richert *et al.* 2000). Any single one of these tissue compartments could express ALS. To address this issue, we tried to localize ALS protein by immunohistochemistry. ALS protein was detected in the lumen of the ducts and/or alveoli, but we were unable to visualize ALS protein within the epithelial

cells or adipocytes. At this time, we do not know exactly which cell types express ALS throughout the various stages of mammary development. Nevertheless, given what is known about the composition of the gland during development, some general statements are appropriate. First, mammary adipose tissue is likely a site of significant ALS expression during the period of pubertal development and early pregnancy. This is because adipose tissue accounts for more than 70% of the tissue at these times (Silberstein 2001) and because we previously showed that non-mammary adipose tissue expresses ALS at ~52% of the levels seen in liver (Giesy 2004). In contrast, epithelial cells occupy most of the mammary gland during late pregnancy and throughout lactation and involution (Richert *et al.* 2000), and thus must synthesize some ALS at these stages. However, we cannot exclude contribution by the epithelium during pubertal development or contribution by remaining adipocytes at later stages.

Despite these limitations, it is still relevant to put our findings in the context of roles played by the GH-IGF-I system in regulating mammary development, with respect to ductal growth. Ruan *et al.* (1992) demonstrated that IGF-I can substitute for GH mediated ductal growth in hypophysectomized rats. Estrogen also plays a role in ductal elongation. In mice lacking estrogen receptor α (ERα), no ductal development occurs (Mallepell *et al.* 2006). Moreover, estrogen enhances GH-induced expression of IGF-I mRNA in the mammary fat pad and synergizes with IGF-I to stimulate ductal growth (Ruan *et al.* 1995). Our data also show that sexual maturation, assessed by presence of a copulatory plug, proceeds more slowly in null ALS mice. However, neither defect appears related to a deficit in estradiol as null ALS mice had higher plasma estradiol levels.

It is possible that the plasma IGF-I deficit of null ALS mice is responsible for the delay in ductal elongation. Few studies have assessed the role of circulating IGF-I

in pubertal mammary development. In one study, pubertal development was studied in the hypomorphic IGF-I$^{m/m}$ model (Richards *et al.* 2004). In these mice, the IGF-I allele contains a site-specific intronic insertion of the targeting construct which results in a 70% reduction in circulating IGF-I and ~50% reduction in mammary IGF-I mRNA (Richards *et al.* 2004). Ductal elongation was delayed and branching complexity was impaired in IGF-I$^{m/m}$ females (Richards *et al.* 2004). The authors attribute this developmental defect to a decrease in local IGF-I production as branching complexity was normal in the liver-specific IGF-I deficient (LID) females, which have a 75% decrease in circulating IGF-I. However, mammary gland development was only analyzed in 90d old mice, and this design would not detect early defects that are normalized over time such as the one we saw in null ALS mice.

IGF-I is also important in early pregnancy, promoting proliferation of ductal branches and formation of alveolar buds (Richert *et al.* 2000). This was shown in female mice lacking one copy of the IGF-I gene, which have impaired alveolar budding at d5.5 of pregnancy (Loladze *et al.* 2006). Similarly, we show a significant decrease in alveolar budding in null ALS mice at d8 of pregnancy. The null ALS mice have normal IGF-I expression in all tissues examined so far (Ueki *et al.* 2000), and accordingly, are also expected to have normal mammary IGF-I expression. If this is the case, this would leave the plasma IGF-I deficit as the common feature in both models.

In an attempt to further study the role of ALS during pregnancy, we created WT or null ALS mice harboring a single functional PRLR allele. Ormandy *et al.* (1997) previously showed that mice harboring a single PRLR allele have normal mammary gland development until d14 of pregnancy, but then suffer for a near complete arrest of lobulo-alveolar expansion. This defect can be rescued by exogenous GH treatment starting at d14 of pregnancy (Allan *et al.* 2002). This rescue

was associated with a 2.5-fold increase in plasma IGF-I on d2 of lactation, raising the possibility that elevated plasma IGF-I was responsible. Our data, however, show that GH induced lobulo-alveolar expansion equally well in null ALS mice carrying one copy of the PRLR gene, demonstrating that effects of GH are mediated by local effects on the mammary gland and not by endocrine IGF-I.

Finally, we observed a delayed progression of involution in the mammary gland of ALS null mice. It is well established that IGF-I acts as a survival factor for the mammary epithelial cell (Green & Streuli 2004). Thus, over-expression of IGF-I in the mammary glands of lactating mice delays the involution process (Neuenschwander *et al.* 1996). Moreover, involution is associated with mammary-specific induction of IGFBP-5 (Tonner *et al.* 1997), which can then neutralize IGF-I and its pro-survival effects (Tonner *et al.* 2002). Consistent with this role, appearance of apoptotic cells and the reappearance of adipocytes were both retarded in IGFBP-5 null mice during involution (Ning *et al.* 2007). This is quite similar to the defect we saw in null ALS mice. This defect appears more likely to relate to local rather than systemic ALS effects. First, if systemic IGF-I did play a role in involution, then one would expect that the lower levels of circulating IGF-I in null ALS mice would accelerate rather than delay mammary involution. Second, locally produced IGFBP-5 neutralizes IGF-I induced proliferation during involution, and ALS is known to form ternary complexes by interacting with IGF-I/IGFBP-5 complexes (Twigg & Baxter 1998). It is tempting to speculate that locally-derived ALS binds IGF-I/IGFBP-5 complexes during involution, and in this manner, increases the neutralization effects of IGFBP-5.

In summary, we have shown that null ALS mice have reduced ductal elongation in the virgin state as well as reduced branching and alveolar budding in early pregnancy. Moreover, involution is delayed in null ALS mice. We detect ALS

mRNA expression and presence of the protein in the mammary gland. In order to understand the mechanism of action of ALS, it is now essential to identify which cell type expresses ALS at each stage of mammary development. This is the first step before specific approaches, such as cell specific ablation of ALS expression, can be considered to address whether the defects arise from plasma or locally produced ALS. Cell specific gene ablation in the mammary gland, particularly at specific stages of development, is not currently feasible. A more realistic approach at this time may be the development of a liver-specific ALS knockout. In this model, any remaining mammary defects could be attributed to the effects of ALS on the circulating IGF-I system.

CHAPTER FIVE:

CONCLUSIONS AND FUTURE DIRECTIONS

Growth hormone (GH) can act directly on target tissues, or it can act indirectly by stimulating insulin-like growth factor (IGF-I) production (Le Roith *et al.* 2001). IGF-I can act either in an autocrine/paracrine fashion via locally produced IGF-I or in an endocrine fashion through circulating IGF-I (Le Roith *et al.* 2001). In plasma, ALS associates with IGF-I in a ternary complex and is responsible for development of the endocrine pool of IGF-I. GH regulation of postnatal growth and liver-derived IGF-I is mediated via the signaling intermediate, Stat5 (Waters *et al.* 2006; Woelfle & Rotwein 2004).

Our first objective was to test whether exogenous GH could stimulate growth, development, and insulin resistance in Stat5 mutant mice. Upon initiation of this work, three independent Stat5 mouse mutants had been created, null Stat5a (Liu *et al.* 1997), null Stat5b (Udy *et al.* 1997), and a mutant thought to combine null Stat5a and 5b alleles ($Stat5^{\Delta N}$) (Teglund *et al.* 1998). These models demonstrated that Stat5a is involved in mammary development (Liu *et al.* 1997), and Stat5b is involved in hepatic gene regulation and postnatal growth (Udy *et al.* 1997). As expected, the $Stat5^{\Delta N}$ mice combined all the defects seen in the individual mutants (Teglund *et al.* 1998). These mice were believed to be true knockouts, but it has since been shown that they express hypomorphic N-terminally deleted Stat5 proteins. Presence of truncated Stat5 proteins has been described in liver (Engblom *et al.* 2007). We show that muscle and adipose tissue also express the truncated proteins. Abundance of the truncated Stat5 proteins in $Stat5^{\Delta N}$ tissues was less than that of Stat5 in WT tissues. Nevertheless, GH was able to activate the truncated Stat5 proteins in all tissues.

Previous studies showed that postnatal growth is impaired in Stat5$^{\Delta N}$ mice (Teglund *et al.* 1998), but whether all effects of GH are lost is unknown. More recently, total Stat5 knockouts were created by ablating the entire Stat5 locus. Total loss of both Stat5 isoforms, however, resulted in perinatal lethality (Cui *et al.* 2004). Because Stat5$^{\Delta N}$ mice are viable and combine the defects seen in null Stat5a and null Stat5b mice, they provide a model in which to study Stat5-mediated GH action.

Similar to previous studies, we show that saline-treated Stat5$^{\Delta N}$ mice grew at a slower rate and had lower hepatic IGF-I expression and plasma IGF-I than WT mice (Teglund *et al.* 1998; Engblom *et al.* 2007). IGF-I expression in muscle and adipose tissue of Stat5$^{\Delta N}$ also was reduced. GH is known to stimulate hepatic IGF-I transcription via Stat5 (Woelfle & Rotwein 2004). More significantly, we show that the impairment in growth is predominantly due to a lack of GH responsiveness. GH treatment increased body weight gain in WT mice, but Stat5$^{\Delta N}$ mice completely failed to respond to GH. Circulating IGF-I and hepatic IGF-I expression increased in GH-treated WT mice while Stat5$^{\Delta N}$ mice were completely insensitive to GH. Furthermore, GH stimulated IGF-I expression in WT mice while Stat5$^{\Delta N}$ mice fail to respond.

Recently, Engblom *et al.* (2007) have shown that regulation of postnatal growth and hepatic IGF-I gene expression required an interaction between Stat5 and the glucocorticoid receptor (GR). Chromatin immunoprecipitation (ChIP) assays demonstrate that the Stat5$^{\Delta N}$ protein is able to bind its cis-elements located in the GH-regulated IGF-I and ALS genes. The Stat5$^{\Delta N}$ protein, however, does not associate with the glucocorticoid receptor as wild type Stat5 does, suggesting that the N-terminal domain of Stat5 serves as a docking platform for GR (Engblom *et al.* 2007). Our results suggest that the Stat5-GR interaction is important for GH-mediated IGF-I transcription not only in liver but also in muscle and adipose tissue. This could be tested by performing ChIP assays in muscle and adipose of WT and Stat5$^{\Delta N}$.

Chronic elevation of GH leads to insulin resistance (Dominici *et al.* 1999b). We show that a functional Stat5 protein is required for GH-induced insulin resistance. Recent studies have identified a molecular mechanism whereby GH antagonizes insulin signaling. In muscle, GH-induction of the p85α subunit of PI3K reduces PI3K activity, resulting in insulin resistance (Barbour *et al.* 2005). GH stimulated p85α expression in WT but not in Stat5$^{\Delta N}$ mice. These results suggest that GH-activated Stat5 binds to the p85α promoter and stimulates expression. Promoter analysis of p85α could be used to test whether Stat5 mediates GH-stimulated p85α expression. This work would involve cloning of the p85α promoter and creation of a reporter construct driven by this promoter. First, we would verify that GH induces p85α expression in vitro. The reporter construct could then be used in cell culture studies to determine whether GH activates the p85α promoter and whether it does so via Stat5 binding to specific cis-elements.

The second experimental chapter of this dissertation focused on the role of the GH-IGF-I system in mammary development. As reviewed in Chapter 2, ALS recruits liver-derived IGF-I in ternary complexes and in doing so, allows the development of the endocrine IGF-I system. Characterization of null ALS mice demonstrated that ALS and IGF-I are needed for normal growth (Ueki *et al.* 2000). Mammary gland development is also highly dependent on the GH-IGF-I system (Kleinberg & Ruan 2008). Thus, our second objective was to assess the role of ALS in mammary gland development. In this survey, we found three specific defects in null ALS mice; delayed ductal elongation, impaired ductal branching and alveolar budding in early pregnancy, and delayed involution. In addition, we detected significant ALS expression in the mammary gland at all stages examined, making it difficult to attribute exclusively any of these defects to disruption of the circulating IGF-I system.

An additional complication is that the mammary gland is a heterogeneous tissue composed of epithelia, adipocytes, and connective tissue (Richert *et al.* 2000). The proportion of these compartments varies significantly throughout the different developmental stages. We attempted to localize ALS protein in the mammary gland by immunohistochemistry in the virgin state, pregnancy, lactation, and involution. During all the developmental stages, ALS was present in the lumen of the ducts and/or alveoli, but we were unable to detect ALS within epithelial cells or adipocytes. Clearly, in situ hybridization studies will be necessary to identify the cell compartment expressing ALS during each phase of mammary development. In the virgin state and during early pregnancy, the gland is composed predominantly of adipose tissue (Silberstein 2001), and we previously have shown that ALS is expressed in other adipose tissue depots (Giesy 2004). In late pregnancy and throughout lactation, however, epithelial cells replace most of the adipocytes (Richert *et al.* 2000). Therefore, we speculate that mammary adipose tissue is likely the major site of ALS expression in pubertal development and early pregnancy, whereas epithelial cell expression predominates in late pregnancy, lactation, and involution.

Mammary ductal elongation is dependent upon estrogen, GH, and IGF-I. Ruan *et al.* (1992) demonstrated that IGF-I can substitute for GH mediated mammary gland development in hypophysectomized rats. Estrogen also plays a role in ductal elongation. In mice lacking estrogen receptor α (ERα), no ductal development occurs (Mallepell *et al.* 2006). Moreover, estrogen enhances GH-induced expression of IGF-I mRNA in the mammary fat pad and synergizes with IGF-I to stimulate ductal growth (Ruan *et al.* 1995). The delay in ductal elongation is likely an IGF-I effect as plasma estradiol levels were adequate in null ALS mice.

IGF-I is also important in early pregnancy, promoting proliferation of ductal branches and formation of alveolar buds (Richert *et al.* 2000). Mice lacking one copy

of the IGF-I gene have a systemic decrease in IGF-I expression, including the mammary gland and reduced circulating IGF-I levels. During early pregnancy, these mice have impaired alveolar budding (Loladze *et al.* 2006), similar to what we observe in null ALS mice. Presumably, mammary expression of IGF-I is normal in null ALS mice, leaving a plasma IGF-I deficit as the common feature between these models.

Perhaps the most interesting result with respect to mammary development was the delayed involution seen in null ALS mice. This defect is more likely to relate to local rather than systemic ALS effects. IGF-I promotes epithelial cell survival in WT mice (Green & Streuli 2004). So, if systemic IGF-I did play a role in involution, then one would expect that the low levels of circulating IGF-I in null ALS mice would in fact accelerate the involution process. Second, ALS is known to also form ternary complexes by interacting with IGF:IGFBP-5 complexes, perhaps providing a more effective mechanism to neutralize IGF-I. The process of involution is irreversible after two days without milk removal (Richert *et al.* 2000). Lactation can be re-established in models having delayed involution, such as null Stat3 mice (Humphreys *et al.* 2002). Given the slower rate of involution in null ALS mice, it would be interesting to determine if lactation could be resumed 4 or 6 days after pup removal. This would involve allowing WT and null ALS dams to nurse pups for 10 days, transferring their pups onto foster dams, and then after 4 or 6 days, transferring the pups back to their dams.

Clearly, we need to establish the spatial and temporal pattern of ALS expression in the mammary gland during development. The other issue to address is whether ALS is affecting mammary gland development via alterations in the circulating IGF-I system or via local mechanisms. This can be approached by ablating ALS expression specifically in liver. We anticipate that such a model would recapitulate the low plasma IGF-I seen in null ALS mice. Any mammary defect

remaining in a liver-specific null ALS model would implicate systemic ALS effects, such as the plasma IGF-I deficiency, rather than mammary ALS. Another approach would be to eliminate ALS specifically in the mammary gland. However, targeted deletion in the mammary gland is difficult, especially during pubertal development, early pregnancy, and involution when the tissue is a heterogeneous composite of adipocytes and epithelial cells. Thus, studying mammary development in a liver-specific ALS knockout model might be the best approach at this time.

REFERENCES

Abell K, Bilancio A, Clarkson RW, Tiffen PG, Altaparmakov AI, Burdon TG, Asano T, Vanhaesebroeck B & Watson CJ 2005 Stat3-induced apoptosis requires a molecular switch in PI(3)K subunit composition. *Nat.Cell Biol.* **7** 392-398.

Albiston AL & Herington AC 1992 Tissue distribution and regulation of insulin-like growth factor (IGF)-binding protein-3 messenger ribonucleic acid (mRNA) in the rat: comparison with IGF-I mRNA expression. *Endocrinology* **130** 497-502.

Allan GJ, Tonner E, Barber MC, Travers MT, Shand JH, Vernon RG, Kelly PA, Binart N & Flint DJ 2002 Growth hormone, acting in part through the insulin-like growth factor axis, rescues developmental, but not metabolic, activity in the mammary gland of mice expressing a single allele of the prolactin receptor. *Endocrinology* **143** 4310-4319.

Allar MA & Wood TL 2004 Expression of the insulin-like growth factor binding proteins during postnatal development of the murine mammary gland. *Endocrinology* **145** 2467-2477.

Baker J, Liu JP, Robertson EJ & Efstratiadis A 1993 Role of insulin-like growth factors in embryonic and postnatal growth. *Cell* **75** 73-82.

Barbour LA, Mizanoor RS, Gurevich I, Leitner JW, Fischer SJ, Roper MD, Knotts TA, Vo Y, McCurdy CE, Yakar S, LeRoith D, Kahn CR, Cantley LC, Friedman JE & Draznin B 2005 Increased P85alpha is a potent negative regulator of skeletal muscle insulin signaling and induces in vivo insulin resistance associated with growth hormone excess. *J.Biol.Chem.* **280** 37489-37494.

Baxter RC 1988 Characterization of the acid-labile subunit of the growth hormone-dependent insulin-like growth factor binding protein complex. *J.Clin.Endocrinol.Metab* **67** 265-272.

Baxter RC 1990 Circulating levels and molecular distribution of the acid-labile (alpha) subunit of the high molecular weight insulin-like growth factor-binding protein complex. *J.Clin.Endocrinol.Metab* **70** 1347-1353.

Baxter RC 1994 Insulin-like growth factor binding proteins in the human circulation: a review. *Horm.Res.* **42** 140-144.

Baxter RC 2000 Insulin-like growth factor (IGF)-binding proteins: interactions with IGFs and intrinsic bioactivities. *Am.J.Physiol Endocrinol.Metab* **278** E967-E976.

Baxter RC & Dai J 1994 Purification and characterization of the acid-labile subunit of rat serum insulin-like growth factor binding protein complex. *Endocrinology* **134** 848-852.

Baxter RC, Martin JL & Beniac VA 1989 High molecular weight insulin-like growth factor binding protein complex. Purification and properties of the acid-labile subunit from human serum. *J.Biol.Chem.* **264** 11843-11848.

Baxter RC, Meka S & Firth SM 2002 Molecular distribution of IGF binding protein-5 in human serum. *J.Clin.Endocrinol.Metab* **87** 271-276.

Bichell DP, Kikuchi K & Rotwein P 1992 Growth hormone rapidly activates insulin-like growth factor I gene transcription in vivo. *Mol.Endocrinol.* **6** 1899-1908.

Biddinger SB & Kahn CR 2006 From mice to men: insights into the insulin resistance syndromes. *Annu.Rev.Physiol* **68** 123-158.

Binoux M & Hossenlopp P 1988 Insulin-like growth factor (IGF) and IGF-binding proteins: comparison of human serum and lymph. *J.Clin.Endocrinol.Metab* **67** 509-514.

Boisclair YR, Rhoads RP, Ueki I, Wang J & Ooi GT 2001 The acid-labile subunit (ALS) of the 150 kDa IGF-binding protein complex: an important but forgotten component of the circulating IGF system. *J.Endocrinol.* **170** 63-70.

Boisclair YR, Seto D, Hsieh S, Hurst KR & Ooi GT 1996 Organization and chromosomal localization of the gene encoding the mouse acid labile subunit of the insulin-like growth factor binding complex. *Proc.Natl.Acad.Sci.U.S.A* **93** 10028-10033.

Bonnette SG & Hadsell DL 2001 Targeted disruption of the IGF-I receptor gene decreases cellular proliferation in mammary terminal end buds. *Endocrinology* **142** 4937-4945.

Brisken C 2002 Hormonal control of alveolar development and its implications for breast carcinogenesis. *J.Mammary.Gland.Biol.Neoplasia.* **7** 39-48.

Brisken C & Rajaram RD 2006 Alveolar and lactogenic differentiation. *J.Mammary.Gland.Biol.Neoplasia.* **11** 239-248.

Brooks AJ, Wooh JW, Tunny KA & Waters MJ 2008 Growth hormone receptor; mechanism of action. *Int.J.Biochem.Cell Biol.* **40** 1984-1989.

Brown AL, Graham DE, Nissley SP, Hill DJ, Strain AJ & Rechler MM 1986 Developmental regulation of insulin-like growth factor II mRNA in different rat tissues. *J.Biol.Chem.* **261** 13144-13150.

Carter-Su C, Rui L & Herrington J 2000 Role of the tyrosine kinase JAK2 in signal transduction by growth hormone. *Pediatr.Nephrol.* **14** 550-557.

Cerro JA, Grewal A, Wood TL & Pintar JE 1993 Tissue-specific expression of the insulin-like growth factor binding protein (IGFBP) mRNAs in mouse and rat development. *Regul.Pept.* **48** 189-198.

Chen WY, White ME, Wagner TE & Kopchick JJ 1991 Functional antagonism between endogenous mouse growth hormone (GH) and a GH analog results in dwarf transgenic mice. *Endocrinology* **129** 1402-1408.

Chin E, Zhou J, Dai J, Baxter RC & Bondy CA 1994 Cellular localization and regulation of gene expression for components of the insulin-like growth factor ternary binding protein complex. *Endocrinology* **134** 2498-2504.

Clemmons DR 2001 Use of mutagenesis to probe IGF-binding protein structure/function relationships. *Endocr.Rev.* **22** 800-817.

Cui Y, Hosui A, Sun R, Shen K, Gavrilova O, Chen W, Cam MC, Gao B, Robinson GW & Hennighausen L 2007 Loss of signal transducer and activator of transcription 5 leads to hepatosteatosis and impaired liver regeneration. *Hepatology* **46** 504-513.

Cui Y, Riedlinger G, Miyoshi K, Tang W, Li C, Deng CX, Robinson GW & Hennighausen L 2004 Inactivation of Stat5 in mouse mammary epithelium during pregnancy reveals distinct functions in cell proliferation, survival, and differentiation. *Mol.Cell Biol.* **24** 8037-8047.

D'Ercole AJ, Stiles AD & Underwood LE 1984 Tissue concentrations of somatomedin C: further evidence for multiple sites of synthesis and paracrine or autocrine mechanisms of action. *Proc.Natl.Acad.Sci.U.S.A* **81** 935-939.

Dai J & Baxter RC 1992 Molecular cloning of the acid-labile subunit of the rat insulin-like growth factor binding protein complex. *Biochem.Biophys.Res.Commun.* **188** 304-309.

Dai J & Baxter RC 1994 Regulation in vivo of the acid-labile subunit of the rat serum insulin-like growth factor-binding protein complex. *Endocrinology* **135** 2335-2341.

Dai J, Scott CD & Baxter RC 1994 Regulation of the acid-labile subunit of the insulin-like growth factor complex in cultured rat hepatocytes. *Endocrinology* **135** 1066-1072.

Daughaday WH, Parker KA, Borowsky S, Trivedi B & Kapadia M 1982 Measurement of somatomedin-related peptides in fetal, neonatal, and maternal rat serum by insulin-like growth factor (IGF) I radioimmunoassay, IGF-II radioreceptor assay (RRA), and multiplication-stimulating activity RRA after acid-ethanol extraction. *Endocrinology* **110** 575-581.

Daughaday WH & Rotwein P 1989 Insulin-like growth factors I and II. Peptide, messenger ribonucleic acid and gene structures, serum, and tissue concentrations. *Endocr.Rev.* **10** 68-91.

Davey HW, Wilkins RJ & Waxman DJ 1999 STAT5 signaling in sexually dimorphic gene expression and growth patterns. *Am.J.Hum.Genet.* **65** 959-965.

Deindl E 2001 18S ribosomal RNA detection on Northern blot employing a specific oligonucleotide. *Biotechniques* **31** 1250, 1252.

Del Rincon JP, Iida K, Gaylinn BD, McCurdy CE, Leitner JW, Barbour LA, Kopchick JJ, Friedman JE, Draznin B & Thorner MO 2007 Growth hormone regulation of p85alpha expression and phosphoinositide 3-kinase activity in adipose tissue: mechanism for growth hormone-mediated insulin resistance. *Diabetes* **56** 1638-1646.

Delhanty P & Baxter RC 1996 The cloning and expression of the baboon acid-labile subunit of the insulin-like growth factor binding protein complex. *Biochem.Biophys.Res.Commun.* **227** 897-902.

Divisova J, Kuiatse I, Lazard Z, Weiss H, Vreeland F, Hadsell DL, Schiff R, Osborne CK & Lee AV 2006 The growth hormone receptor antagonist pegvisomant blocks both mammary gland development and MCF-7 breast cancer xenograft growth. *Breast Cancer Res.Treat.* **98** 315-327.

Dominici FP, Argentino DP, Munoz MC, Miquet JG, Sotelo AI & Turyn D 2005 Influence of the crosstalk between growth hormone and insulin signalling on the modulation of insulin sensitivity. *Growth Horm.IGF.Res.* **15** 324-336.

Dominici FP, Arostegui DG, Bartke A, Kopchick JJ & Turyn D 2000 Compensatory alterations of insulin signal transduction in liver of growth hormone receptor knockout mice. *J.Endocrinol.* **166** 579-590.

Dominici FP, Cifone D, Bartke A & Turyn D 1999a Alterations in the early steps of the insulin-signaling system in skeletal muscle of GH-transgenic mice. *Am.J.Physiol* **277** E447-E454.

Dominici FP, Cifone D, Bartke A & Turyn D 1999b Loss of sensitivity to insulin at early events of the insulin signaling pathway in the liver of growth hormone-transgenic mice. *J.Endocrinol.* **161** 383-392.

Eleswarapu S, Gu Z & Jiang H 2008 Growth hormone regulation of insulin-like growth factor-I gene expression may be mediated by multiple distal signal transducer and activator of transcription 5 binding sites. *Endocrinology* **149** 2230-2240.

Engblom D, Kornfeld JW, Schwake L, Tronche F, Reimann A, Beug H, Hennighausen L, Moriggl R & Schutz G 2007 Direct glucocorticoid receptor-Stat5

interaction in hepatocytes controls body size and maturation-related gene expression. *Genes Dev.* **21** 1157-1162.

Engelman JA, Luo J & Cantley LC 2006 The evolution of phosphatidylinositol 3-kinases as regulators of growth and metabolism. *Nat.Rev.Genet.* **7** 606-619.

Fielder PJ, Mortensen DL, Mallet P, Carlsson B, Baxter RC & Clark RG 1996 Differential long-term effects of insulin-like growth factor-I (IGF-I) growth hormone (GH), and IGF-I plus GH on body growth and IGF binding proteins in hypophysectomized rats. *Endocrinology* **137** 1913-1920.

Firth SM & Baxter RC 2002 Cellular actions of the insulin-like growth factor binding proteins. *Endocr.Rev.* **23** 824-854.

Flint DJ, Beattie J & Allan GJ 2003 Modulation of the Actions of IGFs by IGFBP-5 in the Mammary Gland. *Horm.Metab Res.* **35** 809-815.

Flint DJ, Tonner E, Beattie J & Allan GJ 2008 Role of Insulin-Like Growth Factor Binding Proteins in Mammary Gland Development. *J.Mammary.Gland.Biol.Neoplasia.*

Flores-Morales A, Greenhalgh CJ, Norstedt G & Rico-Bautista E 2006 Negative regulation of growth hormone receptor signaling. *Mol.Endocrinol.* **20** 241-253.

Friedrichsen BN, Galsgaard ED, Nielsen JH & Moldrup A 2001 Growth hormone- and prolactin-induced proliferation of insulinoma cells, INS-1, depends on activation of STAT5 (signal transducer and activator of transcription 5). *Mol.Endocrinol.* **15** 136-148.

Gallego MI, Binart N, Robinson GW, Okagaki R, Coschigano KT, Perry J, Kopchick JJ, Oka T, Kelly PA & Hennighausen L 2001 Prolactin, growth hormone, and epidermal growth factor activate Stat5 in different compartments of mammary tissue and exert different and overlapping developmental effects. *Dev.Biol.* **229** 163-175.

Gatford KL, Egan AR, Clarke IJ & Owens PC 1998 Sexual dimorphism of the somatotrophic axis. *J.Endocrinol.* **157** 373-389.

Gebert CA, Park SH & Waxman DJ 1999 Down-regulation of liver JAK2-STAT5b signaling by the female plasma pattern of continuous growth hormone stimulation. *Mol.Endocrinol.* **13** 213-227.

Giesy, S. L. Regulation of ALS mRNA expression in the mouse. 2004. Ithaca, NY, Cornell University.

Giustina A, Mazziotti G & Canalis E 2008 Growth hormone, insulin-like growth factors, and the skeleton. *Endocr.Rev.* **29** 535-559.

Graham DE, Rechler MM, Brown AL, Frunzio R, Romanus JA, Bruni CB, Whitfield HJ, Nissley SP, Seelig S & Berry S 1986 Coordinate developmental regulation of high and low molecular weight mRNAs for rat insulin-like growth factor II. *Proc.Natl.Acad.Sci.U.S.A* **83** 4519-4523.

Green KA & Streuli CH 2004 Apoptosis regulation in the mammary gland. *Cell Mol.Life Sci.* **61** 1867-1883.

Gronowski AM & Rotwein P 1995 Rapid changes in gene expression after in vivo growth hormone treatment. *Endocrinology* **136** 4741-4748.

Guler HP, Zapf J, Schmid C & Froesch ER 1989 Insulin-like growth factors I and II in healthy man. Estimations of half-lives and production rates. *Acta Endocrinol.(Copenh)* **121** 753-758.

Hadsell DL, Bonnette SG & Lee AV 2002 Genetic manipulation of the IGF-I axis to regulate mammary gland development and function. *J.Dairy Sci.* **85** 365-377.

Haluzik M, Yakar S, Gavrilova O, Setser J, Boisclair Y & LeRoith D 2003 Insulin Resistance in the Liver-Specific IGF-1 Gene-Deleted Mouse Is Abrogated by Deletion of the Acid-Labile Subunit of the IGF-Binding Protein-3 Complex: Relative Roles of Growth Hormone and IGF-1 in Insulin Resistance. *Diabetes* **52** 2483-2489.

Hansen LH, Wang X, Kopchick JJ, Bouchelouche P, Nielsen JH, Galsgaard ED & Billestrup N 1996 Identification of tyrosine residues in the intracellular domain of the growth hormone receptor required for transcriptional signaling and Stat5 activation. *J.Biol.Chem.* **271** 12669-12673.

Hennighausen L & Robinson GW 2008 Interpretation of cytokine signaling through the transcription factors STAT5A and STAT5B. *Genes Dev.* **22** 711-721.

Herrington J, Smit LS, Schwartz J & Carter-Su C 2000 The role of STAT proteins in growth hormone signaling. *Oncogene* **19** 2585-2597.

Hirsch E, Costa C & Ciraolo E 2007 Phosphoinositide 3-kinases as a common platform for multi-hormone signaling. *J.Endocrinol.* **194** 243-256.

Holloway MG, Cui Y, Laz EV, Hosui A, Hennighausen L & Waxman DJ 2007 Loss of sexually dimorphic liver gene expression upon hepatocyte-specific deletion of Stat5a-Stat5b locus. *Endocrinology* **148** 1977-1986.

Hosui A & Hennighausen L 2008 Genomic dissection of the cytokine-controlled STAT5 signaling network in liver. *Physiol Genomics* **34** 135-143.

Hovey RC, Trott JF & Vonderhaar BK 2002 Establishing a framework for the functional mammary gland: from endocrinology to morphology. *J.Mammary.Gland.Biol.Neoplasia.* **7** 17-38.

Howlin J, McBryan J & Martin F 2006 Pubertal mammary gland development: insights from mouse models. *J.Mammary.Gland.Biol.Neoplasia.* **11** 283-297.

Humbel RE 1990 Insulin-like growth factors I and II. *Eur.J.Biochem.* **190** 445-462.

Humphreys RC, Bierie B, Zhao L, Raz R, Levy D & Hennighausen L 2002 Deletion of Stat3 blocks mammary gland involution and extends functional competence of the secretory epithelium in the absence of lactogenic stimuli. *Endocrinology* **143** 3641-3650.

Hwang DL, Lee PD & Cohen P 2008 Quantitative ontogeny of murine insulin-like growth factor (IGF)-I, IGF-binding protein-3 and the IGF-related acid-labile subunit. *Growth Horm.IGF.Res.* **18** 65-74.

Hynes MA, Van Wyk JJ, Brooks PJ, D'Ercole AJ, Jansen M & Lund PK 1987 Growth hormone dependence of somatomedin-C/insulin-like growth factor-I and insulin-like growth factor-II messenger ribonucleic acids. *Mol.Endocrinol.* **1** 233-242.

James PL, Jones SB, Busby WH, Jr., Clemmons DR & Rotwein P 1993 A highly conserved insulin-like growth factor-binding protein (IGFBP-5) is expressed during myoblast differentiation. *J.Biol.Chem.* **268** 22305-22312.

Jones JI & Clemmons DR 1995 Insulin-like growth factors and their binding proteins: biological actions. *Endocr.Rev.* **16** 3-34.

Kasukawa Y, Baylink DJ, Guo R & Mohan S 2003 Evidence that sensitivity to growth hormone (GH) is growth period and tissue type dependent: studies in GH-deficient lit/lit mice. *Endocrinology* **144** 3950-3957.

Kelley KM, Oh Y, Gargosky SE, Gucev Z, Matsumoto T, Hwa V, Ng L, Simpson DM & Rosenfeld RG 1996 Insulin-like growth factor-binding proteins (IGFBPs) and their regulatory dynamics. *Int.J.Biochem.Cell Biol.* **28** 619-637.

Kim JW, Rhoads RP, Segoale N, Kristensen NB, Bauman DE & Boisclair YR 2006 Isolation of the cDNA encoding the acid labile subunit (ALS) of the 150 kDa IGF-binding protein complex in cattle and ALS regulation during the transition from pregnancy to lactation. *J.Endocrinol.* **189** 583-593.

Kleinberg DL 1997 Early mammary development: growth hormone and IGF-1. *J.Mammary.Gland.Biol.Neoplasia.* **2** 49-57.

Kleinberg DL, Feldman M & Ruan W 2000 IGF-I: an essential factor in terminal end bud formation and ductal morphogenesis. *J.Mammary.Gland.Biol.Neoplasia.* **5** 7-17.

Kleinberg DL & Ruan W 2008 IGF-I, GH, and Sex Steroid Effects in Normal Mammary Gland Development. *J.Mammary.Gland.Biol.Neoplasia.*

Klover P & Hennighausen L 2007 Postnatal body growth is dependent on the transcription factors signal transducers and activators of transcription 5a/b in muscle: a role for autocrine/paracrine insulin-like growth factor I. *Endocrinology* **148** 1489-1497.

Kopchick JJ & Laron Z 1999 Is the Laron mouse an accurate model of Laron syndrome? *Mol.Genet.Metab* **68** 232-236.

Kornfeld JW, Grebien F, Kerenyi MA, Friedbichler K, Kovacic B, Zankl B, Hoelbl A, Nivarti H, Beug H, Sexl V, Muller M, Kenner L, Mullner EW, Gouilleux F & Moriggl R 2008 The different functions of Stat5 and chromatin alteration through Stat5 proteins. *Front Biosci.* **13** 6237-6254.

Kou K, Jenkins NA, Gilbert DJ, Copeland NG & Rotwein P 1994 Organization, expression, and chromosomal location of the mouse insulin-like growth factor binding protein 5 gene. *Genomics* **20** 412-418.

Labarta JI, Gargosky SE, Simpson DM, Lee PD, Argente J, Guevara-Aguirre J & Rosenfeld RG 1997 Immunoblot studies of the acid-labile subunit (ALS) in biological fluids, normal human serum and in children with GH deficiency and GH receptor deficiency before and after long-term therapy with GH or IGF-I respectively. *Clin.Endocrinol.(Oxf)* **47** 657-666.

Lamote I, Meyer E, Massart-Leen AM & Burvenich C 2004 Sex steroids and growth factors in the regulation of mammary gland proliferation, differentiation, and involution. *Steroids* **69** 145-159.

Landwehr J, Kaupmann K, Heinrich G & Schwander J 1993 Cloning and characterization of the gene encoding murine insulin-like growth factor-binding protein-2, mIGFBP-2. *Gene* **124** 281-286.

Lanning NJ & Carter-Su C 2006 Recent advances in growth hormone signaling. *Rev.Endocr.Metab Disord.* **7** 225-235.

Laviola L, Natalicchio A & Giorgino F 2007 The IGF-I signaling pathway. *Curr.Pharm.Des* **13** 663-669.

Le Roith D, Bondy C, Yakar S, Liu JL & Butler A 2001 The somatomedin hypothesis: 2001. *Endocr.Rev.* **22** 53-74.

Lee CY, Kwak I, Chung CS, Choi WS, Simmen RC & Simmen FA 2001 Molecular cloning of the porcine acid-labile subunit (ALS) of the insulin-like growth factor-binding protein complex and detection of ALS gene expression in hepatic and non-hepatic tissues. *J.Mol.Endocrinol.* **26** 135-144.

Lee JY, Gavrilova O, Davani B, Na R, Robinson GW & Hennighausen L 2007 The transcription factors Stat5a/b are not required for islet development but modulate pancreatic beta-cell physiology upon aging. *Biochim.Biophys.Acta* **1773** 1455-1461.

Liu JL, Coschigano KT, Robertson K, Lipsett M, Guo Y, Kopchick JJ, Kumar U & Liu YL 2004 Disruption of growth hormone receptor gene causes diminished pancreatic islet size and increased insulin sensitivity in mice. *Am.J.Physiol Endocrinol.Metab* **287** E405-E413.

Liu JL, Grinberg A, Westphal H, Sauer B, Accili D, Karas M & LeRoith D 1998 Insulin-like growth factor-I affects perinatal lethality and postnatal development in a gene dosage-dependent manner: manipulation using the Cre/loxP system in transgenic mice. *Mol.Endocrinol.* **12** 1452-1462.

Liu JL & LeRoith D 1999 Insulin-like growth factor I is essential for postnatal growth in response to growth hormone. *Endocrinology* **140** 5178-5184.

Liu JL, Yakar S & LeRoith D 2000a Conditional knockout of mouse insulin-like growth factor-1 gene using the Cre/loxP system. *Proc.Soc.Exp.Biol.Med.* **223** 344-351.

Liu JL, Yakar S & LeRoith D 2000b Mice deficient in liver production of insulin-like growth factor I display sexual dimorphism in growth hormone-stimulated postnatal growth. *Endocrinology* **141** 4436-4441.

Liu JP, Baker J, Perkins AS, Robertson EJ & Efstratiadis A 1993 Mice carrying null mutations of the genes encoding insulin-like growth factor I (Igf-1) and type 1 IGF receptor (Igf1r). *Cell* **75** 59-72.

Liu X, Robinson GW, Gouilleux F, Groner B & Hennighausen L 1995 Cloning and expression of Stat5 and an additional homologue (Stat5b) involved in prolactin signal transduction in mouse mammary tissue. *Proc.Natl.Acad.Sci.U.S.A* **92** 8831-8835.

Liu X, Robinson GW, Wagner KU, Garrett L, Wynshaw-Boris A & Hennighausen L 1997 Stat5a is mandatory for adult mammary gland development and lactogenesis. *Genes Dev.* **11** 179-186.

Loladze AV, Stull MA, Rowzee AM, Demarco J, Lantry JH, III, Rosen CJ, LeRoith D, Wagner KU, Hennighausen L & Wood TL 2006 Epithelial-Specific and Stage-Specific Functions of Insulin-Like Growth Factor-I during Postnatal Mammary Development. *Endocrinology* **147** 5412-5423.

Lupu F, Terwilliger JD, Lee K, Segre GV & Efstratiadis A 2001 Roles of growth hormone and insulin-like growth factor 1 in mouse postnatal growth. *Dev.Biol.* **229** 141-162.

MacLeod JN, Pampori NA & Shapiro BH 1991 Sex differences in the ultradian pattern of plasma growth hormone concentrations in mice. *J.Endocrinol.* **131** 395-399.

Maiter D, Underwood LE, Maes M, Davenport ML & Ketelslegers JM 1988 Different effects of intermittent and continuous growth hormone (GH) administration on serum somatomedin-C/insulin-like growth factor I and liver GH receptors in hypophysectomized rats. *Endocrinology* **123** 1053-1059.

Mallepell S, Krust A, Chambon P & Brisken C 2006 Paracrine signaling through the epithelial estrogen receptor alpha is required for proliferation and morphogenesis in the mammary gland. *Proc.Natl.Acad.Sci.U.S.A* **103** 2196-2201.

Margot JB, Binkert C, Mary JL, Landwehr J, Heinrich G & Schwander J 1989 A low molecular weight insulin-like growth factor binding protein from rat: cDNA cloning and tissue distribution of its messenger RNA. *Mol.Endocrinol.* **3** 1053-1060.

Marshman E, Green KA, Flint DJ, White A, Streuli CH & Westwood M 2003 Insulin-like growth factor binding protein 5 and apoptosis in mammary epithelial cells. *J.Cell Sci.* **116** 675-682.

Mathews LS, Norstedt G & Palmiter RD 1986 Regulation of insulin-like growth factor I gene expression by growth hormone. *Proc.Natl.Acad.Sci.U.S.A* **83** 9343-9347.

Miyoshi K, Cui Y, Riedlinger G, Robinson P, Lehoczky J, Zon L, Oka T, Dewar K & Hennighausen L 2001 Structure of the mouse Stat 3/5 locus: evolution from Drosophila to zebrafish to mouse. *Genomics* **71** 150-155.

Moses AC, Nissley SP, Short PA, Rechler MM, White RM, Knight AB & Higa OZ 1980 Increased levels of multiplication-stimulating activity, an insulin-like growth factor, in fetal rat serum. *Proc.Natl.Acad.Sci.U.S.A* **77** 3649-3653.

Murphy LJ, Bell GI, Duckworth ML & Friesen HG 1987 Identification, characterization, and regulation of a rat complementary deoxyribonucleic acid which encodes insulin-like growth factor-I. *Endocrinology* **121** 684-691.

Neuenschwander S, Schwartz A, Wood TL, Roberts CT, Jr., Henninghausen L & LeRoith D 1996 Involution of the lactating mammary gland is inhibited by the IGF system in a transgenic mouse model. *J.Clin.Invest* **97** 2225-2232.

Ning Y, Hoang B, Schuller AG, Cominski TP, Hsu MS, Wood TL & Pintar JE 2007 Delayed mammary gland involution in mice with mutation of the insulin-like growth factor binding protein 5 gene. *Endocrinology* **148** 2138-2147.

O'Dell SD & Day IN 1998 Insulin-like growth factor II (IGF-II). *Int.J.Biochem.Cell Biol.* **30** 767-771.

Ohlsson C, Sjogren K, Jansson JO & Isaksson OG 2000 The relative importance of endocrine versus autocrine/paracrine insulin-like growth factor-I in the regulation of body growth. *Pediatr.Nephrol.* **14** 541-543.

Olivecrona H, Hilding A, Ekstrom C, Barle H, Nyberg B, Moller C, Delhanty PJ, Baxter RC, Angelin B, Ekstrom TJ & Tally M 1999 Acute and short-term effects of growth hormone on insulin-like growth factors and their binding proteins: serum levels and hepatic messenger ribonucleic acid responses in humans. *J.Clin.Endocrinol.Metab* **84** 553-560.

Ooi GT, Cohen FJ, Tseng LY, Rechler MM & Boisclair YR 1997 Growth hormone stimulates transcription of the gene encoding the acid-labile subunit (ALS) of the circulating insulin-like growth factor-binding protein complex and ALS promoter activity in rat liver. *Mol.Endocrinol.* **11** 997-1007.

Ooi GT, Hurst KR, Poy MN, Rechler MM & Boisclair YR 1998 Binding of STAT5a and STAT5b to a single element resembling a gamma-interferon-activated sequence mediates the growth hormone induction of the mouse acid-labile subunit promoter in liver cells. *Mol.Endocrinol.* **12** 675-687.

Ormandy CJ, Binart N & Kelly PA 1997 Mammary gland development in prolactin receptor knockout mice. *J.Mammary.Gland.Biol.Neoplasia.* **2** 355-364.

Piwien-Pilipuk G, Huo JS & Schwartz J 2002 Growth hormone signal transduction. *J.Pediatr.Endocrinol.Metab* **15** 771-786.

Powell-Braxton L, Hollingshead P, Warburton C, Dowd M, Pitts-Meek S, Dalton D, Gillett N & Stewart TA 1993 IGF-I is required for normal embryonic growth in mice. *Genes Dev.* **7** 2609-2617.

Rajaram S, Baylink DJ & Mohan S 1997 Insulin-like growth factor-binding proteins in serum and other biological fluids: regulation and functions. *Endocr.Rev.* **18** 801-831.

Ram PA & Waxman DJ 1999 SOCS/CIS protein inhibition of growth hormone-stimulated STAT5 signaling by multiple mechanisms. *J.Biol.Chem.* **274** 35553-35561.

Rechler, M. M. Insulin-like Growth Factor Binding Proteins. Vitamins and Hormones 47, 1-114. 1993.

Rhoads RP, Greenwood PL, Bell AW & Boisclair YR 2000 Organization and regulation of the gene encoding the sheep acid-labile subunit of the 150-kilodalton insulin-like growth factor-binding protein complex. *Endocrinology* **141** 1425-1433.

Richards RG, Klotz DM, Walker MP & Diaugustine RP 2004 Mammary gland branching morphogenesis is diminished in mice with a deficiency of insulin-like

growth factor-I (IGF-I), but not in mice with a liver-specific deletion of IGF-I. *Endocrinology* **145** 3106-3110.

Richert MM, Schwertfeger KL, Ryder JW & Anderson SM 2000 An atlas of mouse mammary gland development. *J.Mammary.Gland.Biol.Neoplasia.* **5** 227-241.

Richert MM & Wood TL 1999 The insulin-like growth factors (IGF) and IGF type I receptor during postnatal growth of the murine mammary gland: sites of messenger ribonucleic acid expression and potential functions. *Endocrinology* **140** 454-461.

Riedlinger G, Okagaki R, Wagner KU, Rucker EB, III, Oka T, Miyoshi K, Flaws JA & Hennighausen L 2002 Bcl-x is not required for maintenance of follicles and corpus luteum in the postnatal mouse ovary. *Biol.Reprod.* **66** 438-444.

Roberts CT, Jr., Lasky SR, Lowe WL, Jr., Seaman WT & LeRoith D 1987 Molecular cloning of rat insulin-like growth factor I complementary deoxyribonucleic acids: differential messenger ribonucleic acid processing and regulation by growth hormone in extrahepatic tissues. *Mol.Endocrinol.* **1** 243-248.

Rotwein P, Bichell DP & Kikuchi K 1993 Multifactorial regulation of IGF-I gene expression. *Mol.Reprod.Dev.* **35** 358-363.

Rowland JE, Kerr LM, White M, Noakes PG & Waters MJ 2005a Heterozygote effects in mice with partial truncations in the growth hormone receptor cytoplasmic domain: assessment of growth parameters and phenotype. *Endocrinology* **146** 5278-5286.

Rowland JE, Lichanska AM, Kerr LM, White M, d'Aniello EM, Maher SL, Brown R, Teasdale RD, Noakes PG & Waters MJ 2005b In vivo analysis of growth hormone receptor signaling domains and their associated transcripts. *Mol.Cell Biol.* **25** 66-77.

Ruan W, Catanese V, Wieczorek R, Feldman M & Kleinberg DL 1995 Estradiol enhances the stimulatory effect of insulin-like growth factor-I (IGF-I) on mammary development and growth hormone-induced IGF-I messenger ribonucleic acid. *Endocrinology* **136** 1296-1302.

Ruan W & Kleinberg DL 1999 Insulin-like growth factor I is essential for terminal end bud formation and ductal morphogenesis during mammary development. *Endocrinology* **140** 5075-5081.

Ruan W, Newman CB & Kleinberg DL 1992 Intact and amino-terminally shortened forms of insulin-like growth factor I induce mammary gland differentiation and development. *Proc.Natl.Acad.Sci.U.S.A* **89** 10872-10876.

Scharf J, Ramadori G, Braulke T & Hartmann H 1996 Synthesis of insulinlike growth factor binding proteins and of the acid-labile subunit in primary cultures of rat

hepatocytes, of Kupffer cells, and in cocultures: regulation by insulin, insulinlike growth factor, and growth hormone. *Hepatology* **23** 818-827.

Schneider MR, Wolf E, Hoeflich A & Lahm H 2002 IGF-binding protein-5: flexible player in the IGF system and effector on its own. *J.Endocrinol.* **172** 423-440.

Schuller AG, Groffen C, van Neck JW, Zwarthoff EC & Drop SL 1994 cDNA cloning and mRNA expression of the six mouse insulin-like growth factor binding proteins. *Mol.Cell Endocrinol.* **104** 57-66.

Shimasaki S, Shimonaka M, Zhang HP & Ling N 1991 Identification of five different insulin-like growth factor binding proteins (IGFBPs) from adult rat serum and molecular cloning of a novel IGFBP-5 in rat and human. *J.Biol.Chem.* **266** 10646-10653.

Silberstein GB 2001 Postnatal mammary gland morphogenesis. *Microsc.Res.Tech.* **52** 155-162.

Singh JS, Rall LB & Styne DM 1991 Insulin-like growth factor I and II gene expression in Balb/C mouse liver during postnatal development. *Biol.Neonate* **60** 7-18.

Sjogren K, Liu JL, Blad K, Skrtic S, Vidal O, Wallenius V, LeRoith D, Tornell J, Isaksson OG, Jansson JO & Ohlsson C 1999 Liver-derived insulin-like growth factor I (IGF-I) is the principal source of IGF-I in blood but is not required for postnatal body growth in mice. *Proc.Natl.Acad.Sci.U.S.A* **96** 7088-7092.

Smit LS, Meyer DJ, Billestrup N, Norstedt G, Schwartz J & Carter-Su C 1996 The role of the growth hormone (GH) receptor and JAK1 and JAK2 kinases in the activation of Stats 1, 3, and 5 by GH. *Mol.Endocrinol.* **10** 519-533.

Stein T, Salomonis N & Gusterson BA 2007 Mammary gland involution as a multi-step process. *J.Mammary.Gland.Biol.Neoplasia.* **12** 25-35.

Stempien MM, Fong NM, Rall LB & Bell GI 1986 Sequence of a placental cDNA encoding the mouse insulin-like growth factor II precursor. *DNA* **5** 357-361.

Stewart CE & Rotwein P 1996 Growth, differentiation, and survival: multiple physiological functions for insulin-like growth factors. *Physiol Rev.* **76** 1005-1026.

Tang Z, Yu R, Lu Y, Parlow AF & Liu JL 2005 Age-dependent onset of liver-specific IGF-I gene deficiency and its persistence in old age: implications for postnatal growth and insulin resistance in LID mice. *Am.J.Physiol Endocrinol.Metab* **289** E288-E295.

Teglund S, McKay C, Schuetz E, van Deursen JM, Stravopodis D, Wang D, Brown M, Bodner S, Grosveld G & Ihle JN 1998 Stat5a and Stat5b proteins have essential and nonessential, or redundant, roles in cytokine responses. *Cell* **93** 841-850.

Thoren M, Hilding A, Baxter RC, Degerblad M, Wivall-Helleryd IL & Hall K 1997 Serum insulin-like growth factor I (IGF-I), IGF-binding protein-1 and -3, and the acid-labile subunit as serum markers of body composition during growth hormone (GH) therapy in adults with GH deficiency. *J.Clin.Endocrinol.Metab* **82** 223-228.

Tonner E, Barber MC, Allan GJ, Beattie J, Webster J, Whitelaw CB & Flint DJ 2002 Insulin-like growth factor binding protein-5 (IGFBP-5) induces premature cell death in the mammary glands of transgenic mice. *Development* **129** 4547-4557.

Tonner E, Barber MC, Travers MT, Logan A & Flint DJ 1997 Hormonal control of insulin-like growth factor-binding protein-5 production in the involuting mammary gland of the rat. *Endocrinology* **138** 5101-5107.

Truett GE, Heeger P, Mynatt RL, Truett AA, Walker JA & Warman ML 2000 Preparation of PCR-quality mouse genomic DNA with hot sodium hydroxide and tris (HotSHOT). *Biotechniques* **29** 52, 54.

Twigg SM & Baxter RC 1998 Insulin-like growth factor (IGF)-binding protein 5 forms an alternative ternary complex with IGFs and the acid-labile subunit. *J.Biol.Chem.* **273** 6074-6079.

Udy GB, Towers RP, Snell RG, Wilkins RJ, Park SH, Ram PA, Waxman DJ & Davey HW 1997 Requirement of STAT5b for sexual dimorphism of body growth rates and liver gene expression. *Proc.Natl.Acad.Sci.U.S.A* **94** 7239-7244.

Ueki, I. Regulation of the acid labile subunit gene and function of the protein during anabolic and catabolic states. 2006. Ithaca, NY, Cornell University.

Ueki I, Ooi GT, Tremblay ML, Hurst KR, Bach LA & Boisclair YR 2000 Inactivation of the acid labile subunit gene in mice results in mild retardation of postnatal growth despite profound disruptions in the circulating insulin-like growth factor system. *Proc.Natl.Acad.Sci.U.S.A* **97** 6868-6873.

Ungureanu D, Saharinen P, Junttila I, Hilton DJ & Silvennoinen O 2002 Regulation of Jak2 through the ubiquitin-proteasome pathway involves phosphorylation of Jak2 on Y1007 and interaction with SOCS-1. *Mol.Cell Biol.* **22** 3316-3326.

Walden PD, Ruan W, Feldman M & Kleinberg DL 1998 Evidence that the mammary fat pad mediates the action of growth hormone in mammary gland development. *Endocrinology* **139** 659-662.

Wang Y & Jiang H 2005 Identification of a distal STAT5-binding DNA region that may mediate growth hormone regulation of insulin-like growth factor-I gene expression. *J.Biol.Chem.* **280** 10955-10963.

Waters MJ, Hoang HN, Fairlie DP, Pelekanos RA & Brown RJ 2006 New insights into growth hormone action. *J.Mol.Endocrinol.* **36** 1-7.

Watson CJ & Khaled WT 2008 Mammary development in the embryo and adult: a journey of morphogenesis and commitment. *Development* **135** 995-1003.

Waxman DJ, Ram PA, Park SH & Choi HK 1995 Intermittent plasma growth hormone triggers tyrosine phosphorylation and nuclear translocation of a liver-expressed, Stat 5-related DNA binding protein. Proposed role as an intracellular regulator of male-specific liver gene transcription. *J.Biol.Chem.* **270** 13262-13270.

Werner H, Woloschak M, Adamo M, Shen-Orr Z, Roberts CT, Jr. & LeRoith D 1989 Developmental regulation of the rat insulin-like growth factor I receptor gene. *Proc.Natl.Acad.Sci.U.S.A* **86** 7451-7455.

Wetterau LA, Moore MG, Lee KW, Shim ML & Cohen P 1999 Novel aspects of the insulin-like growth factor binding proteins. *Mol.Genet.Metab* **68** 161-181.

Woelfle J, Chia DJ, Massart-Schlesinger MB, Moyano P & Rotwein P 2005 Molecular physiology, pathology, and regulation of the growth hormone/insulin-like growth factor-I system. *Pediatr.Nephrol.* **20** 295-302.

Woelfle J, Chia DJ & Rotwein P 2003 Mechanisms of Growth Hormone (GH) Action: IDENTIFICATION OF CONSERVED Stat5 BINDING SITES THAT MEDIATE GH-INDUCED INSULIN-LIKE GROWTH FACTOR-I GENE ACTIVATION. *J.Biol.Chem.* **278** 51261-51266.

Woelfle J & Rotwein P 2004 In vivo regulation of growth hormone-stimulated gene transcription by STAT5b. *Am.J.Physiol Endocrinol.Metab* **286** E393-E401.

Wood TL, Richert MM, Stull MA & Allar MA 2000 The insulin-like growth factors (IGFs) and IGF binding proteins in postnatal development of murine mammary glands. *J.Mammary.Gland.Biol.Neoplasia.* **5** 31-42.

Wormald S & Hilton DJ 2004 Inhibitors of cytokine signal transduction. *J.Biol.Chem.* **279** 821-824.

Wu, Y., Sun, H., Kawashima, Y., Yakar, S., and LeRoith, D. Liver-Derived, Circulating (Endocrine) Insulin-Like Growth Factor-1 Is Sufficient To Support Normal Post-Natal Growth. ENDO 2008 , 103. 2008.

Yakar S, Liu JL, Fernandez AM, Wu Y, Schally AV, Frystyk J, Chernausek SD, Mejia W & Le Roith D 2001 Liver-specific igf-1 gene deletion leads to muscle insulin insensitivity. *Diabetes* **50** 1110-1118.

Yakar S, Liu JL, Stannard B, Butler A, Accili D, Sauer B & LeRoith D 1999 Normal growth and development in the absence of hepatic insulin-like growth factor I. *Proc.Natl.Acad.Sci.U.S.A* **96** 7324-7329.

Yakar S, Rosen CJ, Beamer WG, Ackert-Bicknell CL, Wu Y, Liu JL, Ooi GT, Setser J, Frystyk J, Boisclair YR & LeRoith D 2002 Circulating levels of IGF-1 directly regulate bone growth and density. *J.Clin.Invest* **110** 771-781.

Yakar S, Setser J, Zhao H, Stannard B, Haluzik M, Glatt V, Bouxsein ML, Kopchick JJ & LeRoith D 2004 Inhibition of growth hormone action improves insulin sensitivity in liver IGF-1-deficient mice. *J.Clin.Invest* **113** 96-105.

Zapf J, Hauri C, Futo E, Hussain M, Rutishauser J, Maack CA & Froesch ER 1995 Intravenously injected insulin-like growth factor (IGF) I/IGF binding protein-3 complex exerts insulin-like effects in hypophysectomized, but not in normal rats. *J.Clin.Invest* **95** 179-186.

Zapf J, Hauri C, Waldvogel M & Froesch ER 1986 Acute metabolic effects and half-lives of intravenously administered insulinlike growth factors I and II in normal and hypophysectomized rats. *J.Clin.Invest* **77** 1768-1775.

Zhou Y, Xu BC, Maheshwari HG, He L, Reed M, Lozykowski M, Okada S, Cataldo L, Coschigamo K, Wagner TE, Baumann G & Kopchick JJ 1997 A mammalian model for Laron syndrome produced by targeted disruption of the mouse growth hormone receptor/binding protein gene (the Laron mouse). *Proc.Natl.Acad.Sci.U.S.A* **94** 13215-13220.